Two-loop electroweak next-to-leading logarithms for processes involving heavy quarks

A. Denner and B. Jantzen

Paul Scherrer Institut,
CH-5232 Villigen PSI, Switzerland
E-mail: `Ansgar.Denner@psi.ch`, `physics@bernd-jantzen.de`

S. Pozzorini

Max-Planck-Institut für Physik,
Föhringer Ring 6, D-80805 München, Germany
E-mail: `pozzorin@mppmu.mpg.de`

ABSTRACT: We derive logarithmically enhanced two-loop virtual electroweak corrections for arbitrary fermion-scattering processes at the TeV scale. This extends results previously obtained for massless fermion scattering to processes that involve also bottom and top quarks. The contributions resulting from soft, collinear, and ultraviolet singularities in the complete electroweak Standard Model are explicitly extracted from two-loop diagrams to next-to-leading-logarithmic accuracy including all effects associated with symmetry breaking and Yukawa interactions.

Contents

1. Introduction

At TeV colliders, electroweak radiative corrections are strongly enhanced by logarithms of the type $\ln(Q^2/M_{W,Z}^2)$ [1–4]. These logarithmic corrections affect every reaction that involves electroweakly interacting particles and is characterized by scattering energies $Q \gg M_{W,Z}$. The impact of the enhanced electroweak corrections at high-energy colliders has been investigated both in complete one-loop calculations and in logarithmic approximation for several specific reactions, including gauge-boson pair production at the ILC [4, 5] and the LHC [6], gauge-boson scattering [2, 7], fermion-pair production in e^+e^- collisions [3, 8], Drell-Yan processes at the LHC [9], heavy-quark production [10], single-gauge-boson plus jet production at the LHC [11], Higgs production in vector-boson fusion at the LHC [12], and three-jet production in e^+e^- collisions [13]. The results of these studies demonstrate that at energies $Q \sim 1\,\text{TeV}$ the size of the electroweak corrections can reach, depending on the process, up to tens of per cent at one loop and several per cent at two loops.

At high energies, the dominant effects can be described in a systematic way by treating the electroweak corrections in the asymptotic limit $Q/M_{W,Z} \to \infty$, where all masses of order M_W are formally handled as infinitesimally small parameters. In this limit, the electroweak corrections appear as a sequence of logarithms of the form $\alpha^l \ln^j \left(Q^2/M_{W,Z}^2 \right)$, with $j \leq 2l$, which diverge asymptotically. These logarithms have a two-fold origin. The renormalization of ultraviolet (UV) singularities at the scale $\mu_R \lesssim M_{W,Z}$ yields terms of the form $\ln(Q^2/\mu_R^2)$ and, in addition, the interactions of the initial- and final-state particles with soft and/or collinear gauge bosons give rise to $\ln(Q^2/M_{W,Z}^2)$ terms that represent mass singularities.

As pointed out in ref. [14], soft and collinear electroweak logarithms are present not only in those physical observables that are exclusive with respect to real radiation of Z and W bosons, but even in fully inclusive observables [14, 15]. However, there is no need to combine corrections resulting from virtual and real Z/W bosons in the same observable. Thus, in this paper we will consider only exclusive observables, which do not include real Z/W-boson emission and contain only virtual contributions.

Since they originate from UV, soft, and collinear singularities, electroweak logarithmic corrections have universal properties that can be studied in a process-independent way and reveal interesting analogies between QED, QCD, and electroweak interactions. At one loop, the leading logarithms (LLs) and next-to-leading logarithms (NLLs) factorize and are described by a general formula that applies to arbitrary Standard-Model processes [16, 17].

The properties of electroweak logarithmic corrections beyond one loop can be investigated by means of infrared evolution equations that describe the electroweak interactions in terms of two regimes corresponding to $SU(2) \times U(1)$ and $U_{em}(1)$ symmetric gauge theories [18–22]. This approach makes use of resummation techniques that were derived in the context of symmetric gauge theories (QED, QCD), thereby assuming that electroweak symmetry-breaking effects other than the splitting into two symmetric regimes are negligible in next-to-next-to-leading logarithmic (NNLL) approximation. An alternative method, which also relies on factorization and exponentiation of the logarithmic corrections, is based on soft-collinear effective theory [23]. Using this method, $\ln(Q^2/M_{W,Z}^2)$ corrections to the Sudakov form factor for massless and massive fermions have been calculated and used to compute electroweak corrections to four-fermion processes at the LHC [24, 25]. Alternatively, the electroweak logarithms can be extracted explicitly from Feynman diagrams at two loops [26–32]. Calculations of this type explicitly implement all aspects of electroweak symmetry breaking through the Feynman rules and thus provide a strong check of the results obtained via evolution equations or effective theories.

So far, all existing diagrammatic results are in agreement with the resummation prescriptions. However, up to now only a small subset of logarithms and processes has been computed explicitly at two loops: while the LLs [26] and the angular-dependent subset of the NLLs [27] have been derived for arbitrary processes, complete diagrammatic calculations at (or beyond) the NLL level exist only for matrix elements involving massless external fermions [28–32]. In the literature, no explicit 2-loop NLL calculation exists for reactions involving massive scattering particles.

In this paper we derive the two-loop NLL corrections for general n-fermion processes $f_1 f_2 \rightarrow f_3 \ldots f_n$ involving an arbitrary number of massless and massive fermions, i.e. leptons, light or heavy quarks. We consider the limit where all kinematical invariants are of order $Q^2 \gg M_{W,Z}^2$, and the top mass — as well as the Higgs mass — is of the same order as $M_{W,Z}$. Apart from the top quark all other fermions, including bottom quarks, are treated as massless particles. Soft and collinear singularities from virtual photons are regularized dimensionally and arise as ϵ-poles in $D = 4 - 2\epsilon$ dimensions. For consistency, the same power counting is applied to $\ln(Q^2/M_W^2)$ and $1/\epsilon$ singularities. Thus, in NLL approximation we include all $\epsilon^{-k} \ln^{j-k}(Q^2/M_W^2)$ terms with total power $j = 2, 1$ at one loop and $j = 4, 3$ at two loops. We explicitly show that the photonic singularities can be factorized in a gauge-invariant electromagnetic term, in such a way that the remaining part of the corrections — which is finite, gauge invariant, and does not depend on the scheme adopted to regularize photonic singularities — contains only $\ln(Q^2/M_W^2)$ terms. The divergences contained in the electromagnetic term cancel if real-photon emission is included.

We utilize the technique that we introduced in ref. [32] to derive the NLL two-loop corrections for massless n-fermion processes. This method is based on collinear Ward identities which permit to factorize the soft-collinear contributions from the n-fermion tree-level amplitude and isolate them in process-independent two-loop integrals. The latter are evaluated to NLL accuracy using an automatized algorithm based on the sector-decomposition technique [33] and, alternatively, the method of expansion by regions combined with Mellin-Barnes representations (see ref. [31] and references therein).

The treatment of n-fermion processes that involve massive top quarks implies two new aspects: additional Feynman diagrams resulting from Yukawa interactions, and top-mass terms that render the loop integrals more involved. The latter is the one that requires more effort from the calculational point of view, since every topology has to be evaluated for several different combinations of massive/massless internal and external lines. This part of the calculation was automatized in the framework of the above-mentioned algorithms, thereby doing an important step towards a complete NLL analysis of all processes that involve massive particles. A brief summary of the results presented here was anticipated in ref. [34].

The paper is organized as follows. Section 2 contains definitions and conventions used in the calculation. In section 3 we review the techniques used to extract UV and mass singularities for the case of massless fermion scattering [32] and extend them to the case of massive fermions. The one-loop counterterms and explicit results for the renormalized one-loop amplitude are given in section 4. The complete two-loop results are presented in section 5 including a discussion of the Yukawa-coupling contributions and the two-loop renormalization. Section 6 is devoted to the discussion of our final results. Explicit results for the various contributing one- and two-loop diagrams are presented in appendix A. Further appendices contain the definition of the loop integrals (appendix B) and relations between them (appendix C). Specific results for four-particle processes involving external fermions and gluons, including a comparison with the results of refs. [24, 25], can be found in appendix D.

2. Definitions and conventions

The calculation is based on the formalism introduced in ref. [32] for massless fermion scattering. Here we summarize the most important conventions and introduce new definitions that are needed to describe massive fermions. For more details we refer to section 2 of ref. [32].

We consider a generic $n \rightarrow 0$ process involving an even number n of polarized fermionic particles,

$$\varphi_1(p_1)\dots\varphi_n(p_n) \rightarrow 0. \tag{2.1}$$

The symbols φ_i represent $n/2$ antifermions and $n/2$ fermions: $\varphi_i = \bar{f}^{\kappa_i}_{\sigma_i}$ for $i = 1,\dots,n/2$ and $\varphi_i = f^{\kappa_i}_{\sigma_i}$ for $i = n/2+1,\dots,n$. The indices $\kappa_i = \mathrm{R},\mathrm{L}$ and σ_i characterize the chirality (see below) and the fermion type ($f_{\sigma_i} = \nu_e, e, \dots, \tau, u, d, \dots, t$), respectively. All external momenta are incoming and on shell, $p_k^2 = m_k^2$. Apart from the top quarks, all other fermions (including bottom quarks) are treated as massless particles.

The matrix element for the process (2.1) reads

$$\mathcal{M}^{\varphi_1\dots\varphi_n} = \left[\prod_{i=1}^{n/2} \bar{v}(p_i, \kappa_i)\right] G^{\underline{\varphi}_1\cdots\underline{\varphi}_n}(p_1,\dots,p_n) \left[\prod_{j=n/2+1}^{n} u(p_j, \kappa_j)\right], \tag{2.2}$$

where $G^{\underline{\varphi}_1\cdots\underline{\varphi}_n}$ is the corresponding truncated Green function. The spinors fulfil the Dirac equation,

$$(\not{p} - m)u(p,\kappa) = 0, \qquad (\not{p} + m)v(p,\kappa) = 0, \tag{2.3}$$

and the argument κ denotes their chirality. More precisely, the polarization states $\kappa = \mathrm{R}, \mathrm{L}$ are defined in such a way that in the massless limit the spinors are eigenstates of the chiral projectors

$$\omega_{\mathrm{R}} = \bar{\omega}_{\mathrm{L}} = \frac{1}{2}(1 + \gamma^5), \qquad \omega_{\mathrm{L}} = \bar{\omega}_{\mathrm{R}} = \frac{1}{2}(1 - \gamma^5), \qquad (2.4)$$

i.e.

$$\omega_\rho u(p, \kappa) = \delta_{\kappa\rho} u(p, \kappa) + \mathcal{O}\left(\frac{m}{p^0} u\right), \qquad \omega_\rho v(p, \kappa) = \delta_{\kappa\rho} v(p, \kappa) + \mathcal{O}\left(\frac{m}{p^0} v\right) \qquad (2.5)$$

for $m/p^0 \ll 1$. While massless spinors are exact eigenstates of the chiral projectors, in the massive case the spinors are constructed by means of helicity projectors

$$\Omega_{\mathrm{R}} = \hat{\Omega}_{\mathrm{L}} = \frac{1}{2}(1 + \gamma^5 \not{r}), \qquad \Omega_{\mathrm{L}} = \hat{\Omega}_{\mathrm{R}} = \frac{1}{2}(1 - \gamma^5 \not{r}) \qquad (2.6)$$

where

$$r^\mu = \pm \frac{1}{m}\left(|\vec{p}|, p^0 \frac{\vec{p}}{|\vec{p}|}\right), \qquad \text{for} \quad \mathrm{sign}(p^0) = \pm 1, \qquad (2.7)$$

with $(rp) = 0$, $r^2 = -1$ and

$$\Omega_\rho u(p, \kappa) = \delta_{\kappa\rho} u(p, \kappa), \qquad \hat{\Omega}_\rho v(p, \kappa) = \delta_{\kappa\rho} v(p, \kappa). \qquad (2.8)$$

For $m/p^0 \to 0$, we have $r^\mu \to p^\mu/m$, and the spinors satisfy (2.5) in the high-energy limit. Note that in the case of antifermions, chirality and helicity play the opposite role, and we always use chirality to label the spinors.

The amplitudes for physical scattering processes, i.e. $2 \to n - 2$ reactions, are easily obtained from our results for $n \to 0$ reactions using crossing symmetry.

2.1 Perturbative and asymptotic expansions

For the perturbative expansion of matrix elements we write

$$\mathcal{M} = \sum_{l=0}^{\infty} \mathcal{M}_l, \qquad \mathcal{M}_l = \left(\frac{\alpha_\epsilon}{4\pi}\right)^l \tilde{\mathcal{M}}_l, \qquad \alpha_\epsilon = \left(\frac{4\pi\mu_{\mathrm{D}}^2}{\mathrm{e}^{\gamma_{\mathrm{E}}} Q^2}\right)^\epsilon \alpha, \qquad (2.9)$$

where $\alpha = e^2/(4\pi)$ and in $D = 4 - 2\epsilon$ dimensions we include in the definition of α_ϵ a normalization factor depending on ϵ, the scale μ_{D} of dimensional regularization, and the characteristic energy Q of the scattering process.

The electroweak corrections are evaluated in the region where all kinematical invariants, $r_{j\ldots k} = (p_j + \cdots + p_k)^2$, are much larger than the squared masses of the heavy particles that enter the loops,

$$|r_{j\ldots k}| \sim Q^2 \gg M_{\mathrm{W}}^2 \sim M_{\mathrm{Z}}^2 \sim m_{\mathrm{t}}^2 \sim M_{\mathrm{H}}^2. \qquad (2.10)$$

In this region, the electroweak corrections are dominated by mass-singular logarithms,

$$L = \ln\left(\frac{Q^2}{M_{\mathrm{W}}^2}\right), \qquad (2.11)$$

and logarithms of UV origin. Mass singularities that originate from soft and collinear massless photons and UV singularities are regularized dimensionally and give rise to $1/\epsilon$ poles. The amplitudes are computed as series in L and ϵ, classifying the terms $\epsilon^n L^{m+n}$ according to the total power m of logarithms L and $1/\epsilon$ poles. At l loops, terms with $m = 2l, 2l - 1, \ldots$ are denoted as leading logarithms (LLs), next-to-leading logarithms (NLLs), and so on. The calculation is performed in NLL approximation expanding the one- and two-loop terms up to order ϵ^2 and ϵ^0, respectively,

$$\mathcal{M}_1 \overset{\text{NLL}}{=} \sum_{m=1}^{2} \sum_{n=-m}^{2} \mathcal{M}_{1,m,n}\, \epsilon^n L^{m+n}, \qquad \mathcal{M}_2 \overset{\text{NLL}}{=} \sum_{m=3}^{4} \sum_{n=-m}^{0} \mathcal{M}_{2,m,n}\, \epsilon^n L^{m+n}. \quad (2.12)$$

Since the loop corrections depend on various masses, $M_{\mathrm{W}} \sim M_{\mathrm{Z}} \sim m_{\mathrm{t}} \sim M_{\mathrm{H}}$, and different invariants r_{jk}, the coefficients $\mathcal{M}_{l,m,n}$ in (2.12) involve logarithms of type[1]

$$l_i = \ln\left(\frac{M_i^2}{M_{\mathrm{W}}^2}\right), \qquad l_{jk} = \ln\left(\frac{-r_{jk} - \mathrm{i}0}{Q^2}\right) \quad \text{for } j \neq k. \quad (2.13)$$

For convenience we also define $l_{jj} = 0$ and

$$L_{\mathrm{t}} = \ln\left(\frac{Q^2}{m_{\mathrm{t}}^2}\right). \quad (2.14)$$

To distinguish terms associated with massless and massive fermions we use the symbols

$$\delta_{i,\mathrm{t}} = \left\{ \begin{array}{l} 1,\ m_i = m_{\mathrm{t}} \\ 0,\ m_i = 0 \end{array} \right\}, \qquad \delta_{i,0} = \left\{ \begin{array}{l} 1,\ m_i = 0 \\ 0,\ m_i = m_{\mathrm{t}} \end{array} \right\}. \quad (2.15)$$

Mass-suppressed corrections of order M_{W}^2/Q^2 are systematically neglected.

2.2 Gauge and Yukawa couplings

The generators associated with the gauge bosons $V = A, Z, W^{\pm}$ are related to the weak isospin generators T^i, the hypercharge Y, and the electromagnetic charge Q through

$$eI^{W^{\pm}} = \frac{g_2}{\sqrt{2}}\left(T^1 \pm \mathrm{i}T^2\right), \qquad eI^A = -eQ = -g_2 s_{\mathrm{w}} T^3 - g_1 c_{\mathrm{w}} \frac{Y}{2},$$

$$eI^Z = g_2 c_{\mathrm{w}} T^3 - g_1 s_{\mathrm{w}} \frac{Y}{2} = \frac{g_2}{c_{\mathrm{w}}} T^3 - e \frac{s_{\mathrm{w}}}{c_{\mathrm{w}}} Q, \quad (2.16)$$

where $c_{\mathrm{w}} = \cos\theta_{\mathrm{w}}$ and $s_{\mathrm{w}} = \sin\theta_{\mathrm{w}}$ denote the sine and cosine of the weak mixing angle, and g_1 and g_2 are the coupling constants associated with the U(1) and SU(2) groups, respectively. The generators (2.16) obey the commutation relations

$$e\left[I^{V_1}, I^{V_2}\right] = \mathrm{i}g_2 \sum_{V_3 = A, Z, W^{\pm}} \varepsilon^{V_1 V_2 V_3} I^{\bar{V}_3}, \quad (2.17)$$

---

[1]This dependence only appears at the next-to-leading level, i.e. for $m = 2l - 1$.

where $\bar{V}$ denotes the complex conjugate of V and the ε-tensor is defined in ref. [32]. The SU(2) × U(1) Casimir operator reads
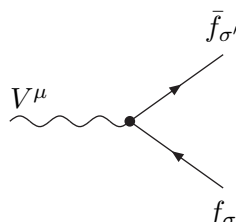
$$\sum_{V=A,Z,W^\pm} I^{\bar{V}} I^V = \frac{g_1^2}{e^2}\left(\frac{Y}{2}\right)^2 + \frac{g_2^2}{e^2} C, \qquad \text{with} \quad C = \sum_{i=1}^3 (T^i)^2. \qquad (2.18)$$

The gauge-boson masses, the vacuum expectation value v, and the couplings fulfil

$$M_{W^\pm} = \frac{1}{2} g_2 v, \qquad M_Z = \frac{1}{2c_W} g_2 v, \qquad c_W = \frac{M_W}{M_Z}, \qquad c_W g_1 Y_\Phi = s_W g_2, \qquad (2.19)$$

where Y_Φ is the hypercharge of the Higgs doublet. Leaving Y_Φ as a free parameter and identifying $e = c_W g_1$, the Gell-Mann-Nishijima relation, which determines the hypercharges of the fermions, reads $Q = Y/2 + Y_\Phi T^3$.

The Feynman rules for the vector-boson-fermion-antifermion vertices read

$$= \mathrm{i} e \gamma^\mu \sum_{\kappa=\mathrm{R,L}} \omega_\kappa I^V_{f^\kappa_{\sigma'} f^\kappa_\sigma}, \qquad (2.20)$$

where $I^V_{f^\kappa_{\sigma'} f^\kappa_\sigma}$ denote the SU(2) × U(1) generators in the fundamental ($\kappa = \mathrm{L}$) or trivial ($\kappa = \mathrm{R}$) representation. The chiral projectors ω_κ in (2.20) can easily be shifted along the fermionic lines using anticommutation relations[2] until they meet the spinor of an external fermion or antifermion and can be eliminated using (2.5).

It is convenient to adopt a notation that describes the interactions of fermions and antifermions in a generic way. To this end, for a generic incoming particle $\varphi_i = f^{\kappa_i}_\sigma$ or $\bar{f}^{\kappa_i}_\sigma$, we define

$$I^V_{\varphi''_i \varphi_i} = \begin{cases} I^V_{f^{\kappa_i}_{\sigma''} f^{\kappa_i}_{\sigma'}} & \text{for} \quad \varphi_i = f^{\kappa_i}_\sigma \\ I^V_{\bar{f}^{\kappa_i}_{\sigma''} \bar{f}^{\kappa_i}_{\sigma'}} = -I^V_{f^{\kappa_i}_{\sigma'} f^{\kappa_i}_{\sigma''}} & \text{for} \quad \varphi_i = \bar{f}^{\kappa_i}_\sigma \end{cases}. \qquad (2.21)$$

With this notation the interaction of a gauge boson V with incoming fermions and antifermions yields

$$\frac{\mathrm{i}(\slashed{p}_i + \slashed{q} + m_i)}{(p_i+q)^2 - m_i^2} \mathrm{i} e \gamma^\mu I^V_{\varphi'_i \varphi_i} u(p_i, \kappa_i) \qquad \text{and} \qquad \bar{v}(p_i, \kappa_i) \mathrm{i} e \gamma^\mu I^V_{\varphi'_i \varphi_i} \frac{\mathrm{i}(\slashed{p}_i + \slashed{q} - m_i)}{(p_i+q)^2 - m_i^2}. \qquad (2.22)$$
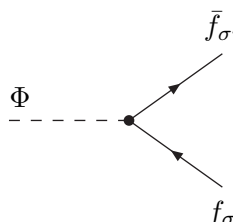
Similar expressions are obtained for multiple gauge-boson interactions. Apart from the spinors and the reversed order of the Dirac matrices, these expressions differ only in the sign of the mass terms in the Dirac propagators.[3] In practice we perform the calculations

---

[2]In the high-energy NLL approximation diagrams involving chiral anomalies are irrelevant. Thus we can use $\{\gamma^\mu, \gamma^5\} = 0$ in $D = 4 - 2\epsilon$ dimensions.

[3]For antifermions the negative sign in the coupling (2.21) compensates the negative sign (of slashed momenta) due to the opposite fermion and momentum flow. This yields $-(-\slashed{p}_i - \slashed{q} + m_i) = (\slashed{p}_i + \slashed{q} - m_i)$.

assuming that certain legs $(i, j, \dots)$ are incoming fermions and we find that the results are independent of the sign of the mass terms in the propagators (only squared mass terms give rise to unsuppressed contributions). Thus, the results are directly applicable to fermions and antifermions.

The Feynman rules for the scalar-fermion-antifermion vertices read

$$= \mathrm{i} \left(\omega_{\mathrm{R}} G^{\Phi}_{f^{\mathrm{L}}_{\sigma'} f^{\mathrm{R}}_{\sigma}} + \omega_{\mathrm{L}} G^{\Phi}_{f^{\mathrm{R}}_{\sigma'} f^{\mathrm{L}}_{\sigma}} \right) , \qquad (2.23)$$

where $\Phi = H, \chi, \phi^{\pm}$. Unitarity implies the following relation between left- and right-handed coupling matrices:

$$G^{\Phi}_{f^{\mathrm{R}}_{\sigma'} f^{\mathrm{L}}_{\sigma}} = \left(G^{\Phi^{+}}_{f^{\mathrm{L}}_{\sigma} f^{\mathrm{R}}_{\sigma'}} \right)^{*}. \qquad (2.24)$$

We consider only contributions proportional to the top-quark Yukawa coupling,

$$\lambda_t = \frac{g_2 m_{\mathrm{t}}}{\sqrt{2} M_{\mathrm{W}}}, \qquad (2.25)$$

and neglect the bottom-quark mass. The non-vanishing components of the right-handed coupling matrix read

$$G^{H}_{t^{\mathrm{L}} t^{\mathrm{R}}} = -\frac{\lambda_t}{\sqrt{2}}, \qquad G^{\chi}_{t^{\mathrm{L}} t^{\mathrm{R}}} = \mathrm{i} \frac{\lambda_t}{\sqrt{2}}, \qquad G^{\phi^{-}}_{b^{\mathrm{L}} t^{\mathrm{R}}} = \lambda_t. \qquad (2.26)$$

In analogy with (2.21), we define

$$G^{\Phi}_{\varphi''_i \varphi'_i} = \begin{cases} G^{\Phi}_{f^{\mathrm{L}}_{\sigma''} f^{\mathrm{R}}_{\sigma'}} & \text{for} \quad \varphi_i = f^{\mathrm{R}}_{\sigma} \\ G^{\Phi}_{\bar{f}^{\mathrm{L}}_{\sigma''} \bar{f}^{\mathrm{R}}_{\sigma'}} = -G^{\Phi}_{f^{\mathrm{R}}_{\sigma'} f^{\mathrm{L}}_{\sigma''}} & \text{for} \quad \varphi_i = \bar{f}^{\mathrm{R}}_{\sigma} \end{cases} , \qquad (2.27)$$

and similarly for $\mathrm{R} \leftrightarrow \mathrm{L}$. With this notation the interaction of a boson Φ with incoming fermions $\varphi_i = f^{\kappa_i}_{\sigma}$ and antifermions $\varphi_i = \bar{f}^{\kappa_i}_{\sigma}$ yields similar expressions as in the case of gauge interactions (2.22),

$$\frac{\mathrm{i}(\not{p}_i + \not{q} + m_i)}{(p_i + q)^2 - m_i^2} \mathrm{i} G^{\Phi}_{\varphi'_i \varphi_i} u(p_i, \kappa_i) \qquad \text{and} \qquad \bar{v}(p_i, \kappa_i) \mathrm{i} G^{\Phi}_{\varphi'_i \varphi_i} \frac{\mathrm{i}(\not{p}_i + \not{q} - m_i)}{(p_i + q)^2 - m_i^2}. \qquad (2.28)$$

In the case of light (anti)fermions ($\varphi_i =$ lepton or quark of the first two generations), the subsequent interaction with gauge bosons V_1, V_2, V_3 yields coupling factors $I^{V_3}_{\varphi'''_i \varphi''_i} I^{V_2}_{\varphi''_i \varphi'_i} I^{V_1}_{\varphi'_i \varphi_i}$, where the representation of all generators I^{V} corresponds to the chirality κ_i given by the spinor of the external particle φ_i [see (2.21)]. For quarks of the third generation ($\varphi_i =$ top or bottom), due to Yukawa interactions and top-mass terms in the fermion propagators, also couplings with opposite chirality contribute. These are denoted as

$$\hat{I}^{V}_{\varphi''_i \varphi'_i} = I^{V}_{\varphi''_i \varphi'_i} \Big|_{\mathrm{R} \leftrightarrow \mathrm{L}}, \qquad \hat{G}^{\Phi}_{\varphi''_i \varphi'_i} = G^{\Phi}_{\varphi''_i \varphi'_i} \Big|_{\mathrm{R} \leftrightarrow \mathrm{L}}. \qquad (2.29)$$

For instance, the subsequent emission of scalars and gauge bosons Φ_1, V_2, Φ_3 along a heavy-quark line yields coupling factors $\hat{G}^{\Phi_3}_{\varphi'''_i \varphi''_i} \hat{I}^{V_2}_{\varphi''_i \varphi'_i} G^{\Phi_1}_{\varphi'_i \varphi_i}$.

In our results the matrix elements (2.2) are often abbreviated as

$$\mathcal{M} \equiv \mathcal{M}^{\varphi_1 \cdots \varphi_n}, \tag{2.30}$$

and when they are multiplied by gauge- and Yukawa-coupling matrices we write

$$\mathcal{M} I^{V_1}_k = \sum_{\varphi'_k} \mathcal{M}^{\varphi_1 \cdots \varphi'_k \cdots \varphi_n} I^{V_1}_{\varphi'_k \varphi_k}, \qquad \mathcal{M} G^{\Phi_1}_k = \sum_{\varphi'_k} \mathcal{M}^{\varphi_1 \cdots \varphi'_k \cdots \varphi_n} G^{\Phi_1}_{\varphi'_k \varphi_k},$$

$$\mathcal{M} G^{\Phi_1}_k I^{V_2}_k = \sum_{\varphi'_k, \varphi''_k} \mathcal{M}^{\varphi_1 \cdots \varphi''_k \cdots \varphi_n} G^{\Phi_1}_{\varphi''_k \varphi'_k} I^{V_2}_{\varphi'_k \varphi_k}, \quad \text{etc.} \tag{2.31}$$

Similar shorthands are used for the coupling matrices (2.29). Global gauge invariance implies the relation

$$\hat{I}^V_k G^{\Phi_i}_k - G^{\Phi_i}_k I^V_k = \sum_{\Phi_j = H, \chi, \phi^\pm} G^{\Phi_j}_k I^V_{\Phi_j \Phi_i} \tag{2.32}$$

between combinations of gauge and Yukawa couplings as well as the charge-conservation identity

$$\mathcal{M} \sum_{k=1}^{n} I^V_k = 0, \tag{2.33}$$

which is fulfilled up to mass-suppressed terms in the high-energy limit. In (2.32), $I^V_{\Phi_j \Phi_i}$ denotes the $\mathrm{SU}(2) \times \mathrm{U}(1)$ generators for the Higgs doublet, which enter the gauge couplings of the Higgs boson.

3. Treatment of ultraviolet and mass singularities

Large logarithms and $1/\epsilon$ poles originate from UV and mass singularities. These contributions can be extracted from one- and two-loop Feynman diagrams within the 't Hooft-Feynman gauge, using the technique introduced in ref. [32]. In section 3.1 we review this method for the case of massless fermion scattering. The new aspects that emerge in the presence of massive fermions are discussed in section 3.2. Finally, in section 3.3, we report on a calculation of the fermionic form factor as a check of the validity of our methods.

3.1 Massless fermions

Here we give a concise summary of the method presented in ref. [32]. For a detailed discussion we refer to the original paper.

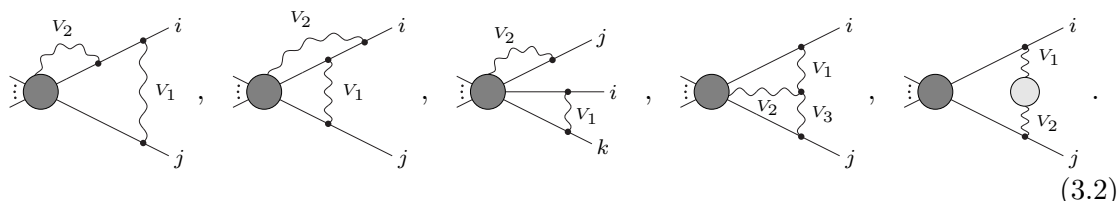#### 3.1.1 Origin of mass singularities

Mass singularities appear in loop diagrams involving soft and/or collinear gauge bosons that couple to external legs. At one loop, the mass singularities of the n-fermion amplitude

originate from diagrams of the type

$$(3.1)$$

where an electroweak gauge boson, $V = A, Z, W^\pm$, couples to one of the external fermions $(i = 1, \ldots, n)$ and to either (i) another external fermion or (ii) an internal propagator. While diagrams of type (ii) produce only single logarithms of collinear origin, diagrams of type (i) give rise to single and double logarithms. The latter originate from the region where the gauge-boson momentum is soft and collinear to one of the external fermions. At two loops, the following five types of diagrams give rise to NLL mass singularities

$$(3.2)$$

Here the NLL mass singularities originate from the regions where the gauge boson V_1 is simultaneously soft and collinear, and the gauge bosons V_2 and V_3 in the first four types of diagrams are soft and/or collinear.

3.1.2 Factorizable and non-factorizable contributions

The soft-collinear NLL contributions resulting from the diagrams (3.1) and (3.2) are split into factorizable and non-factorizable ones. The one- and two-loop factorizable (F) parts result from those diagrams where the virtual gauge bosons couple only to external lines. Including sums over gauge bosons and external legs we have

$$\mathcal{M}_1^{\mathrm{F}} = \frac{1}{2} \sum_{i=1}^{n} \sum_{\substack{j=1 \\ j \neq i}}^{n} \sum_{V=A,Z,W^\pm} \left[\quad \right]_{q^\mu \to x p^\mu}, \qquad (3.3)$$

and

$$\mathcal{M}_2^{\mathrm{F}} = \sum_{i=1}^{n} \sum_{\substack{j=1 \\ j \neq i}}^{n} \sum_{V_m=A,Z,W^\pm} \left\{ \frac{1}{2} \left[\quad + \quad \right] \right.$$

$$\left. + \quad + \quad + \quad + \frac{1}{2} \quad \right.$$

$$+\sum_{\substack{k=1\\k\neq i,j}}^{n}\left[\;\cdots\;\text{F}\underset{V_2}{\overset{V_1}{\diagdown}}\genfrac{}{}{0pt}{}{j}{i}\;+\;\frac{1}{6}\;\cdots\;\text{F}\overset{V_2\,V_1\,V_3}{\diagdown}\genfrac{}{}{0pt}{}{j}{i}\;\right]+\frac{1}{8}\sum_{\substack{k=1\\k\neq i,j}}^{n}\sum_{\substack{l=1\\l\neq i,j,k}}^{n}\;\cdots\;\text{F}\overset{V_1\,V_2}{\diagdown}\left.\genfrac{}{}{0pt}{}{i}{l}\right\}_{q^\mu\to xp^\mu}.$$

$$(3.4)$$

The limit $q^\mu \to xp^\mu$ in (3.3) and (3.4) indicates that the above diagrams are evaluated in the approximation where each of the four-momenta q^μ of the various gauge bosons is collinear to one of the momenta p^μ of the external legs or soft. Where relevant, also the contributions of hard regions are taken into account (see section 3.1.4). The label F in the n-fermion tree subdiagrams in (3.3) and (3.4) indicates that, by definition, the factorizable contributions include only those parts of the above diagrams that are obtained by performing the loop integration with the momenta q_m of the gauge bosons V_m set to zero in the n-fermion tree subdiagrams.

These contributions are called factorizable since their logarithmic soft-collinear singularities factorize from the n-fermion tree amplitude (see below). The remaining contributions are called non-factorizable (NF). They comprise those diagrams of type (3.1) and (3.2) that involve gauge bosons V_i coupling to internal (hard) propagators, and the non-factorizable parts of the diagrams in (3.3) and (3.4). In ref. [32], using collinear Ward identities, it was explicitly shown that all non-factorizable one- and two-loop contributions cancel at the amplitude level.

3.1.3 Soft-collinear approximation

The soft-collinear singularities are extracted from the above Feynman diagrams using the following soft-collinear approximation for the interactions of virtual gauge bosons $V_1 \ldots V_n$ with an incoming (anti)fermion line i

$$\lim_{q_k^\mu\to x_k p_i^\mu}\;\cdots\;i\;=\;\cdots\;i\;\times\;\frac{-2eI_i^{V_n}(p_i+\tilde q_n)^{\mu_n}}{(p_i+\tilde q_n)^2}\cdots\frac{-2eI_i^{V_1}(p_i+q_1)^{\mu_1}}{(p_i+q_1)^2}.$$

$$(3.5)$$

Here q_k are the loop momenta of the gauge bosons V_k, and $\tilde q_k = q_1+\cdots+q_k$. In practice, the coupling of each soft/collinear gauge boson gives rise to a factor $-2eI_i^{V_k}(p_i+\tilde q_k)^\mu$. When applied to the factorizable diagrams in (3.3)–(3.4), this approximation removes all Dirac matrices occuring along the fermionic lines and yields factorized expressions of the form

$$\mathcal{M}_{1,2}^{\mathrm{F}} = \mathcal{M}_0\, K_{1,2}, \tag{3.6}$$

where the NLL corrections $K_{1,2}$, involving coupling factors and logarithmically divergent loop integrals, factorize from the n-fermion tree amplitude $\mathcal{M}_0$.

As discussed in ref. [32], the soft-collinear approximation (3.5) provides a correct description of the gauge-boson-fermion couplings in all soft/collinear regions that are relevant

for an NLL analysis at one and two loops, with the following exception: The soft-collinear approximation is not applicable to topologies of type

which contain UV singularities associated with a subdiagram with characteristic scale $\mu_{\mathrm{loop}}^2 \ll Q^2$ (see next section) or give rise to power singularities of $\mathcal{O}(1/M^2)$. For these diagrams, the soft-collinear approximation (3.5) can be applied only to the vertices that occur outside the one-loop subdiagrams that are depicted as grey blobs in (3.7), whereas for the vertices and propagators inside the one-loop subdiagrams we have to apply the usual Feynman rules.

To bring these diagrams in the factorized form (3.6), we have to simplify the Dirac matrices along the fermionic lines where the soft-collinear approximation is not applicable. To this end we utilize trace projectors that reduce these Dirac matrices to scalar quantities. In practice, for the second and third diagram in (3.7), the Dirac matrices along the line i are eliminated using [32]

$$X u(p_i, \kappa_i) = \sum_\rho \omega_\rho \Pi_{ij} \left(\omega_\rho X \right) u(p_i, \kappa_i) = \Pi_{ij} \left(\omega_{\kappa_i} X \right) u(p_i, \kappa_i), \qquad (3.8)$$

where X represents the diagram without $\vdots\!\!\text{F}$ and external spinors, and the projector is defined as

$$\Pi_{ij} \left(\Gamma \right) = \frac{1}{2 p_i p_j} \, \mathrm{Tr} \left[\Gamma \not{p}_i \not{p}_j \right] \qquad (3.9)$$

if $m_i = m_j = 0$. For a detailed discussion we refer to section 3.2 of ref. [32].

3.1.4 Treatment of ultraviolet singularities

In addition to logarithmic soft-collinear singularities, also the logarithms originating from UV singularities need to be taken into account. Moreover, the soft-collinear approximation (3.5) can give rise to fake UV logarithms that must carefully be avoided or subtracted.

Since UV singularities produce only a single logarithm per loop, in NLL approximation we need to consider only UV-divergent diagrams of one-loop order and their insertion in one-loop diagrams (3.3) involving leading soft-collinear singularities. The UV logarithms originate from the UV cancellations between bare diagrams and counterterms as

$$\left(\frac{\mu_{\mathrm{D}}^2}{Q^2} \right)^\epsilon \left[\underbrace{\frac{1}{\epsilon} \left(\frac{Q^2}{\mu_{\mathrm{loop}}^2} \right)^\epsilon}_{\text{bare diagrams}} - \underbrace{\frac{1}{\epsilon} \left(\frac{Q^2}{\mu_{\mathrm{R}}^2} \right)^\epsilon}_{\text{counterterms}} \right] = \ln \left(\frac{\mu_{\mathrm{R}}^2}{\mu_{\mathrm{loop}}^2} \right) + \mathcal{O}(\epsilon), \qquad (3.10)$$

where μ_{loop} is the characteristic scale of the UV-singular loop diagram, μ_{R} is the renormalization scale, and the term $\left(\mu_{\mathrm{D}}^2 / Q^2 \right)^\epsilon$ — that we always absorb in α_ϵ [see (2.9)] — is

factorized. In our calculation, the UV poles of bare loop diagrams and counterterms are removed by means of a minimal subtraction at the scale Q^2. As a result, the UV divergent terms take the form

$$\left(\frac{\mu_{\rm D}^2}{Q^2}\right)^\epsilon \left\{ \underbrace{\frac{1}{\epsilon}\left[\left(\frac{Q^2}{\mu_{\rm loop}^2}\right)^\epsilon - 1\right]}_{\text{bare diagrams}} - \underbrace{\frac{1}{\epsilon}\left[\left(\frac{Q^2}{\mu_{\rm R}^2}\right)^\epsilon - 1\right]}_{\text{counterterms}} \right\}, \tag{3.11}$$

which is obviously equivalent to (3.10). The advantage of this subtraction is that for all bare (sub)diagrams with $\mu_{\rm loop}^2 \sim Q^2$ the UV singularities $\epsilon^{-1}[(Q^2/\mu_{\rm loop}^2)^\epsilon - 1]$ do not produce large logarithms and are thus negligible. This holds also for fake UV singularities resulting from the soft-collinear approximation. Thus, apart from the counterterms, we must consider only those (subtracted) UV contributions that originate from bare (sub)diagrams with $\mu_{\rm loop}^2 \ll Q^2$. At one loop this condition is never realized in the high-energy limit (2.10), and in practice we need to consider only the two-loop UV contributions which result from the diagrams in (3.3) through insertion of UV-divergent subdiagrams in the lines that are not hard ($\mu_{\rm loop}^2 \ll Q^2$). These contributions correspond to the diagrams depicted in (3.7), for which we use — instead of the soft-collinear approximation — the projectors (3.8)–(3.9), thereby ensuring a correct description of the UV regions.

3.2 Massive fermions

The method outlined in section 3.1 is applicable also to processes involving external top and/or bottom quarks. However, in the presence of massive fermions, two new aspects must be taken into account: mass terms in the top-quark propagators and new diagrams resulting from Yukawa interactions.

3.2.1 Top-mass terms

Let us recall that, in the high-energy limit (2.10), the top-quark mass is treated as a small parameter and terms of $\mathcal{O}(\text{NLL} \times m_{\rm t}/Q)$ are systematically neglected. In this approximation, only the following types of $m_{\rm t}$-terms must be considered:

(i) Yukawa couplings proportional to $m_{\rm t}/M_{\rm W}$;

(ii) $m_{\rm t}$-terms acting as collinear regulators in the denominator of propagators;

(iii) $m_{\rm t}$-terms in the numerator of loop integrals of $\mathcal{O}(\text{NLL}/m_{\rm t})$ or $\mathcal{O}(\text{NLL}/M_{\rm W,Z,H})$, i.e. integrals that involve power singularities.

The majority of the $m_{\rm t}$-terms occuring in one- and two-loop diagrams does not belong to these categories and can be set to zero. In particular, by explicit inspection of the relevant one- and two-loop integrals, we find that $m_{\rm t}$-terms of type (iii) occur only inside the one-loop insertions in the diagrams (3.7). Apart from these special cases all other $m_{\rm t}$-terms in the numerators of loop integrals can be set to zero.

3.2.2 NLL contributions from gauge interactions

As in the case of massless fermion scattering, the diagrams (3.1)–(3.2) with external-leg interactions of soft/collinear gauge bosons produce logarithmic mass singularities. These diagrams are split into factorizable and non-factorizable parts as discussed in section 3.1.2 and, in the presence of massive fermions, the Ward identities that are responsible for the cancellation of the non-factorizable contributions [32] receive only negligible corrections of $\mathcal{O}(m_t/Q)$. Thus, as in the case of massless fermions, the non-factorizable parts do not contribute and we can restrict ourselves to the calculation of the factorizable parts (3.3) and (3.4).

The soft-collinear approximation (3.5) can easily be adapted to massive fermions by including the m_t-terms in the denominator of the top-quark propagators and leaving the numerator as in the massless case. In principle m_t-terms modify also the numerator of (3.5). However, as observed above, such terms are relevant only in the one-loop insertion diagrams in (3.7). Here, as discussed in section 3.1.3, we employ the usual Feynman rules — and not the soft-collinear approximation — due to the presence of UV divergences or power singularities of $\mathcal{O}(1/M^2)$.

To bring the diagrams of type (3.7) in the factorized form (3.6), we utilize projections analogous to (3.8). In the case of massive fermions, using the two projectors

$$\Pi_{ij}\left(\Gamma\right) = \frac{2p_i p_j}{(2p_i p_j)^2 - 4m_i^2 m_j^2} \operatorname{Tr}\left[\Gamma(\not{p}_i + m_i)\left(\not{p}_j - \frac{m_i m_j^2}{p_i p_j}\right)\right] \tag{3.12}$$

and

$$\tilde{\Pi}_{ij}\left(\Gamma\right) = \frac{2p_i p_j}{(2p_i p_j)^2 - 4m_i^2 m_j^2} \operatorname{Tr}\left[\Gamma(\not{p}_i + m_i)\left(1 - \frac{\not{p}_i \not{p}_j}{p_i p_j}\right)\right] \tag{3.13}$$

we obtain

$$Xu(p_i,\kappa_i) = \sum_\rho \omega_\rho \left[\Pi_{ij}\left(\omega_\rho X\right) + \tilde{\Pi}_{ij}\left(\omega_\rho X\right)\not{p}_j\right] u(p_i,\kappa_i). \tag{3.14}$$

Here, in contrast to the massless case, the Dirac matrices are not projected out completely and a term proportional to $\tilde{\Pi}_{ij}(\omega_\rho X)\not{p}_j$ remains, which cannot be cast in the factorized form (3.6). However, after explicit evaluation of the loop integration, we find that these $\tilde{\Pi}_{ij}$-terms are suppressed in the high-energy limit and only the factorizable terms associated with the projector Π_{ij} contribute.

The projectors (3.12)–(3.14) are applicable in the case where particle i is an incoming fermion. For antifermions similar projectors can be constructed, which differ only in the sign of the m_i-terms. As discussed in section 2.2, this difference is irrelevant since only squared mass terms produce NLL contributions. Thus, the results derived for fermions are directly applicable to antifermions.

All logarithms of UV origin — also in the presence of Yukawa interactions — are treated by means of a minimal subtraction at the scale Q^2 as explained in section 3.1.4.

3.2.3 NLL contributions from Yukawa interactions

The interaction of external bottom or top legs with scalar bosons is suppressed in all soft/collinear regions. Thus, Yukawa interactions can produce NLL contributions only through the counterterms (see section 4.1) and the topologies of type (3.7), which contain UV singularities or power singularities of $\mathcal{O}(1/M^2)$. In addition to the diagrams of type (3.7) that are present in the massless case, the following new bare diagrams must be taken into account:

$$
\mathcal{M}_2^{\mathrm{Yuk}} = \sum_{i=1}^{n} \sum_{\substack{j=1 \\ j \neq i}}^{n} \sum_{V_m = A, Z, W^{\pm}} \sum_{\Phi_l = H, \chi, \phi^{\pm}} \left\{ \begin{array}{c} \end{array} \right. \quad + \quad \cdots
$$

$$
\left. + \quad \cdots \quad + \quad \cdots \quad + \quad \cdots \right\} . \tag{3.15}
$$

By explicit inspection we find that the last two diagrams in (3.15) are suppressed in NLL accuracy since the $VV\Phi$ couplings of $\mathcal{O}(M_{\mathrm{W,Z}})$ are not compensated by $1/M$ terms from the loop integrals. The NLL terms resulting from the first three diagrams in (3.15) are worked out in section 5.1.

3.3 Form-factor checks

When evaluating the factorizable contributions of arbitrary n-fermion processes, we have to eliminate the Dirac matrices along the fermionic lines in order to separate the loop integrals from the tree amplitude $\mathcal{M}_0$. For this purpose we use the soft-collinear approximation for gauge interactions presented in section 3.1.3 and the fact that the Yukawa interactions are suppressed in all soft/collinear regions (see section 3.2.3).

We have checked the validity of this procedure for the case of the form factor which couples a fermion-antifermion pair to an external Abelian field. In our approach, the radiative corrections to this form factor are given by the factorizable contributions (3.3), (3.4), and (3.15) with $n = 2$ external fermions (in this case the diagrams with three and four legs in (3.4) do not contribute). Alternatively, we have calculated the one- and two-loop corrections to the form factor in the high-energy limit including all Feynman diagrams, without neglecting m_{t}-terms in the numerator, and employing projection techniques (see e.g. ref. [35]) instead of the soft-collinear approximation. After performing the minimal subtraction of the UV divergences as explained in section 3.1.4, the results of the complete form-factor calculation agree with the ones resulting from the factorizable contributions (3.3), (3.4), and (3.15) in soft-collinear approximation. We have also verified by explicit evaluation that, as expected from the discussion in section 3.2.3, the form-factor diagrams with Yukawa interactions that are not included in (3.15) are either suppressed or

vanish in NLL accuracy. Two of these additional Yukawa diagrams[4] yield non-vanishing NLL contributions which are, however, of pure UV origin and are completely removed by the minimal UV subtraction.

4. One-loop results

The one-loop amplitude gets contributions from the factorizable one-loop diagrams (3.3) and from counterterms,

$$\tilde{\mathcal{M}}_1 = \tilde{\mathcal{M}}_1^{\mathrm{F}} + \tilde{\mathcal{M}}_1^{\mathrm{CT}}. \tag{4.1}$$

The results for the loop diagrams are summarized in appendix A.1. Here we discuss the one-loop renormalization and list the final results for the renormalized one-loop amplitude. As shown in ref. [16] the one-loop NLL corrections factorize, i.e. they can be expressed through correction factors that multiply the Born amplitude. Moreover, they can be split in a symmetric-electroweak part, an electromagnetic part, which in particular contains all soft/collinear singularities associated with photons, and an M_{Z}-dependent part that results from the difference in the W- and Z-boson masses. This splitting permits to separate the soft/collinear singularities resulting from photons in a gauge-invariant way and is very important in view of the discussion of the two-loop contributions.

4.1 One-loop renormalization

As discussed in ref. [32], mass renormalization is not relevant in NLL approximation. Thus, counterterm contributions result only from the renormalization of the electroweak gauge couplings and the top-quark Yukawa coupling,

$$g_{k,0} = g_k + \sum_{l=1}^{\infty} \left(\frac{\alpha_\epsilon}{4\pi} \right)^l \delta g_k^{(l)}, \quad e_0 = e + \sum_{l=1}^{\infty} \left(\frac{\alpha_\epsilon}{4\pi} \right)^l \delta e^{(l)}, \quad \lambda_{t,0} = \lambda_t + \sum_{l=1}^{\infty} \left(\frac{\alpha_\epsilon}{4\pi} \right)^l \delta \lambda_t^{(l)}, \tag{4.2}$$

and from the renormalization constants associated with the wave functions of the external fermions $i = 1, \ldots, n$,

$$Z_i = 1 + \sum_{l=1}^{\infty} \left(\frac{\alpha_\epsilon}{4\pi} \right)^l \delta Z_i^{(l)}. \tag{4.3}$$

All couplings are renormalized in the $\overline{\mathrm{MS}}$ scheme, but we moreover subtract the UV singularities both in the bare and the counterterm contributions as explained in section 3.1.4. The counterterm for the Yukawa coupling can be determined from the divergent parts of the counterterms to g_2, M_{W} and m_{t} using tree-level relations. Assuming that the renormalization scale[5] μ_{R} is of the order of or larger than M_{W}, we find for the counterterms

$$\delta g_k^{(1)} \stackrel{\mathrm{NLL}}{=} -\frac{g_k}{2} \frac{1}{\epsilon} b_k^{(1)} \left[\left(\frac{Q^2}{\mu_{\mathrm{R}}^2} \right)^\epsilon - 1 \right], \qquad \delta e^{(1)} \stackrel{\mathrm{NLL}}{=} -\frac{e}{2} \frac{1}{\epsilon} b_e^{(1)} \left[\left(\frac{Q^2}{\mu_{\mathrm{R}}^2} \right)^\epsilon - 1 \right],$$

$$\delta \lambda_t^{(1)} \stackrel{\mathrm{NLL}}{=} -\frac{\lambda_t}{2} \frac{1}{\epsilon} b_{\lambda_t}^{(1)} \left[\left(\frac{Q^2}{\mu_{\mathrm{R}}^2} \right)^\epsilon - 1 \right], \tag{4.4}$$

---

[4]These are the one-loop diagram (A.2) with the gauge boson V_1 replaced by a scalar boson and the two-loop diagram (A.7) with the gauge boson V_2 replaced by a scalar boson.

[5]We do not identify the renormalization scale μ_{R} and the scale of dimensional regularization μ_{D}.

where the dependence on the factor $(Q^2/\mu_{\mathrm{R}})^\epsilon$ is due to the normalization of the expansion parameter α_ϵ in (4.2), and the one-loop β-function coefficients in the electroweak Standard Model ($Y_\Phi = 1$) are given by

$$b_1^{(1)} = -\frac{41}{6c_{\mathrm{W}}^2}, \qquad b_2^{(1)} = \frac{19}{6s_{\mathrm{W}}^2}, \qquad b_e^{(1)} = -\frac{11}{3}, \qquad b_{\lambda_t}^{(1)} = \frac{9}{4s_{\mathrm{W}}^2} + \frac{17}{12c_{\mathrm{W}}^2} - \frac{9m_{\mathrm{t}}^2}{4s_{\mathrm{W}}^2 M_{\mathrm{W}}^2}. \quad (4.5)$$

For later convenience we also define the QED β-function coefficient, which is determined by the light-fermion contributions only,

$$b_{\mathrm{QED}}^{(1)} = -\frac{4}{3} \sum_{f \neq t} N_{\mathrm{c}}^f Q_f^2 = -\frac{80}{9}, \quad (4.6)$$

where N_{c}^f represents the colour factor, i.e. $N_{\mathrm{c}}^f = 1$ for leptons and $N_{\mathrm{c}}^f = 3$ for quarks. The renormalization of the mixing parameters c_{W} and s_{W} can be determined via (2.19) from the renormalization of the coupling constants.

The contribution of the counterterms (4.4) can easily be absorbed into the Born amplitude

$$\mathcal{M}_0(Q^2) \equiv \mathcal{M}_0 \Big|_{g_k = g_k(Q^2),\, e = e(Q^2),\, \lambda_t = \lambda_t(Q^2)} \quad (4.7)$$

via the running couplings

$$g_k^2(Q^2) \overset{\mathrm{NLL}}{=} g_k^2(\mu_{\mathrm{R}}^2) \left\{ 1 - \frac{\alpha_\epsilon}{4\pi} b_k^{(1)} \frac{1}{\epsilon} \left[\left(\frac{Q^2}{\mu_{\mathrm{R}}^2} \right)^\epsilon - 1 \right] \right\} = g_k^2(\mu_{\mathrm{R}}^2) \left\{ 1 - \frac{\alpha_\epsilon}{4\pi} b_k^{(1)} \ln\left(\frac{Q^2}{\mu_{\mathrm{R}}^2} \right) + \mathcal{O}(\epsilon) \right\},$$

$$e^2(Q^2) \overset{\mathrm{NLL}}{=} e^2(\mu_{\mathrm{R}}^2) \left\{ 1 - \frac{\alpha_\epsilon}{4\pi} b_e^{(1)} \frac{1}{\epsilon} \left[\left(\frac{Q^2}{\mu_{\mathrm{R}}^2} \right)^\epsilon - 1 \right] \right\} = e^2(\mu_{\mathrm{R}}^2) \left\{ 1 - \frac{\alpha_\epsilon}{4\pi} b_e^{(1)} \ln\left(\frac{Q^2}{\mu_{\mathrm{R}}^2} \right) + \mathcal{O}(\epsilon) \right\}, \quad (4.8)$$

$$\lambda_t^2(Q^2) \overset{\mathrm{NLL}}{=} \lambda_t^2(\mu_{\mathrm{R}}^2) \left\{ 1 - \frac{\alpha_\epsilon}{4\pi} b_{\lambda_t}^{(1)} \frac{1}{\epsilon} \left[\left(\frac{Q^2}{\mu_{\mathrm{R}}^2} \right)^\epsilon - 1 \right] \right\} = \lambda_t^2(\mu_{\mathrm{R}}^2) \left\{ 1 - \frac{\alpha_\epsilon}{4\pi} b_{\lambda_t}^{(1)} \ln\left(\frac{Q^2}{\mu_{\mathrm{R}}^2} \right) + \mathcal{O}(\epsilon) \right\}.$$

For practical applications one can use $\overline{\mathrm{MS}}$ input parameters at the scale $\mu_{\mathrm{R}} = M_{\mathrm{Z}}$, or alternatively the on-shell input parameters $\alpha(M_{\mathrm{Z}})$, M_{Z} and M_{W}, or the G_μ input scheme. These different schemes are based on input parameters at the electroweak scale and are thus equivalent in NLL approximation. In the following we express all one- and two-loop results in terms of the Born amplitude at the scale Q^2. The notation $\mathcal{M}_0(Q^2)$ emphasizes the fact that the Born amplitude implicitly depends on logarithms $\ln(Q^2/\mu_{\mathrm{R}}^2)$ via the running of the couplings.

In this setup, the only one-loop NLL counterterm contribution arises from the on-shell wave-function renormalization constants $\delta Z_i^{(1)}$ for the fermionic external legs. All legs receive contributions from massive weak bosons, whereas the photonic contribution to the counterterm for massless external fermions vanishes owing to a cancellation between UV and mass singularities within dimensional regularization. The legs with top or bottom

quarks additionally get Yukawa contributions. After subtraction of the UV poles we find

$$\delta Z_i^{(1)} \overset{\mathrm{NLL}}{=} -\frac{1}{\epsilon} \left\{ \sum_{V=Z,W^\pm} I_i^{\bar{V}} I_i^V \left[\left(\frac{Q^2}{M_V^2} \right)^\epsilon - 1 \right] + I_i^A I_i^A \left[3\delta_{i,\mathrm{t}} \left(\frac{Q^2}{m_\mathrm{t}^2} \right)^\epsilon - 1 \right] \right.$$
$$\left. + z_i^{\mathrm{Y}} \frac{\lambda_t^2}{2e^2} \left[\left(\frac{Q^2}{m_\mathrm{t}^2} \right)^\epsilon - 1 \right] \right\}. \tag{4.9}$$

The Kronecker symbol $\delta_{i,\mathrm{t}}$ is defined in (2.15). Compared with the massless case two extra terms appear, one related to the massive top quark in photonic diagrams and one originating from the Yukawa couplings. The Yukawa factors z_i^{Y} are obtained from

$$\sum_{\Phi=H,\chi,\phi^\pm} \hat{G}_i^{\Phi^+} G_i^\Phi = z_i^{\mathrm{Y}} \lambda_t^2 \tag{4.10}$$

and read

$$z_i^{\mathrm{Y}} = \begin{cases} 1, & \text{for left-handed third-generation quarks } \varphi_i = t^\mathrm{L}, \bar{t}^\mathrm{L}, b^\mathrm{L}, \bar{b}^\mathrm{L}, \\ 2, & \text{for right-handed top quarks}, \varphi_i = t^\mathrm{R}, \bar{t}^\mathrm{R}, \\ 0, & \text{otherwise.} \end{cases} \tag{4.11}$$

Finally, the one-loop counterterm for a process with n external fermions in NLL approximation is obtained as

$$\tilde{\mathcal{M}}_1^{\mathrm{CT}} = \mathcal{M}_0(Q^2) \sum_{i=1}^n \frac{1}{2} \delta Z_i^{(1)}. \tag{4.12}$$

4.2 Renormalized one-loop amplitude

Inserting the results from (A.5), (A.6) and (4.9)–(4.12) into (4.1), we can write for the renormalized one-loop matrix element for a process with n external fermions

$$\tilde{\mathcal{M}}_1 \overset{\mathrm{NLL}}{=} \mathcal{M}_0(Q^2) \left[F_1^{\mathrm{sew}} + \Delta F_1^{\mathrm{em}} + \Delta F_1^{\mathrm{Z}} \right]. \tag{4.13}$$

Here the corrections are split into a symmetric-electroweak (sew) part,

$$F_1^{\mathrm{sew}} \overset{\mathrm{NLL}}{=} -\frac{1}{2} \sum_{i=1}^n \sum_{\substack{j=1 \\ j \neq i}}^n \sum_{V=A,Z,W^\pm} I_i^{\bar{V}} I_j^V \, I(\epsilon, M_\mathrm{W}; p_i, p_j) - \frac{\lambda_t^2}{4e^2} C(m_\mathrm{t}) \sum_{i=1}^n z_i^{\mathrm{Y}}, \tag{4.14}$$

which is obtained by setting the masses of all gauge bosons, A, Z and $\mathrm{W}^\pm$, equal to M_W everywhere, an electromagnetic (em) part

$$\Delta F_1^{\mathrm{em}} = -\frac{1}{2} \sum_{i=1}^n \sum_{\substack{j=1 \\ j \neq i}}^n I_i^A I_j^A \, \Delta I(\epsilon, 0; p_i, p_j), \tag{4.15}$$

resulting from the mass gap between the W boson and the massless photon, and an M_Z-dependent part

$$\Delta F_1^{\mathrm{Z}} = -\frac{1}{2} \sum_{i=1}^n \sum_{\substack{j=1 \\ j \neq i}}^n I_i^Z I_j^Z \, \Delta I(\epsilon, M_\mathrm{Z}; p_i, p_j), \tag{4.16}$$

describing the effect that results from the difference between M_W and M_Z. The functions

$$\Delta I(\epsilon, m; p_i, p_j) = I(\epsilon, m; p_i, p_j) - I(\epsilon, M_W; p_i, p_j), \tag{4.17}$$

which are associated with the exchange of gauge bosons of mass m, describe the effect resulting from the difference between m and M_W.

We have expressed the large logarithms in the Yukawa contribution

$$C(m_t) \overset{\text{NLL}}{=} L_t + \frac{1}{2}L_t^2\epsilon + \frac{1}{6}L_t^3\epsilon^2 + \mathcal{O}(\epsilon^3), \tag{4.18}$$

which originates only from the counterterm (4.9), through their natural scale m_t in $L_t = \ln(Q^2/m_t^2)$, while all the gauge-interaction contributions are written in terms of $L = \ln(Q^2/M_W^2)$ as usual. In order to build squared one-loop expressions to order ϵ^0, which enter the two-loop amplitude, we need to expand all one-loop terms up to order ϵ^2. For the functions I and ΔI we obtain

$$I(\epsilon, M_W; p_i, p_j) \overset{\text{NLL}}{=} -L^2 - \frac{2}{3}L^3\epsilon - \frac{1}{4}L^4\epsilon^2 + (3 - 2l_{ij})\left(L + \frac{1}{2}L^2\epsilon + \frac{1}{6}L^3\epsilon^2\right) + \mathcal{O}(\epsilon^3),$$

$$\Delta I(\epsilon, M_Z; p_i, p_j) \overset{\text{NLL}}{=} l_Z\left(2L + 2L^2\epsilon + L^3\epsilon^2\right) + \mathcal{O}(\epsilon^3),$$

$$\Delta I(\epsilon, 0; p_i, p_j) \overset{\text{NLL}}{=} (\delta_{i,0} + \delta_{j,0})\left(-\epsilon^{-2} + \frac{1}{2}L^2 + \frac{1}{3}L^3\epsilon + \frac{1}{8}L^4\epsilon^2\right) + (\delta_{i,t} + \delta_{j,t})\left(L\epsilon^{-1} + L^2\right.$$

$$\left. + \frac{1}{2}L^3\epsilon + \frac{1}{6}L^4\epsilon^2\right) + \left[2l_{ij} - \frac{3}{2}(\delta_{i,0} + \delta_{j,0}) - \delta_{i,t}(1 + l_i)\right.$$

$$\left. - \delta_{j,t}(1 + l_j)\right]\left(\epsilon^{-1} + L + \frac{1}{2}L^2\epsilon + \frac{1}{6}L^3\epsilon^2\right) + \mathcal{O}(\epsilon^3). \tag{4.19}$$

Only the function $\Delta I(\epsilon, 0; p_i, p_j)$, which incorporates the interactions with massless photons, depends on the fermion masses m_i through the symbols $\delta_{i,0}$ and $\delta_{i,t}$ defined in (2.15). The functions $I(\epsilon, M_W; p_i, p_j)$ and $\Delta I(\epsilon, M_Z; p_i, p_j)$, which correspond to the exchange of massive gauge bosons, are independent of the fermion masses and agree with the results for massless fermions in ref. [32].

The functions I and ΔI are symmetric with respect to an exchange of the external legs i, j, and apart from the angular-dependent l_{ij}-terms, the dependence on p_i and p_j can be separated:

$$I(\epsilon, m; p_i, p_j)\Big|_{l_{ij}=0} = \frac{1}{2}\left[I(\epsilon, m; p_i, p_i) + I(\epsilon, m; p_j, p_j)\right], \tag{4.20}$$

where $l_{ii} = l_{jj} = 0$ is understood. Under the sums over i, j in (4.13)–(4.16) we can replace $I(\epsilon, m; p_j, p_j) \to I(\epsilon, m; p_i, p_i)$, use the charge-conservation identity (2.33) and write

$$\mathcal{M}_0(Q^2) \sum_{i=1}^{n} \sum_{\substack{j=1 \\ j \neq i}}^{n} I_i^{\bar{V}} I_j^V\, I(\epsilon, M_V; p_i, p_j)\Bigg|_{l_{ij}=0} = -\mathcal{M}_0(Q^2) \sum_{i=1}^{n} I_i^V I_i^{\bar{V}}\, I(\epsilon, M_V; p_i, p_i),$$

$$\tag{4.21}$$

and similarly for ΔI. This relation turns out to be useful later.

5. Two-loop results

The renormalized two-loop matrix element gets contributions from the factorizable two-loop diagrams (3.4) and (3.15), from wave-function renormalization, and from parameter renormalization,

$$\tilde{\mathcal{M}}_2 = \tilde{\mathcal{M}}_2^{\mathrm{F}} + \mathcal{M}_2^{\mathrm{Yuk}} + \tilde{\mathcal{M}}_2^{\mathrm{WF}} + \tilde{\mathcal{M}}_2^{\mathrm{PR}}. \tag{5.1}$$

The results for the two-loop diagrams (3.4), which involve only gauge interactions, are summarized in appendix A.2. Here we first show that the Yukawa contribution of the factorizable two-loop diagrams in (3.15) vanishes in NLL accuracy. Then we list the two-loop renormalization contributions and finally combine the factorizable contributions from two-loop diagrams with gauge interactions and the renormalization contributions into the complete renormalized two-loop amplitude.

As discussed in section 3, the NLL corrections factorize, i.e. they can be expressed through correction factors that multiply the Born amplitude. Moreover, as we show, the two-loop correction factors can be expressed entirely in terms of one-loop quantities.

5.1 Two-loop Yukawa contributions

As explained in section 3.2.3, the only non-suppressed NLL contributions involving Yukawa interactions, apart from counterterms, arise from the first three diagrams in (3.15),

$$\mathcal{M}_2^{\mathrm{Yuk}} \stackrel{\mathrm{NLL}}{=} \sum_{i=1}^{n} \sum_{\substack{j=1 \\ j \neq i}}^{n} \sum_{V_1=A,Z,W^\pm} \sum_{\Phi_2=H,\chi,\phi^\pm} \left\{ + \right.$$

$$\left. + \sum_{\Phi_3=H,\chi,\phi^\pm} \right\}. \tag{5.2}$$

The evaluation of these three diagrams is presented in section A.3. In NLL approximation we find that, up to a minus sign, the integral functions associated with the three individual diagrams equal each other, and combining all diagrams we get

$$\mathcal{M}_2^{\mathrm{Yuk}} \stackrel{\mathrm{NLL}}{=} -\frac{1}{e^2} \mathcal{M}_0 \sum_{i=1}^{n} \sum_{\substack{j=1 \\ j \neq i}}^{n} \sum_{V_1=A,Z,W^\pm} \sum_{\Phi_2=H,\chi,\phi^\pm} D_{\mathrm{Y}}(M_{V_1}; p_i, p_j) \, I_j^{\bar{V}_1} \hat{G}_i^{\Phi_2^+}$$

$$\times \left\{ G_i^{\Phi_2} I_i^{V_1} - \hat{I}_i^{V_1} G_i^{\Phi_2} + \sum_{\Phi_3=H,\chi,\phi^\pm} G_i^{\Phi_3} I_{\Phi_3\Phi_2}^{V_1} \right\} = 0, \tag{5.3}$$

where the result for the function D_{Y} is given in (A.53). Owing to global gauge invariance the combination of gauge and Yukawa couplings in the curly brackets of (5.3) vanishes [cf. (2.32)], so the only two-loop NLL contributions from Yukawa interactions originate from

the wave-function counterterms discussed in section 5.2. This observation confirms the prediction of refs. [24, 25], where in soft-collinear effective theory at scales below Q scalar particles contribute only via wave-function renormalization.

5.2 Two-loop renormalization

At two loops, the mass renormalization leads to non-suppressed logarithmic terms only through the insertion of the one-loop mass counterterms in the one-loop logarithmic corrections. However, these contributions are of NNLL order and can thus be neglected in NLL approximation. In this approximation also the purely two-loop counterterms that are associated with the renormalization of the external-fermion wave functions and the couplings, i.e. $\delta Z_i^{(2)}$, $\delta g_k^{(2)}$, $\delta e^{(2)}$ and $\delta\lambda_t^{(2)}$, do not contribute.

The only NLL two-loop counterterm contributions are those that result from the combination of the one-loop amplitude with the one-loop counterterms $\delta Z_i^{(1)}$, $\delta g_k^{(1)}$, $\delta e^{(1)}$ and $\delta\lambda_t^{(1)}$. The wave-function counterterms yield

$$\tilde{\mathcal{M}}_2^{\mathrm{WF}} = \tilde{\mathcal{M}}_1^{\mathrm{F}} \sum_{i=1}^n \frac{1}{2}\delta Z_i^{(1)}. \tag{5.4}$$

The unrenormalized one-loop amplitude $\tilde{\mathcal{M}}_1^{\mathrm{F}}$ and the wave-function renormalization constants $\delta Z_i^{(1)}$ are given in (A.5) and (4.9), respectively. In NLL approximation only the LL part of $\tilde{\mathcal{M}}_1^{\mathrm{F}}$ contributes to (5.4). At this level of accuracy, the unrenormalized amplitude $\tilde{\mathcal{M}}_1^{\mathrm{F}}$ and the renormalized amplitude $\tilde{\mathcal{M}}_1$ (4.13) are equal, and we can use (4.21) in order to write $\tilde{\mathcal{M}}_1^{\mathrm{F}}$ and $\delta Z_i^{(1)}$ such that all gauge-group generators I_i^V appear only in terms of the Casimir operators $\sum_{V=A,Z,W^\pm} I_i^{\bar{V}} I_i^V$ and $I_j^A I_j^A$, which commute with each other. This enables us to combine the counterterms $\tilde{\mathcal{M}}_2^{\mathrm{WF}}$ (5.4) with the unrenormalized result $\tilde{\mathcal{M}}_2^{\mathrm{F}}$ (A.46) into the form presented in section 5.3.

The remaining NLL two-loop counterterms result from the insertion of the one-loop coupling-constant counterterms (4.4) in the one-loop amplitude (4.13) and read

$$e^2 \tilde{\mathcal{M}}_2^{\mathrm{PR}} \stackrel{\mathrm{NLL}}{=} -\frac{1}{2\epsilon}\left[\left(\frac{Q^2}{\mu_{\mathrm{R}}^2}\right)^\epsilon - 1\right] \mathcal{M}_0(Q^2) \sum_{i=1}^n \Bigg\{ \left[b_1^{(1)} g_1^2 \left(\frac{Y_i}{2}\right)^2 + b_2^{(1)} g_2^2 C_i\right] I(\epsilon, M_{\mathrm{W}}; p_i, p_i) $$
$$+ b_e^{(1)} e^2 Q_i^2 \, \Delta I(\epsilon, 0; p_i, p_i) \Bigg\}. \tag{5.5}$$

Again only the LL parts of the one-loop amplitude contribute to $\tilde{\mathcal{M}}_2^{\mathrm{PR}}$, so (4.21) has been used to arrive at the form (5.5), and the Yukawa terms in F_1^{sew} as well as the corresponding counterterms $\delta\lambda_t^{(1)}$ are irrelevant.

5.3 Renormalized two-loop amplitude

Using the results of appendices A and C, we find that the renormalized two-loop matrix

element can be written as

$$\tilde{\mathcal{M}}_2 \overset{\mathrm{NLL}}{=} \mathcal{M}_0(Q^2) \left\{ \frac{1}{2} [F_1^{\mathrm{sew}}]^2 + F_1^{\mathrm{sew}} \Delta F_1^{\mathrm{em}} + F_1^{\mathrm{sew}} \Delta F_1^{\mathrm{Z}} + \frac{1}{2} [\Delta F_1^{\mathrm{em}}]^2 + \Delta F_1^{\mathrm{Z}} \Delta F_1^{\mathrm{em}} \right.$$
$$\left. + G_2^{\mathrm{sew}} + \Delta G_2^{\mathrm{em}} \right\}, \tag{5.6}$$

in terms of the one-loop correction factors defined in (4.14)–(4.16) and the additional two-loop terms

$$e^2 G_2^{\mathrm{sew}} = \frac{1}{2} \sum_{i=1}^{n} \left[b_1^{(1)} g_1^2 \left(\frac{Y_i}{2} \right)^2 + b_2^{(1)} g_2^2 C_i \right] J(\epsilon, M_{\mathrm{W}}, \mu_{\mathrm{R}}^2; p_i, p_i),$$
$$\Delta G_2^{\mathrm{em}} = \frac{1}{2} \sum_{i=1}^{n} Q_i^2 \left\{ b_e^{(1)} \left[\Delta J(\epsilon, 0, \mu_{\mathrm{R}}^2; p_i, p_i) - \Delta J(\epsilon, 0, M_{\mathrm{W}}^2; p_i, p_i) \right] \right.$$
$$\left. + b_{\mathrm{QED}}^{(1)} \Delta J(\epsilon, 0, M_{\mathrm{W}}^2; p_i, p_i) \right\}. \tag{5.7}$$

The two-loop functions J and ΔJ are defined in (A.48) through the one-loop functions I and ΔI, so the entire two-loop amplitude is expressed in terms of one-loop quantities. The relevant J-functions read explicitly

$$J(\epsilon, M_{\mathrm{W}}, \mu_{\mathrm{R}}^2; p_i, p_i) \overset{\mathrm{NLL}}{=} \frac{1}{3} L^3 - l_{\mu_{\mathrm{R}}} L^2 + \mathcal{O}(\epsilon),$$
$$\Delta J(\epsilon, 0, M_{\mathrm{W}}^2; p_i, p_i) \overset{\mathrm{NLL}}{=} \delta_{i,0} \left(\frac{3}{2} \epsilon^{-3} + 2L \epsilon^{-2} + L^2 \epsilon^{-1} \right)$$
$$- \delta_{i,\mathrm{t}} \left(L \epsilon^{-2} + 2L^2 \epsilon^{-1} + 2L^3 \right) + \mathcal{O}(\epsilon),$$
$$\Delta J(\epsilon, 0, \mu_{\mathrm{R}}^2; p_i, p_i) - \Delta J(\epsilon, 0, M_{\mathrm{W}}^2; p_i, p_i) \overset{\mathrm{NLL}}{=} l_{\mu_{\mathrm{R}}} \left\{ \delta_{i,0} \left[-2\epsilon^{-2} + \epsilon^{-1}(l_{\mu_{\mathrm{R}}} - 2L) \right. \right.$$
$$\left. \left. + l_{\mu_{\mathrm{R}}} L - \frac{1}{3} l_{\mu_{\mathrm{R}}}^2 \right] + \delta_{i,\mathrm{t}} \left(2L\epsilon^{-1} + 4L^2 - l_{\mu_{\mathrm{R}}} L \right) \right\} + \mathcal{O}(\epsilon), \tag{5.8}$$

where

$$l_{\mu_{\mathrm{R}}} = \ln \left(\frac{\mu_{\mathrm{R}}^2}{M_{\mathrm{W}}^2} \right). \tag{5.9}$$

Note that the terms G_2^{sew} and ΔG_2^{em} in (5.7) only involve NLLs.

In order to be able to express (5.6) in terms of the one-loop operators (4.14)–(4.16) it is crucial that terms up to order ϵ^2 are included in the latter.

The coefficients $b_e^{(1)}$ and $b_{\mathrm{QED}}^{(1)}$ describe the running of the electromagnetic coupling above and below the electroweak scale, respectively. The former receives contributions from all charged fermions and bosons, whereas the latter receives contributions only from light fermions, i.e. all charged leptons and quarks apart from the top quark.

The couplings that enter the one- and two-loop correction factors[6] are renormalized at the general scale $\mu_{\rm R} \gtrsim M_{\rm W}$. The renormalization of the coupling constants g_1, g_2, e, and λ_t in the lowest-order matrix element $\mathcal{M}_0(Q^2)$ in (4.13) and (5.6) is discussed in section 4.1. The $\mu_{\rm R}$-dependence of $\mathcal{M}_0(Q^2)$ is implicitly defined by (4.8), and the dependence of the one- and two-loop correction factors on $\mu_{\rm R}$ is described by the terms (5.7). The contributions (5.7) originate from combinations of UV and mass singularities. We observe that the term proportional to $b_e^{(1)}$ vanishes for $\mu_{\rm R} = M_{\rm W}$. Instead, the terms proportional to $b_1^{(1)}$, $b_2^{(1)}$, and $b_{\rm QED}^{(1)}$ cannot be eliminated through an appropriate choice of the renormalization scale. This reflects the fact that such two-loop terms do not originate exclusively from the running of the couplings in the one-loop amplitude.

Combining the Born amplitude with the one- and two-loop NLL corrections we can write

$$\mathcal{M} \stackrel{\rm NLL}{=} \mathcal{M}_0(Q^2)\, F^{\rm sew}\, F^{\rm Z}\, F^{\rm em}, \tag{5.10}$$

where we observe a factorization of the symmetric-electroweak contributions,

$$F^{\rm sew} \stackrel{\rm NLL}{=} 1 + \frac{\alpha_\epsilon}{4\pi} F_1^{\rm sew} + \left(\frac{\alpha_\epsilon}{4\pi}\right)^2 \left[\frac{1}{2}\left(F_1^{\rm sew}\right)^2 + G_2^{\rm sew}\right], \tag{5.11}$$

the terms resulting from the difference between $M_{\rm W}$ and $M_{\rm Z}$,

$$F^{\rm Z} \stackrel{\rm NLL}{=} 1 + \frac{\alpha_\epsilon}{4\pi}\Delta F_1^{\rm Z}, \tag{5.12}$$

and the electromagnetic terms resulting from the mass gap between the photon and the W boson,

$$F^{\rm em} \stackrel{\rm NLL}{=} 1 + \frac{\alpha_\epsilon}{4\pi}\Delta F_1^{\rm em} + \left(\frac{\alpha_\epsilon}{4\pi}\right)^2 \left[\frac{1}{2}\left(\Delta F_1^{\rm em}\right)^2 + \Delta G_2^{\rm em}\right]. \tag{5.13}$$

We also observe that the symmetric-electroweak and electromagnetic terms are consistent with the exponentiated expressions

$$F^{\rm sew} \stackrel{\rm NLL}{=} \exp\left[\frac{\alpha_\epsilon}{4\pi}F_1^{\rm sew} + \left(\frac{\alpha_\epsilon}{4\pi}\right)^2 G_2^{\rm sew}\right],$$
$$F^{\rm em} \stackrel{\rm NLL}{=} \exp\left[\frac{\alpha_\epsilon}{4\pi}\Delta F_1^{\rm em} + \left(\frac{\alpha_\epsilon}{4\pi}\right)^2 \Delta G_2^{\rm em}\right]. \tag{5.14}$$

In particular, these two contributions exponentiate separately. This double-exponentiating structure is indicated by the ordering of the non-commuting one-loop operators $F_1^{\rm sew}$ and $\Delta F_1^{\rm em}$ in the interference term $F_1^{\rm sew}\Delta F_1^{\rm em}$ in our result (5.6). The commutator of these two operators yields a non-vanishing NLL two-loop contribution.

Note that the $\mathcal{O}(\alpha^2)$ LL contributions in (5.14) are entirely given by the exponentiation of the one-loop term. On the other hand, at the NLL level the presence of the $\mathcal{O}(\alpha^2)$ terms

---

[6]These are the coupling α in the perturbative expansion (2.9) and the couplings g_1, g_2, e and λ_t that appear explicitly in (4.14), (5.7) and enter implicitly in (4.14)–(4.16) through the dependence of the generators (2.16) on the couplings and the mixing parameters $c_{\rm W}$ and $s_{\rm W}$.

G_2^{sew} and ΔG_2^{em} in our result (5.14) seems to spoil exponentiation. However, this is an artifact of the fixed-order expansion of the argument of the exponential and must not be interpreted as a breaking of exponentiation. This can easily be seen in the framework of evolution equations, were the $\mathcal{O}(\alpha^2)$ terms in (5.14) naturally emerge from the running of the coupling associated with the one-loop contribution. To illustrate this feature we restrict ourselves to a gauge theory with a simple gauge group and consider a form factor. In this case the structure of our result F^{sew} in (5.14) is easily obtained from the manifestly exponentiated expression (15) in ref. [30],

$$\mathcal{F} = F_0 \exp\left\{ \int_{M_{\text{W}}^2}^{Q^2} \frac{\mathrm{d}x}{x} \left[\int_{M_{\text{W}}^2}^{x} \frac{\mathrm{d}x'}{x'} \gamma(\alpha(x')) + \zeta(\alpha(x)) + \xi(\alpha(M_{\text{W}}^2)) \right] \right\}. \tag{5.15}$$

The NLL approximation requires the one-loop values of the various anomalous dimensions as well as the one-loop running of α in $\gamma(\alpha)$,

$$\gamma(\alpha(x')) \overset{\text{NLL}}{=} \frac{\alpha(x')}{4\pi}\gamma^{(1)} \overset{\text{NLL}}{=} \frac{\alpha(\mu_{\text{R}}^2)}{4\pi} \left[1 - \frac{\alpha(\mu_{\text{R}}^2)}{4\pi}b^{(1)} \ln\left(\frac{x'}{\mu_{\text{R}}^2}\right) \right] \gamma^{(1)},$$

$$\zeta(\alpha(x)) \overset{\text{NLL}}{=} \frac{\alpha(\mu_{\text{R}}^2)}{4\pi}\zeta^{(1)}, \qquad \xi(\alpha(M_{\text{W}}^2)) \overset{\text{NLL}}{=} \frac{\alpha(\mu_{\text{R}}^2)}{4\pi}\xi^{(1)}. \tag{5.16}$$

Inserting these expressions in (5.15) one obtains

$$\mathcal{F} \overset{\text{NLL}}{=} F_0 \exp\left\{ \frac{\alpha(\mu_{\text{R}}^2)}{4\pi} \left[\frac{\gamma^{(1)}}{2}L^2 + \left(\zeta^{(1)} + \xi^{(1)} \right) L \right] \right.$$

$$\left. - \left(\frac{\alpha(\mu_{\text{R}}^2)}{4\pi} \right)^2 \frac{\gamma^{(1)}}{2}b^{(1)} \left(\frac{1}{3}L^3 - l_{\mu_{\text{R}}}L^2 \right) \right\}, \tag{5.17}$$

and one can easily verify that the two-loop term appearing in the argument of the exponential, i.e. the term proportional to the β-function coefficient $b^{(1)}$, corresponds to the term G_2^{sew} in our result.

The one- and two-loop corrections (4.13)–(4.16) and (5.6)–(5.7) contain various combinations of weak-isospin matrices I_i^V, which are in general non-commuting and non-diagonal. These matrices have to be applied to the Born amplitude $\mathcal{M}_0(Q^2)$ according to the definition (2.31). In order to express the results in a form which is more easily applicable to a specific process, it is useful to split the integrals $I(\epsilon, M_V; p_i, p_j)$ and $\Delta I(\epsilon, M_V; p_i, p_j)$ in (4.14)–(4.16) into an angular-dependent part involving logarithms l_{ij} and an angular-independent part. This permits to eliminate the sum over j for the angular-independent parts of (4.14)–(4.16) using (4.21). One can easily see that the angular-independent part of (4.14) gives rise to the Casimir operator (2.18). After these simplifications, all operators that are associated with the angular-independent parts can be replaced by the corresponding eigenvalues, and the one- and two-loop results can be written as

$$\mathcal{M} \overset{\text{NLL}}{=} \mathcal{M}_0(Q^2)\, f^{\text{sew}}\, f^{\text{Z}}\, f^{\text{em}}, \tag{5.18}$$

where the electromagnetic terms read

$$f^{\text{em}} \overset{\text{NLL}}{=} 1 + \frac{\alpha_\epsilon}{4\pi}\Delta f_1^{\text{em}} + \left(\frac{\alpha_\epsilon}{4\pi} \right)^2 \left[\frac{1}{2}(\Delta f_1^{\text{em}})^2 + \Delta g_2^{\text{em}} \right] \tag{5.19}$$

with

$$
\Delta f_1^{\text{em}} \overset{\text{NLL}}{=} \sum_{i=1}^{n} \Bigg\{ \delta_{i,0} \left(-\epsilon^{-2} + \frac{1}{2}L^2 + \frac{1}{3}L^3\epsilon + \frac{1}{8}L^4\epsilon^2 \right) + \delta_{i,\text{t}} \left(L\epsilon^{-1} + L^2 + \frac{1}{2}L^3\epsilon + \frac{1}{6}L^4\epsilon^2 \right)
$$
$$
- \left[\frac{3}{2}\delta_{i,0} + \delta_{i,\text{t}}(1+l_i) \right] \left(\epsilon^{-1} + L + \frac{1}{2}L^2\epsilon + \frac{1}{6}L^3\epsilon^2 \right) \Bigg\} q_i^2
$$
$$
- \left(\epsilon^{-1} + L + \frac{1}{2}L^2\epsilon + \frac{1}{6}L^3\epsilon^2 \right) \sum_{i=1}^{n} \sum_{\substack{j=1 \\ j\neq i}}^{n} l_{ij}q_iq_j + \mathcal{O}(\epsilon^3),
$$

$$
\Delta g_2^{\text{em}} \overset{\text{NLL}}{=} \sum_{i=1}^{n} \Bigg\{ l_{\mu_{\text{R}}} \left[\delta_{i,0} \left(-\epsilon^{-2} - \left(L - \frac{1}{2}l_{\mu_{\text{R}}} \right)\epsilon^{-1} + \frac{1}{2}l_{\mu_{\text{R}}}L - \frac{1}{6}l_{\mu_{\text{R}}}^2 \right) \right.
$$
$$
\left. + \delta_{i,\text{t}} \left(L\epsilon^{-1} + 2L^2 - \frac{1}{2}l_{\mu_{\text{R}}}L \right) \right] b_e^{(1)} + \left[\delta_{i,0} \left(\frac{3}{4}\epsilon^{-3} + L\epsilon^{-2} + \frac{1}{2}L^2\epsilon^{-1} \right) \right.
$$
$$
\left. - \delta_{i,\text{t}} \left(\frac{1}{2}L\epsilon^{-2} + L^2\epsilon^{-1} + L^3 \right) \right] b_{\text{QED}}^{(1)} \Bigg\} q_i^2 + \mathcal{O}(\epsilon). \tag{5.20}
$$

For the term resulting from the difference between M_{W} and M_{Z} we get

$$
f^{\text{Z}} \overset{\text{NLL}}{=} 1 + \frac{\alpha_\epsilon}{4\pi}\Delta f_1^{\text{Z}} \tag{5.21}
$$

with

$$
\Delta f_1^{\text{Z}} \overset{\text{NLL}}{=} \left(L + L^2\epsilon + \frac{1}{2}L^3\epsilon^2 \right) l_{\text{Z}} \sum_{i=1}^{n} \left(\frac{g_2}{e}c_{\text{W}}t_i^3 - \frac{g_1}{e}s_{\text{W}}\frac{y_i}{2} \right)^2 + \mathcal{O}(\epsilon^3), \tag{5.22}
$$

and the symmetric-electroweak contributions yield

$$
f^{\text{sew}} \overset{\text{NLL}}{=} 1 + \frac{\alpha_\epsilon}{4\pi}f_1^{\text{sew}} + \left(\frac{\alpha_\epsilon}{4\pi} \right)^2 \left[\frac{1}{2}(f_1^{\text{sew}})^2 + g_2^{\text{sew}} \right] \tag{5.23}
$$

with

$$
f_1^{\text{sew}} \overset{\text{NLL}}{=} -\left(\frac{1}{2}L^2 + \frac{1}{3}L^3\epsilon + \frac{1}{8}L^4\epsilon^2 - \frac{3}{2}L - \frac{3}{4}L^2 - \frac{1}{4}L^3\epsilon^2 \right) \sum_{i=1}^{n} \left[\frac{g_1^2}{e^2}\left(\frac{y_i}{2} \right)^2 + \frac{g_2^2}{e^2}c_i \right]
$$
$$
+ \left(L + \frac{1}{2}L^2\epsilon + \frac{1}{6}L^3\epsilon^2 \right) \mathcal{K}_1^{\text{ad}} - \frac{\lambda_t^2}{4e^2} \left(L_\text{t} + \frac{1}{2}L_\text{t}^2\epsilon + \frac{1}{6}L_\text{t}^3\epsilon^2 \right) \sum_{i=1}^{n} z_i^{\text{Y}} + \mathcal{O}(\epsilon^3),
$$
$$
g_2^{\text{sew}} \overset{\text{NLL}}{=} \left(\frac{1}{6}L^3 - \frac{1}{2}l_{\mu_{\text{R}}}L^2 \right) \sum_{i=1}^{n} \left[b_1^{(1)}\frac{g_1^2}{e^2}\left(\frac{y_i}{2} \right)^2 + b_2^{(1)}\frac{g_2^2}{e^2}c_i \right] + \mathcal{O}(\epsilon). \tag{5.24}
$$

In the above equations $l_{\mu_{\text{R}}} = \ln\left(\mu_{\text{R}}^2/M_{\text{W}}^2 \right)$, and c_i, t_i^3, y_i, q_i represent the eigenvalues of the operators C_i, T_i^3, Y_i, and Q_i, respectively.

The only matrix-valued expression is the angular-dependent part of the symmetric-electroweak contribution f_1^{sew} in (5.24),

$$
\mathcal{K}_1^{\text{ad}} = \sum_{i=1}^{n} \sum_{\substack{j=1 \\ j\neq i}}^{n} l_{ij} \sum_{V=A,Z,W^{\pm}} I_i^{\bar{V}} I_j^V. \tag{5.25}
$$

The two-loop corrections involve terms proportional to $\mathcal{K}_1^{\text{ad}}$ and $[\mathcal{K}_1^{\text{ad}}]^2$. However, the latter are of NNLL order and thus negligible in NLL approximation. The combination of the matrix (5.25) with the Born amplitude,

$$
\begin{aligned}
\mathcal{M}_0(Q^2)\,\mathcal{K}_1^{\text{ad}} &= \sum_{i=1}^n \sum_{\substack{j=1 \\ j\neq i}}^n l_{ij} \sum_{V=A,Z,W^\pm} \mathcal{M}_0^{\varphi_1\ldots\varphi_i'\ldots\varphi_j'\ldots\varphi_n} I_{\varphi_i'\varphi_i}^{\bar{V}} I_{\varphi_j'\varphi_j}^{V} \\
&= \sum_{i=1}^n \sum_{\substack{j=1 \\ j\neq i}}^n l_{ij} \left\{ \mathcal{M}_0^{\varphi_1\ldots\varphi_i\ldots\varphi_j\ldots\varphi_n} \left[\frac{g_1^2}{e^2} \frac{y_i y_j}{4} + \frac{g_2^2}{e^2} t_i^3 t_j^3 \right] \right. \\
&\left. \quad + \sum_{V=W^\pm} \mathcal{M}_0^{\varphi_1\ldots\varphi_i'\ldots\varphi_j'\ldots\varphi_n} I_{\varphi_i'\varphi_i}^{\bar{V}} I_{\varphi_j'\varphi_j}^{V} \right\}, \quad (5.26)
\end{aligned}
$$

requires the evaluation of matrix elements involving SU(2)-transformed external fermions φ_i', φ_j', i.e. isospin partners of the fermions φ_i, φ_j. Explicit results for four-particle processes are presented in appendix D.

6. Discussion and conclusion

We have studied the asymptotic high-energy behaviour of virtual electroweak corrections to arbitrary fermionic processes in the Standard Model. The present analysis extends results previously obtained for massless fermion scattering [32] to processes that involve also bottom and top quarks. By explicit evaluation of all relevant Feynman diagrams, we have derived a general formula that describes one- and two-loop logarithmic contributions of the form $\ln(Q^2/M_{\text{W}}^2)$. Such logarithmic terms — which dominate the electroweak corrections at TeV colliders — originate from ultraviolet and mass (soft/collinear) singularities in the asymptotic regime where all kinematical invariants are at an energy scale $Q^2 \gg M_{\text{W}}^2$. All masses of the heavy particles have been assumed to be of the same order $M_{\text{W}} \sim M_{\text{Z}} \sim M_{\text{H}} \sim m_{\text{t}}$ but not equal, and all light fermions — including bottom quarks — have been treated as massless particles. We have included all leading (LLs) and next-to-leading (NLLs) logarithms.

The calculation has been performed in the complete spontaneously broken electroweak Standard Model using the 't Hooft-Feynman gauge. The fermionic wave functions are renormalized on shell, and coupling-constant renormalization is performed in the $\overline{\text{MS}}$ scheme, but can be generalized easily. Employing the method developed in ref. [32], we have reduced all NLL contributions to factorizable diagrams. In this way the process-dependent part of the calculation is isolated in a generic tree-level amplitude, which is multiplied by process-independent factors consisting of loop integrals and gauge and Yukawa couplings. Technically this is achieved by means of collinear Ward identities and a soft-collinear approximation. All relevant contributions originating from ultraviolet singularities are consistently taken into account in every step of the calculation. In particular, as discussed in section 3.1.4, the logarithms of ultraviolet origin are isolated in a few bare diagrams [see (3.7) and (3.15)] and counterterms (see sections 4.1 and 5.2) by means of minimal subtractions of the ultraviolet singularities and an appropriate choice of the subtraction

scale. While the ultraviolet logarithms associated with the renormalization of the coupling parameters in the factorized tree-level amplitude are easily absorbed into running couplings, the process-independent correction factors receive additional contributions of ultraviolet origin which result from the bare two-loop diagrams of type (3.7), the wave-function renormalization [see (4.12) and (5.4)], and the renormalization of the couplings in the soft-collinear corrections [see (5.5)].

Since the NLL electroweak corrections originate only from the electroweak interactions of the external legs, our general results for n-fermion processes are also applicable to processes involving external fermions and gluons and, more generally, to hard reactions that involve n fermions plus an arbitrary number of SU(2) × U(1) singlets as external particles. Additional legs associated with external electroweak singlets can only enter the hard part (F) of the factorizable diagrams (3.3), (3.4) and (3.15). This modifies only the process-dependent hard amplitude $\mathcal{M}_0$, which is always factorized in our derivations, while the NLL correction factors receive contributions only from fermionic external legs and do not depend on additional external singlets.

All two-loop integrals have been solved by two independent methods in NLL approximation. One makes use of sector decomposition, the other uses the strategy of regions. Explicit results have been given for all contributing factorizable Feynman diagrams.

The presence of soft/collinear singularities originating from virtual photons and their interplay, at two loops, with logarithmic corrections resulting from massive particles is one of the most delicate aspects of the problem. In order to isolate the finite $\ln(Q^2/M_W^2)$ terms in a meaningful way, one has to separate the photonic divergences in a gauge-invariant contribution that can be cancelled against real-photon corrections. To this end, we have split the corrections into a finite symmetric-electroweak part, which is constructed by setting the masses of all gauge bosons equal to M_W, and remaining subtracted parts, which describe the effects resulting from the γ-W and Z-W mass differences. By combining all one- and two-loop diagrams we found that these three contributions factorize as described in (5.10)–(5.13): the term associated with the γ-W mass splitting (F^{em}) depends only on the masses and charges of the external fermions and behaves as a pure QED correction subtracted at photon mass $M_A = M_W$. The term resulting from the Z-W splitting (F^{Z}) is proportional to $\ln(M_Z^2/M_W^2)$ and depends only on the external-leg Z-boson couplings. Finally, the contribution constructed by setting $M_A = M_Z = M_W$ in all loop diagrams (F^{sew}) turns out to be independent of symmetry-breaking effects such as mixing or couplings proportional to the vacuum expectation value. This contribution, which contains only finite $\ln(Q^2/M_W^2)$ terms, behaves as in a symmetric SU(2) × U(1) theory where mass singularities are regularized by a common mass parameter. Moreover we find that the electromagnetic and the symmetric-electroweak parts exponentiate as described in (5.14): the corresponding two-loop contributions can be written as the second-order terms of exponentials of the one-loop contributions plus additional terms that are proportional to the one-loop β-function coefficients.

These results agree with the resummations that have been proposed in the literature and confirm — for fermion scattering processes — the assumption that the asymptotic high-energy behaviour of electroweak interactions at two loops can be described by a sym-

metric and unmixed $\mathrm{SU(2)} \times \mathrm{U(1)}$ theory matched with QED at the electroweak scale. Indeed, apart from the terms involving $\ln(M_Z^2/M_W^2)$, in the final result we observe a cancellation of all effects associated with symmetry breaking. We have explicitly checked that, upon separation of the QED singularities, our results are consistent with the predictions of ref. [19] and refs. [24, 25].

As an application of our results for general n-fermion processes, we present in appendix D explicit expressions for the case of four-particle processes involving four fermions or two fermions and two gluons. In general, our process-independent results can be applied to any reaction with external fermions and gluons as long as all kinematical invariants are large. We plan to extend these results to processes involving external gauge bosons and Higgs bosons.

Acknowledgments

A. Loop integrals of factorizable contributions

In this appendix, we present explicit results for the loop integrals of the one- and two-loop factorizable contributions defined in section 3.1.2 and the Yukawa contributions in section 3.2.3. These are evaluated within the 't Hooft-Feynman gauge, where the masses of the Faddeev-Popov ghosts $u^A, u^Z, u^{W^\pm}$ and would-be Goldstone bosons $\chi, \phi^\pm$ read $M_{u^A} = M_A = 0$, $M_\chi = M_{u^Z} = M_Z$, and $M_{\phi^\pm} = M_{u^W} = M_W$. Using the soft-collinear approximation and the projectors introduced in sections 3.1.3 and 3.2.2, we express the factorizable contributions resulting from individual diagrams as products of the n-fermion Born amplitude with matrix-valued coupling factors and loop integrals.

The loop integrals associated with the various diagrams are denoted with symbols of the type $D_h(m_1, \ldots, m_n; p_i, p_j, \ldots)$. The definition of these integrals is provided in appendix B. They depend on various internal masses $m_1, m_2, \ldots$ and, through the external momenta $p_i, p_j, \ldots$, on the kinematical invariants r_{ij} and the masses $m_i^2 = p_i^2$. The symbols m_k are always used to denote generic mass parameters, which can assume the values $m_k = M_W, M_Z, m_t, M_H$ or $m_k = 0$. Instead we use the symbols M_k to denote non-zero masses, i.e. $M_k = M_W, M_Z, m_t, M_H$. The integrals are often singular when certain mass parameters tend to zero, and the cases where such parameters are zero or non-zero need to be treated separately. We also define subtracted functions

$$\Delta D_h(m_1, \ldots, m_n; p_i, \ldots) = D_h(m_1, \ldots, m_n; p_i, \ldots) - D_h(M_W, \ldots, M_W; p_i, \ldots), \quad \text{(A.1)}$$
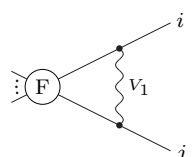
where the integral with all internal mass parameters equal to M_W is subtracted.

The integrals have been computed in NLL accuracy, and the result is expanded in ϵ up to $\mathcal{O}(\epsilon^2)$ at one loop and $\mathcal{O}(\epsilon^0)$ at two loops. The UV poles have been eliminated by means of a minimal subtraction as explained in section 3.1.4 such that the presented results are UV finite. The integrals have been evaluated separately for all physical combinations of gauge-boson and fermion masses on internal and external lines. All loop integrals have been solved and cross-checked using two independent methods: an automatized algorithm based on the sector-decomposition technique [33] and the method of expansion by regions combined with Mellin-Barnes representations (see ref. [31] and references therein).

The one-loop diagrams are treated in section A.1, the two-loop diagrams involving gauge interactions in section A.2, and the diagrams involving Yukawa interactions in section A.3.

A.1 One-loop diagrams

The one-loop factorizable contributions (3.3) originate only from one type of diagram,[7]

$$\tilde{\mathcal{M}}_1^{ij} = \quad \overset{\mathrm{NLL}}{=} -\mathcal{M}_0 \sum_{V_1=A,Z,W^\pm} I_i^{\bar{V}_1} I_j^{V_1} D_0(M_{V_1}; p_i, p_j). \qquad (\mathrm{A.2})$$

In NLL accuracy, the representations of the generators $I_i^{\bar{V}_1}$ and $I_j^{V_1}$ correspond to the chiralities given by the spinors of the external particles i and j, respectively. The loop integral D_0 is defined in (B.6) and to NLL accuracy yields

$$
\begin{aligned}
D_0(M_1; p_i, p_j) &\overset{\mathrm{NLL}}{=} -L^2 - \frac{2}{3}L^3\epsilon - \frac{1}{4}L^4\epsilon^2 + (4 - 2l_{ij})\left(L + \frac{1}{2}L^2\epsilon + \frac{1}{6}L^3\epsilon^2\right) \\
&\quad + l_1\left(2L + 2L^2\epsilon + L^3\epsilon^2\right), \\
D_0(0; p_i, p_j) &\overset{\mathrm{NLL}}{=} 2l_{ij}\epsilon^{-1} - (\delta_{i,0} + \delta_{j,0})\left(\epsilon^{-2} + 2\epsilon^{-1}\right) + \left\{\delta_{i,\mathrm{t}}\left[L\epsilon^{-1} + \frac{1}{2}L^2 + \frac{1}{6}L^3\epsilon\right.\right. \\
&\quad \left.\left. + \frac{1}{24}L^4\epsilon^2 - l_i\epsilon^{-1} + (2 - l_i)\left(L + \frac{1}{2}L^2\epsilon + \frac{1}{6}L^3\epsilon^2\right)\right] + (i \leftrightarrow j)\right\},
\end{aligned}
$$
$$(\mathrm{A.3})$$

where the UV singularities

$$D_0^{\mathrm{UV}}(m_1; p_i, p_j) \overset{\mathrm{NLL}}{=} 4\epsilon^{-1} \qquad (\mathrm{A.4})$$

have been subtracted. The shorthands $L, l_i, l_{ij}, \delta_{i,\mathrm{t}}, \delta_{i,0}$ are defined in section 2.1.

Summing over all external legs, we find for the factorizable one-loop contributions (3.3)

$$\tilde{\mathcal{M}}_1^{\mathrm{F}} \overset{\mathrm{NLL}}{=} \mathcal{M}_0\left[F_1^{\mathrm{F,sew}} + \Delta F_1^{\mathrm{F,em}} + \Delta F_1^{\mathrm{F,Z}}\right] \qquad (\mathrm{A.5})$$

---

[7]The l-loop diagrams depicted in this appendix are understood without factors $(\alpha_\epsilon/4\pi)^l$.
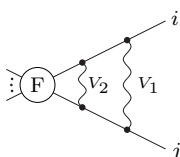
with

$$F_1^{\mathrm{F,sew}} = -\frac{1}{2} \sum_{i=1}^{n} \sum_{\substack{j=1 \\ j \neq i}}^{n} \sum_{V=A,Z,W^\pm} I_i^{\bar{V}} I_j^V \, D_0(M_{\mathrm{W}}; p_i, p_j),$$

$$\Delta F_1^{\mathrm{F,em}} = -\frac{1}{2} \sum_{i=1}^{n} \sum_{\substack{j=1 \\ j \neq i}}^{n} I_i^A I_j^A \, \Delta D_0(0; p_i, p_j),$$

$$\Delta F_1^{\mathrm{F,Z}} = -\frac{1}{2} \sum_{i=1}^{n} \sum_{\substack{j=1 \\ j \neq i}}^{n} I_i^Z I_j^Z \, \Delta D_0(M_{\mathrm{Z}}; p_i, p_j), \tag{A.6}$$

and $\Delta D_0(m; p_i, p_j)$ defined in (A.1).

A.2 Two-loop diagrams involving gauge interactions

The two-loop NLL factorizable terms (3.4) involve fourteen different types of diagrams. The diagrams 1–3, 12 and 14 in this section give rise to LLs and NLLs, whereas all other diagrams yield only NLLs.

Diagram 1.

$$\tilde{\mathcal{M}}_2^{1,ij} = \quad \overset{\mathrm{NLL}}{=} \mathcal{M}_0 \sum_{V_1,V_2=A,Z,W^\pm} I_i^{\bar{V}_2} I_i^{\bar{V}_1} I_j^{V_2} I_j^{V_1} D_1(M_{V_1}, M_{V_2}; p_i, p_j), \tag{A.7}$$

where the loop integral D_1 is defined in (B.6) and yields

$$D_1(M_1, m_2; p_i, p_j) \overset{\mathrm{NLL}}{=} \frac{1}{6} L^4 - \frac{2}{3} \left(2 - l_{ij} + l_1 \right) L^3,$$

$$D_1(0, M_2; p_i, p_j) \overset{\mathrm{NLL}}{=} \left(\delta_{i,0} + \delta_{j,0} \right) \left[L^2 \epsilon^{-2} + \frac{4}{3} L^3 \epsilon^{-1} + L^4 - l_2 \left(2L\epsilon^{-2} + 4L^2\epsilon^{-1} + 4L^3 \right) \right.$$

$$\left. - \left(4 - 2l_{ij} \right) \left(L\epsilon^{-2} + L^2\epsilon^{-1} + \frac{2}{3} L^3 \right) \right]$$

$$+ \left\{ \delta_{i,\mathrm{t}} \left[-L^3\epsilon^{-1} - \frac{23}{12} L^4 + \left(4 - 3l_{ij} + 2l_2 + l_i \right) L^2\epsilon^{-1} \right. \right.$$

$$\left. \left. + \left(\frac{20}{3} - \frac{17}{3} l_{ij} + \frac{16}{3} l_2 + \frac{7}{3} l_i \right) L^3 \right] + (i \leftrightarrow j) \right\},$$

$$D_1(0, 0; p_i, p_j) \overset{\mathrm{NLL}}{=} \delta_{i,0} \delta_{j,0} \left[\epsilon^{-4} + \left(4 - 2l_{ij} \right) \epsilon^{-3} \right] + \left\{ \delta_{i,\mathrm{t}} \delta_{j,0} \left[\frac{1}{3} \epsilon^{-4} - \frac{2}{3} L\epsilon^{-3} - \frac{1}{3} L^2\epsilon^{-2} \right. \right.$$

$$\left. - \frac{1}{9} L^3\epsilon^{-1} - \frac{1}{36} L^4 + \left(\frac{4}{3} - \frac{4}{3} l_{ij} + \frac{2}{3} l_i \right) \epsilon^{-3} \right.$$

$$\left. \left. - \left(4 - l_{ij} - l_i \right) \left(\frac{2}{3} L\epsilon^{-2} + \frac{1}{3} L^2\epsilon^{-1} + \frac{1}{9} L^3 \right) \right] + (i \leftrightarrow j) \right\}$$

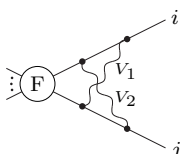$$+ \delta_{i,\mathrm{t}}\delta_{j,\mathrm{t}}\left[2L^2\epsilon^{-2} + \frac{10}{3}L^3\epsilon^{-1} + \frac{7}{2}L^4 + 4l_{ij}L\epsilon^{-2} + (8 + 6l_{ij})\,L^2\epsilon^{-1}\right.$$
$$\left.+ \left(\frac{40}{3} + \frac{22}{3}l_{ij}\right)L^3 - (l_i + l_j)\bigl(2L\epsilon^{-2} + 5L^2\epsilon^{-1} + 7L^3\bigr)\right]. \quad (A.8)$$

Here the UV singularities

$$D_1^{\mathrm{UV}}(M_1, m_2; p_i, p_j) \overset{\mathrm{NLL}}{=} -4L^2\epsilon^{-1} - \frac{8}{3}L^3,$$

$$D_1^{\mathrm{UV}}(0, m_2; p_i, p_j) \overset{\mathrm{NLL}}{=} -4\,(\delta_{i,0} + \delta_{j,0})\,\epsilon^{-3} + (\delta_{i,\mathrm{t}} + \delta_{j,\mathrm{t}})\left(4L\epsilon^{-2} + 2L^2\epsilon^{-1} + \frac{2}{3}L^3\right)$$
$$(A.9)$$

have been subtracted.
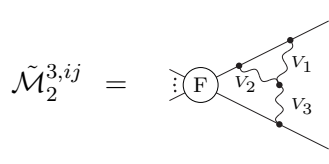
Diagram 2.

$$\tilde{\mathcal{M}}_2^{2,ij} = \quad \quad \overset{\mathrm{NLL}}{=} \mathcal{M}_0 \sum_{V_1,V_2 = A,Z,W^\pm} I_i^{\bar{V}_2} I_i^{\bar{V}_1} I_j^{V_1} I_j^{V_2} D_2(M_{V_1}, M_{V_2}; p_i, p_j),\,(A.10)$$

where the loop integral D_2 is defined in (B.6). This integral is free of UV singularities and yields

$$D_2(M_1, M_2; p_i, p_j) \overset{\mathrm{NLL}}{=} \frac{1}{3}L^4 - \frac{2}{3}\,(4 - 2l_{ij} + l_1 + l_2)\,L^3,$$

$$D_2(0, M_2; p_i, p_j) \overset{\mathrm{NLL}}{=} \delta_{i,0}\left[-\frac{2}{3}L^3\epsilon^{-1} - \frac{5}{6}L^4 + (4 - 2l_{ij})\left(L^2\epsilon^{-1} + L^3\right)\right.$$
$$\left.+ l_2\left(2L^2\epsilon^{-1} + \frac{10}{3}L^3\right)\right] + \delta_{i,\mathrm{t}}\left[\frac{2}{3}L^4 - \left(4 - \frac{8}{3}l_{ij} + 2l_2 + \frac{2}{3}l_i\right)L^3\right],$$

$$D_2(M_1, 0; p_i, p_j) = D_2(0, M_1; p_j, p_i),$$

$$D_2(0, 0; p_i, p_j) \overset{\mathrm{NLL}}{=} \delta_{i,0}\delta_{j,0}\left[\epsilon^{-4} + (4 - 2l_{ij})\,\epsilon^{-3}\right] + \left\{\delta_{i,\mathrm{t}}\delta_{j,0}\left[\frac{1}{6}\epsilon^{-4} - \frac{1}{3}L\epsilon^{-3} + \frac{1}{3}L^2\epsilon^{-2}\right.\right.$$
$$+ \frac{4}{9}L^3\epsilon^{-1} + \frac{5}{18}L^4 + (2 - 2l_{ij} + l_i)\left(\frac{1}{3}\epsilon^{-3} - \frac{2}{3}L\epsilon^{-2}\right)$$
$$\left.+ \left(\frac{4}{3} + \frac{2}{3}l_{ij} - \frac{4}{3}l_i\right)L^2\epsilon^{-1} + \left(\frac{16}{9} + \frac{2}{9}l_{ij} - \frac{10}{9}l_i\right)L^3\right] + (i \leftrightarrow j)\right\}$$
$$+ \delta_{i,\mathrm{t}}\delta_{j,\mathrm{t}}\left[-\frac{4}{3}L^3\epsilon^{-1} - \frac{7}{3}L^4 - 4l_{ij}L^2\epsilon^{-1} - \left(\frac{16}{3} + \frac{20}{3}l_{ij}\right)L^3\right.$$
$$\left.+ (l_i + l_j)\left(2L^2\epsilon^{-1} + \frac{14}{3}L^3\right)\right]. \quad (A.11)$$

Diagram 3.

$$\tilde{\mathcal{M}}_2^{3,ij} \overset{\text{NLL}}{=} -\mathrm{i}\frac{g_2}{e}\mathcal{M}_0 \sum_{V_1,V_2,V_3=A,Z,W^\pm} \varepsilon^{V_1V_2V_3} I_i^{\bar{V}_2} I_i^{\bar{V}_1} I_j^{\bar{V}_3} D_3(M_{V_1},M_{V_2},M_{V_3};p_i,p_j), \quad (\text{A.12})$$

where the ε-tensor is defined in ref. [32] [see also (2.17)]. The loop integral D_3 is defined in (B.6) and yields
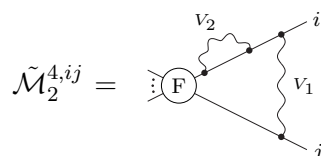
$$D_3(M_1,m_2,M_3;p_i,p_j) \overset{\text{NLL}}{=} \frac{1}{6}L^4 - \left(3 - \frac{2}{3}l_{ij} + \frac{1}{3}l_1 + \frac{1}{3}l_3\right)L^3,$$

$$D_3(0,M_2,M_3;p_i,p_j) \overset{\text{NLL}}{=} \delta_{i,0}\left[-\frac{1}{3}L^3\epsilon^{-1} - \frac{5}{12}L^4 + (2 - l_{ij} + l_3)L^2\epsilon^{-1} + \left(\frac{1}{3} - l_{ij}\right.\right.$$
$$\left.\left. + \frac{5}{3}l_3\right)L^3\right] + \delta_{i,\mathrm{t}}\left[\frac{1}{3}L^4 - \left(\frac{11}{3} - \frac{4}{3}l_{ij} + l_3 + \frac{1}{3}l_i\right)L^3\right],$$

$$D_3(M_1,M_2,0;p_i,p_j) \overset{\text{NLL}}{=} -3\delta_{i,0}L\epsilon^{-2} + \delta_{i,\mathrm{t}}\left(\frac{9}{2}L^2\epsilon^{-1} + \frac{7}{2}L^3\right) + \delta_{j,0}\left[-\frac{1}{3}L^3\epsilon^{-1} - \frac{5}{12}L^4\right.$$
$$\left. - 3L\epsilon^{-2} - (2 + l_{ij} - l_1)L^2\epsilon^{-1} + \left(\frac{2}{3} - l_{ij} + \frac{5}{3}l_1\right)L^3\right]$$
$$+ \delta_{j,\mathrm{t}}\left[\frac{1}{3}L^4 + \frac{3}{2}L^2\epsilon^{-1} + \left(\frac{5}{2} + \frac{4}{3}l_{ij} - l_1 - \frac{1}{3}l_j\right)L^3\right], \quad (\text{A.13})$$

where the UV singularities

$$D_3^{\mathrm{UV}}(m_1,m_2,M_3;p_i,p_j) \overset{\text{NLL}}{=} -3L^2\epsilon^{-1} - 2L^3,$$

$$D_3^{\mathrm{UV}}(m_1,m_2,0;p_i,p_j) \overset{\text{NLL}}{=} -3\left(\delta_{i,0} + \delta_{j,0}\right)\epsilon^{-3} + \left(\delta_{i,\mathrm{t}} + \delta_{j,\mathrm{t}}\right)\left(3L\epsilon^{-2} + \frac{3}{2}L^2\epsilon^{-1} + \frac{1}{2}L^3\right)$$
$$(\text{A.14})$$

have been subtracted.

Diagram 4.

$$\tilde{\mathcal{M}}_2^{4,ij} \overset{\text{NLL}}{=} -\mathcal{M}_0 \sum_{V_1,V_2=A,Z,W^\pm} I_i^{V_2} I_i^{\bar{V}_2} I_i^{V_1} I_j^{\bar{V}_1} D_4(M_{V_1},M_{V_2};p_i,p_j),$$
$$(\text{A.15})$$

where the loop integral D_4 is defined in (B.6) and yields

$$D_4(M_1,m_2;p_i,p_j) \overset{\text{NLL}}{=} \frac{1}{3}L^3,$$

$$D_4(0, M_2; p_i, p_j) \overset{\text{NLL}}{=} (\delta_{i,0} + \delta_{j,0}) \left(L\epsilon^{-2} + L^2\epsilon^{-1} + \frac{2}{3}L^3 \right) - \frac{1}{2}\delta_{i,\text{t}} \left(L^2\epsilon^{-1} + L^3 \right)$$

$$- \delta_{j,\text{t}} \left(\frac{3}{2}L^2\epsilon^{-1} + \frac{17}{6}L^3 \right),$$

$$D_4(0, 0; p_i, p_j) \overset{\text{NLL}}{=} -\delta_{i,0}\delta_{j,0}\,\epsilon^{-3} + \delta_{i,\text{t}}\delta_{j,0} \left(\epsilon^{-3} + 3L\epsilon^{-2} + \frac{5}{2}L^2\epsilon^{-1} + \frac{3}{2}L^2 \right)$$

$$+ \delta_{i,0}\delta_{j,\text{t}} \left(-\frac{2}{3}\epsilon^{-3} + \frac{1}{3}L\epsilon^{-2} + \frac{1}{6}L^2\epsilon^{-1} + \frac{1}{18}L^3 \right)$$

$$- \delta_{i,\text{t}}\delta_{j,\text{t}} \left(2L\epsilon^{-2} + 8L^2\epsilon^{-1} + \frac{38}{3}L^3 \right). \tag{A.16}$$
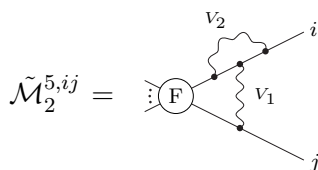
Here the UV singularities

$$D_4^{\text{UV}}(M_1, m_2; p_i, p_j) \overset{\text{NLL}}{=} L^2\epsilon^{-1} + \frac{2}{3}L^3,$$

$$D_4^{\text{UV}}(0, m_2; p_i, p_j) \overset{\text{NLL}}{=} (\delta_{i,0} + \delta_{j,0})\,\epsilon^{-3} - (\delta_{i,\text{t}} + \delta_{j,\text{t}}) \left(L\epsilon^{-2} + \frac{1}{2}L^2\epsilon^{-1} + \frac{1}{6}L^3 \right) \tag{A.17}$$

have been subtracted.

Diagram 4 and the following diagram 5 are the only cases where fermion masses in the numerator of the fermion line i contribute to the result in NLL accuracy. In principle, these fermion-mass terms contribute with generators I_i^V and $\hat{I}_i^V$, belonging to representations with different chiralities [see (2.29)]. But we found that this happens only in the case when both gauge bosons V_1 and V_2 are photons, such that $\hat{I}_i^A = I_i^A$. Thus all contributions to (A.15) and (A.18) can be expressed in terms of the operators I_i^V, I_j^V, which belong to the representations associated with the chiralities κ_i, κ_j of the external fermions.

Diagram 5.

$$\tilde{\mathcal{M}}_2^{5,ij} = \quad \quad \overset{\text{NLL}}{=} -\mathcal{M}_0 \sum_{V_1, V_2 = A, Z, W^\pm} I_i^{V_2} I_i^{V_1} I_j^{\bar{V}_2} I_j^{\bar{V}_1} D_5(M_{V_1}, M_{V_2}; p_i, p_j),$$
$$\tag{A.18}$$

where the loop integral D_5 is defined in (B.6) and to NLL accuracy is given by D_4, up to a minus sign:

$$D_5(m_1, m_2; p_i, p_j) \overset{\text{NLL}}{=} -D_4(m_1, m_2; p_i, p_j). \tag{A.19}$$

Note that this relation only holds if the fermion-mass terms in the numerator along the line i are correctly taken into account.

Diagrams 6.

$$\tilde{\mathcal{M}}_2^{6,ij} \overset{\text{NLL}}{=} \frac{1}{2}\frac{g_2^2}{e^2}\mathcal{M}_0 \sum_{V_1,V_2,V_3,V_4=A,Z,W^\pm} I_i^{\bar{V}_1} I_j^{\bar{V}_4}\, \varepsilon^{V_1\bar{V}_2\bar{V}_3}\varepsilon^{V_4V_2V_3}\, D_6(M_{V_1},M_{V_2},M_{V_3},M_{V_4};p_i,p_j), \tag{A.20}$$

where the loop integral D_6 is defined in (B.6) and yields

$$D_6(M_1,m_2,m_3,M_4;p_i,p_j) \overset{\text{NLL}}{=} \frac{20}{9}L^3,$$

$$D_6(0,M_2,M_3,M_4;p_i,p_j) \overset{\text{NLL}}{=} \frac{20}{9}L^3 + \frac{M_2^2+M_3^2}{2M_4^2}\left[(\delta_{i,0}+\delta_{j,0})\left(-8L\epsilon^{-2}-4L^2\epsilon^{-1}+\frac{8}{3}L^3\right)\right.$$

$$\left. + (\delta_{i,\text{t}}+\delta_{j,\text{t}})\left(8L^2\epsilon^{-1}+12L^3\right)\right],$$

$$D_6(M_1,M_2,M_3,0;p_i,p_j) = D_6(0,M_2,M_3,M_1;p_i,p_j),$$

$$D_6(0,M_2,M_3,0;p_i,p_j) \overset{\text{NLL}}{=} (\delta_{i,0}+\delta_{j,0})\left(\frac{10}{3}L\epsilon^{-2}+\frac{5}{3}L^2\epsilon^{-1}\right)$$

$$- (\delta_{i,\text{t}}+\delta_{j,\text{t}})\left(\frac{10}{3}L^2\epsilon^{-1}+\frac{35}{9}L^3\right). \tag{A.21}$$

Here the UV singularities
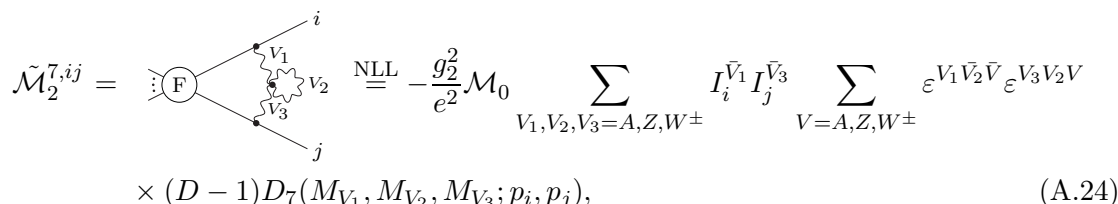
$$D_6^{\text{UV}}(M_1,m_2,m_3,M_4;p_i,p_j) \overset{\text{NLL}}{=} \frac{10}{3}L^2\epsilon^{-1}+\frac{20}{9}L^3,$$

$$D_6^{\text{UV}}(0,m_2,m_3,M_4;p_i,p_j) \overset{\text{NLL}}{=} \frac{10}{3}L^2\epsilon^{-1}+\frac{20}{9}L^3 + \frac{m_2^2+m_3^2}{2M_4^2}\left[(\delta_{i,0}+\delta_{j,0})\left(-8\epsilon^{-3}\right.\right.$$

$$\left.\left. + 4L^2\epsilon^{-1}+\frac{8}{3}L^3\right) + (\delta_{i,\text{t}}+\delta_{j,\text{t}})\left(8L\epsilon^{-2}+8L^2\epsilon^{-1}+4L^3\right)\right],$$

$$D_6^{\text{UV}}(M_1,m_2,m_3,0;p_i,p_j) = D_6^{\text{UV}}(0,m_2,m_3,M_1;p_i,p_j),$$

$$D_6^{\text{UV}}(0,m_2,m_3,0;p_i,p_j) \overset{\text{NLL}}{=} \frac{10}{3}(\delta_{i,0}+\delta_{j,0})\,\epsilon^{-3}$$

$$- (\delta_{i,\text{t}}+\delta_{j,\text{t}})\left(\frac{10}{3}L\epsilon^{-2}+\frac{5}{3}L^2\epsilon^{-1}+\frac{5}{9}L^3\right) \tag{A.22}$$

have been subtracted. We observe that the loop integrals associated with A–Z mixing-energy subdiagrams give rise to the contributions

$$\Delta D_6(0,M_\text{W},M_\text{W},M_\text{Z};p_i,p_j) \overset{\text{NLL}}{=} \frac{M_\text{W}^2}{M_\text{Z}^2}\left[(\delta_{i,0}+\delta_{j,0})\left(-8L\epsilon^{-2}-4L^2\epsilon^{-1}+\frac{8}{3}L^3\right)\right.$$

$$\left. + (\delta_{i,\text{t}}+\delta_{j,\text{t}})\left(8L^2\epsilon^{-1}+12L^3\right)\right], \tag{A.23}$$

which depend linearly on the ratio M_W^2/M_Z^2. Similar terms appear also in diagrams 7, 8, 9, and 10. These terms cancel when adding all contributions owing to relations between these integrals (see appendix C), which hold also in the presence of massive external fermions.

Diagram 7.

$$\tilde{\mathcal{M}}_2^{7,ij} = \;\;\vcenter{\hbox{[F]}}\;\; \overset{\mathrm{NLL}}{=} -\frac{g_2^2}{e^2}\mathcal{M}_0 \sum_{V_1,V_2,V_3=A,Z,W^\pm} I_i^{\bar{V}_1} I_j^{\bar{V}_3} \sum_{V=A,Z,W^\pm} \varepsilon^{V_1\bar{V}_2\bar{V}} \varepsilon^{V_3 V_2 V}$$
$$\times (D-1)D_7(M_{V_1},M_{V_2},M_{V_3};p_i,p_j), \qquad (A.24)$$

where $D = 4 - 2\epsilon$. The loop integral D_7 is defined in (B.6) and yields
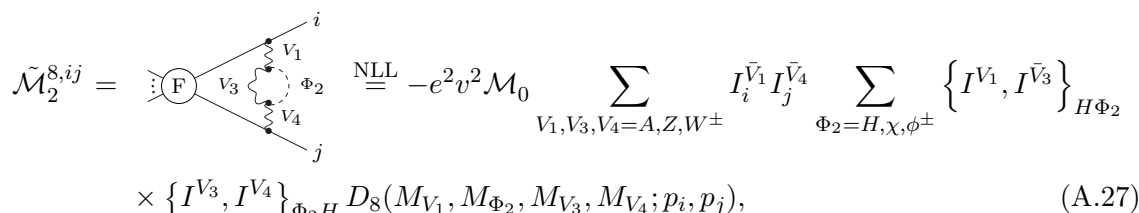
$$D_7(M_1,m_2,M_3;p_i,p_j) \overset{\mathrm{NLL}}{=} 0,$$
$$D_7(0,M_2,M_3;p_i,p_j) \overset{\mathrm{NLL}}{=} \frac{M_2^2}{M_3^2}\left[(\delta_{i,0}+\delta_{j,0})\left(-L\epsilon^{-2}-\frac{1}{2}L^2\epsilon^{-1}+\frac{1}{3}L^3\right)\right.$$
$$\left. + (\delta_{i,\mathrm{t}}+\delta_{j,\mathrm{t}})\left(L^2\epsilon^{-1}+\frac{3}{2}L^3\right)\right],$$
$$D_7(M_1,M_2,0;p_i,p_j) = D_7(0,M_2,M_1;p_i,p_j),$$
$$D_7(0,M_2,0;p_i,p_j) \overset{\mathrm{NLL}}{=} 0, \qquad (A.25)$$

where the UV singularities

$$D_7^{\mathrm{UV}}(0,M_2,M_3;p_i,p_j) \overset{\mathrm{NLL}}{=} \frac{M_2^2}{M_3^2}\left[(\delta_{i,0}+\delta_{j,0})\left(-\epsilon^{-3}+\frac{1}{2}L^2\epsilon^{-1}+\frac{1}{3}L^3\right)\right.$$
$$\left. + (\delta_{i,\mathrm{t}}+\delta_{j,\mathrm{t}})\left(L\epsilon^{-2}+L^2\epsilon^{-1}+\frac{1}{2}L^3\right)\right],$$
$$D_7^{\mathrm{UV}}(M_1,M_2,0;p_i,p_j) = D_7^{\mathrm{UV}}(0,M_2,M_1;p_i,p_j) \qquad (A.26)$$

have been subtracted.

Diagram 8.

$$\tilde{\mathcal{M}}_2^{8,ij} = \;\;\vcenter{\hbox{[F]}}\;\; \overset{\mathrm{NLL}}{=} -e^2v^2\mathcal{M}_0 \sum_{V_1,V_3,V_4=A,Z,W^\pm} I_i^{\bar{V}_1} I_j^{\bar{V}_4} \sum_{\Phi_2=H,\chi,\phi^\pm} \left\{I^{V_1},I^{\bar{V}_3}\right\}_{H\Phi_2}$$
$$\times \left\{I^{V_3},I^{V_4}\right\}_{\Phi_2 H} D_8(M_{V_1},M_{\Phi_2},M_{V_3},M_{V_4};p_i,p_j), \qquad (A.27)$$

where the curly brackets denote anticommutators and v is the vacuum expectation value. The loop integral D_8 is defined in (B.6) and yields

$$M_W^2 D_8(M_1,M_2,m_3,M_4;p_i,p_j) \overset{\mathrm{NLL}}{=} 0,$$

$$D_8(0, M_2, M_3, M_4; p_i, p_j) \overset{\text{NLL}}{=} \frac{1}{M_4^2} \Bigg[(\delta_{i,0} + \delta_{j,0}) \left(-L\epsilon^{-2} - \frac{1}{2}L^2\epsilon^{-1} + \frac{1}{3}L^3 \right)$$

$$+ (\delta_{i,\text{t}} + \delta_{j,\text{t}}) \left(L^2\epsilon^{-1} + \frac{3}{2}L^3 \right) \Bigg],$$

$$D_8(M_1, M_2, M_3, 0; p_i, p_j) = D_8(0, M_2, M_3, M_1; p_i, p_j),$$

$$M_{\text{W}}^2 D_8(0, M_2, M_3, 0; p_i, p_j) \overset{\text{NLL}}{=} 0. \tag{A.28}$$

Here the UV singularities

$$D_8^{\text{UV}}(0, M_2, M_3, M_4; p_i, p_j) \overset{\text{NLL}}{=} \frac{1}{M_4^2} \Bigg[(\delta_{i,0} + \delta_{j,0}) \left(-\epsilon^{-3} + \frac{1}{2}L^2\epsilon^{-1} + \frac{1}{3}L^3 \right)$$

$$+ (\delta_{i,\text{t}} + \delta_{j,\text{t}}) \left(L\epsilon^{-2} + L^2\epsilon^{-1} + \frac{1}{2}L^3 \right) \Bigg],$$

$$D_8^{\text{UV}}(M_1, M_2, M_3, 0; p_i, p_j) = D_8^{\text{UV}}(0, M_2, M_3, M_1; p_i, p_j) \tag{A.29}$$

have been subtracted.

Diagram 9.

$$\tilde{\mathcal{M}}_2^{9,ij} = \text{(diagram)} \overset{\text{NLL}}{=} -\frac{1}{2}\mathcal{M}_0 \sum_{V_1, V_4 = A, Z, W^\pm} I_i^{\bar{V}_1} I_j^{\bar{V}_4} \sum_{\Phi_2, \Phi_3 = H, \chi, \phi^\pm} I_{\Phi_3\Phi_2}^{V_1} I_{\Phi_2\Phi_3}^{V_4}$$

$$\times D_9(M_{V_1}, M_{\Phi_2}, M_{\Phi_3}, M_{V_4}; p_i, p_j), \tag{A.30}$$

where the loop integral D_9 is defined in (B.6) and yields

$$D_9(M_1, M_2, M_3, M_4; p_i, p_j) \overset{\text{NLL}}{=} \frac{2}{9}L^3,$$

$$D_9(0, M_2, M_3, M_4; p_i, p_j) \overset{\text{NLL}}{=} \frac{2}{9}L^3 + \frac{M_2^2 + M_3^2}{2M_4^2} \Bigg[(\delta_{i,0} + \delta_{j,0}) \left(2L\epsilon^{-2} + L^2\epsilon^{-1} - \frac{2}{3}L^3 \right)$$

$$- (\delta_{i,\text{t}} + \delta_{j,\text{t}}) \left(2L^2\epsilon^{-1} + 3L^3 \right) \Bigg],$$

$$D_9(M_1, M_2, M_3, 0; p_i, p_j) = D_9(0, M_2, M_3, M_1; p_i, p_j),$$

$$D_9(0, M_2, M_3, 0; p_i, p_j) \overset{\text{NLL}}{=} (\delta_{i,0} + \delta_{j,0}) \left(\frac{1}{3}L\epsilon^{-2} + \frac{1}{6}L^2\epsilon^{-1} \right)$$

$$- (\delta_{i,\text{t}} + \delta_{j,\text{t}}) \left(\frac{1}{3}L^2\epsilon^{-1} + \frac{7}{18}L^3 \right). \tag{A.31}$$

Here the UV singularities

$$D_9^{\text{UV}}(M_1, M_2, M_3, M_4; p_i, p_j) \overset{\text{NLL}}{=} \frac{1}{3}L^2\epsilon^{-1} + \frac{2}{9}L^3,$$

$$D_9^{\mathrm{UV}}(0, M_2, M_3, M_4; p_i, p_j) \overset{\mathrm{NLL}}{=} \frac{1}{3}L^2\epsilon^{-1} + \frac{2}{9}L^3 + \frac{M_2^2 + M_3^2}{2M_4^2}\left[(\delta_{i,0} + \delta_{j,0})\left(2\epsilon^{-3} - L^2\epsilon^{-1}\right.\right.$$

$$\left.\left. - \frac{2}{3}L^3\right) - (\delta_{i,\mathrm{t}} + \delta_{j,\mathrm{t}})\left(2L\epsilon^{-2} + 2L^2\epsilon^{-1} + L^3\right)\right],$$

$$D_9^{\mathrm{UV}}(M_1, M_2, M_3, 0; p_i, p_j) = D_9^{\mathrm{UV}}(0, M_2, M_3, M_1; p_i, p_j),$$

$$D_9^{\mathrm{UV}}(0, M_2, M_3, 0; p_i, p_j) \overset{\mathrm{NLL}}{=} \frac{1}{3}(\delta_{i,0} + \delta_{j,0})\epsilon^{-3}$$

$$- (\delta_{i,\mathrm{t}} + \delta_{j,\mathrm{t}})\left(\frac{1}{3}L\epsilon^{-2} + \frac{1}{6}L^2\epsilon^{-1} + \frac{1}{18}L^3\right) \qquad (A.32)$$

have been subtracted.

Diagram 10.

$$\tilde{\mathcal{M}}_2^{10,ij} = \quad \text{<image>} \quad \overset{\mathrm{NLL}}{=} -\frac{1}{2}\mathcal{M}_0 \sum_{V_1,V_3 = A,Z,W^\pm} I_i^{\bar{V}_1} I_j^{\bar{V}_3} \sum_{\Phi_2 = H,\chi,\phi^\pm} \{I^{V_1}, I^{V_3}\}_{\Phi_2\Phi_2}$$

$$\times D_{10}(M_{V_1}, M_{\Phi_2}, M_{V_3}; p_i, p_j), \qquad (A.33)$$

where

$$D_{10} \equiv D_7. \qquad (A.34)$$

Diagram 11. For the diagrams involving fermionic self-energy subdiagrams we consider the contributions of a generic fermionic doublet Ψ with components $\Psi_i = u, d$. The sum over the three generations of leptons and quarks is denoted by $\sum_\Psi$, and colour factors are implicitly understood. Assuming that all down-type fermions are massless, $m_d = 0$, and that the masses of up-type fermions are $m_u = 0$ or m_t, we have

$$\tilde{\mathcal{M}}_2^{11,ij} = \quad \text{<image>} \quad \overset{\mathrm{NLL}}{=} -\frac{1}{2}\mathcal{M}_0 \sum_{V_1,V_4 = A,Z,W^\pm} I_i^{\bar{V}_1} I_j^{\bar{V}_4}$$

$$\times \sum_\Psi \left\{ \sum_{\Psi_{i_2},\Psi_{i_3}=u,d} \sum_{\kappa=\mathrm{R},\mathrm{L}} I_{\Psi_{i_3}^\kappa \Psi_{i_2}^\kappa}^{V_1} I_{\Psi_{i_2}^\kappa \Psi_{i_3}^\kappa}^{V_4} D_{11,0}(M_{V_1}, m_{i_2}, m_{i_3}, M_{V_4}; p_i, p_j)\right.$$

$$\left. - \left(I_{u^\mathrm{R}u^\mathrm{R}}^{V_1} I_{u^\mathrm{L}u^\mathrm{L}}^{V_4} + I_{u^\mathrm{L}u^\mathrm{L}}^{V_1} I_{u^\mathrm{R}u^\mathrm{R}}^{V_4}\right)m_u^2 D_{11,m}(M_{V_1}, m_u, m_u, M_{V_4}; p_i, p_j)\right\}, \quad (A.35)$$

where $D_{11,m} \equiv -4D_8$ represents the contribution associated with the m_u-terms in the numerator of the up-type fermion propagators of the loop insertion, whereas the integral $D_{11,0}$, which is defined in (B.6), accounts for the remaining contributions. This latter integral yields

$$D_{11,0}(M_1, m_2, m_3, M_4; p_i, p_j) \overset{\mathrm{NLL}}{=} \frac{8}{9}L^3,$$

$$D_{11,0}(0, m_2, m_3, M_4; p_i, p_j) \stackrel{\mathrm{NLL}}{=} \frac{8}{9}L^3 + \frac{m_2^2 + m_3^2}{2M_4^2}\left[(\delta_{i,0} + \delta_{j,0})\left(4L\epsilon^{-2} + 2L^2\epsilon^{-1} - \frac{4}{3}L^3\right)\right.$$
$$\left. - (\delta_{i,\mathrm{t}} + \delta_{j,\mathrm{t}})\left(4L^2\epsilon^{-1} + 6L^3\right)\right],$$
$$D_{11,0}(M_1, m_2, m_3, 0; p_i, p_j) = D_{11,0}(0, m_2, m_3, M_1; p_i, p_j),$$
$$D_{11,0}(0, M_2, M_3, 0; p_i, p_j) \stackrel{\mathrm{NLL}}{=} (\delta_{i,0} + \delta_{j,0})\left(\frac{4}{3}L\epsilon^{-2} + \frac{2}{3}L^2\epsilon^{-1}\right)$$
$$- (\delta_{i,\mathrm{t}} + \delta_{j,\mathrm{t}})\left(\frac{4}{3}L^2\epsilon^{-1} + \frac{14}{9}L^3\right),$$
$$D_{11,0}(0, 0, 0, 0; p_i, p_j) \stackrel{\mathrm{NLL}}{=} -(\delta_{i,0} + \delta_{j,0})\epsilon^{-3} + (\delta_{i,\mathrm{t}} + \delta_{j,\mathrm{t}})\left(\frac{2}{3}L\epsilon^{-2} - \frac{2}{9}L^3\right), \quad \text{(A.36)}$$

where the UV singularities

$$D_{11,0}^{\mathrm{UV}}(M_1, m_2, m_3, M_4; p_i, p_j) \stackrel{\mathrm{NLL}}{=} \frac{4}{3}L^2\epsilon^{-1} + \frac{8}{9}L^3,$$
$$D_{11,0}^{\mathrm{UV}}(0, m_2, m_3, M_4; p_i, p_j) \stackrel{\mathrm{NLL}}{=} \frac{4}{3}L^2\epsilon^{-1} + \frac{8}{9}L^3 + \frac{m_2^2 + m_3^2}{2M_4^2}\left[(\delta_{i,0} + \delta_{j,0})\left(4\epsilon^{-3} - 2L^2\epsilon^{-1}\right.\right.$$
$$\left.\left. - \frac{4}{3}L^3\right) - (\delta_{i,\mathrm{t}} + \delta_{j,\mathrm{t}})(4L\epsilon^{-2} + 4L^2\epsilon^{-1} + 2L^3)\right],$$
$$D_{11,0}^{\mathrm{UV}}(M_1, m_2, m_3, 0; p_i, p_j) = D_{11,0}^{\mathrm{UV}}(0, m_2, m_3, M_1; p_i, p_j),$$
$$D_{11,0}^{\mathrm{UV}}(0, m_2, m_3, 0; p_i, p_j) \stackrel{\mathrm{NLL}}{=} \frac{4}{3}(\delta_{i,0} + \delta_{j,0})\epsilon^{-3}$$
$$- (\delta_{i,\mathrm{t}} + \delta_{j,\mathrm{t}})\left(\frac{4}{3}L\epsilon^{-2} + \frac{2}{3}L^2\epsilon^{-1} + \frac{2}{9}L^3\right) \quad \text{(A.37)}$$

have been subtracted. As a consequence of

$$\Delta D_{11,0}(0, m_2, m_3, M_4; p_i, p_j) \stackrel{\mathrm{NLL}}{=} \frac{m_2^2 + m_3^2}{2}\Delta D_{11,m}(0, m_2, m_3, M_4; p_i, p_j),$$
$$\Delta D_{11,0}(M_1, m_2, m_3, 0; p_i, p_j) \stackrel{\mathrm{NLL}}{=} \frac{m_2^2 + m_3^2}{2}\Delta D_{11,m}(M_1, m_2, m_3, 0; p_i, p_j), \quad \text{(A.38)}$$

all terms proportional to the fermion masses in $\tilde{\mathcal{M}}_2^{11,ij}$ cancel.

Diagram 12.

$$\tilde{\mathcal{M}}_2^{12,ijk} = \quad \text{} \quad \stackrel{\mathrm{NLL}}{=} \mathcal{M}_0 \sum_{V_1, V_2 = A, Z, W^{\pm}} I_i^{\bar{V}_2} I_i^{\bar{V}_1} I_j^{V_1} I_k^{V_2} D_{12}(M_{V_1}, M_{V_2}; p_i, p_j, p_k),$$
$$\text{(A.39)}$$

where the loop integral D_{12} is defined in (B.6) and yields

$$D_{12}(M_1, M_2; p_i, p_j, p_k) \stackrel{\mathrm{NLL}}{=} \frac{1}{2}L^4 - \left(4 - 2l_{ik} + \frac{4}{3}l_1 + \frac{2}{3}l_2\right)L^3,$$

$$D_{12}(0, M_2; p_i, p_j, p_k) \overset{\mathrm{NLL}}{=} (\delta_{i,0} + \delta_{j,0}) \left[L^2 \epsilon^{-2} + L^3 \epsilon^{-1} + \frac{7}{12} L^4 \right.$$

$$\left. - (2 - l_{ik}) \left(2L\epsilon^{-2} + L^2\epsilon^{-1} + \frac{1}{3} L^3 \right) - l_2 \left(2L\epsilon^{-2} + 3L^2\epsilon^{-1} + \frac{7}{3} L^3 \right) \right]$$

$$+ \delta_{i,\mathrm{t}} \left[-\frac{2}{3} L^3 \epsilon^{-1} - \frac{5}{6} L^4 + (2 - 2l_{ik} + l_2 + l_i) L^2 \epsilon^{-1} + \left(\frac{2}{3} - 2l_{ik} + \frac{5}{3} l_2 + \frac{5}{3} l_i \right) L^3 \right]$$

$$+ \delta_{j,\mathrm{t}} \left[-\frac{4}{3} L^3 \epsilon^{-1} - \frac{7}{3} L^4 + (6 - 2l_{ik} - 2l_{ij} + 3l_2 + l_j) L^2 \epsilon^{-1} \right.$$

$$\left. + \left(\frac{26}{3} - 2l_{ik} - \frac{14}{3} l_{ij} + 7l_2 + \frac{7}{3} l_j \right) L^3 \right],$$

$$D_{12}(M_1, 0; p_i, p_j, p_k) \overset{\mathrm{NLL}}{=} \delta_{k,0} \left[-\frac{2}{3} L^3 \epsilon^{-1} - \frac{2}{3} L^4 + (2 - l_{ik}) \left(2L^2 \epsilon^{-1} + \frac{4}{3} L^3 \right) \right.$$

$$\left. + l_1 \left(2L^2 \epsilon^{-1} + \frac{8}{3} L^3 \right) \right] + \delta_{k,\mathrm{t}} \left[\frac{5}{6} L^4 - \left(\frac{16}{3} - \frac{10}{3} l_{ik} + \frac{8}{3} l_1 + \frac{2}{3} l_k \right) L^3 \right],$$

$$D_{12}(0, 0; p_i, p_j, p_k) \overset{\mathrm{NLL}}{=} \delta_{i,0} \delta_{j,0} \left\{ \delta_{k,0} \left[2\epsilon^{-4} + (8 - 4l_{ik}) \epsilon^{-3} \right] \right.$$

$$+ \delta_{k,\mathrm{t}} \left[\frac{2}{3} \epsilon^{-4} - \frac{4}{3} L\epsilon^{-3} - \frac{2}{3} L^2 \epsilon^{-2} - \frac{2}{9} L^3 \epsilon^{-1} - \frac{1}{18} L^4 + \frac{4}{3} (2 - 2l_{ik} + l_k) \epsilon^{-3} \right.$$

$$\left. \left. - (4 - l_{ik} - l_k) \left(\frac{4}{3} L\epsilon^{-2} + \frac{2}{3} L^2 \epsilon^{-1} + \frac{2}{9} L^3 \right) \right] \right\}$$

$$+ \delta_{i,\mathrm{t}} \delta_{j,0} \left\{ \delta_{k,0} \left[\frac{1}{2} \epsilon^{-4} - L\epsilon^{-3} + \frac{1}{3} L^3 \epsilon^{-1} + \frac{1}{4} L^4 + (2 - 2l_{ik} + l_i) \epsilon^{-3} - (4 - 2l_{ik}) L\epsilon^{-2} \right.$$

$$\left. + (l_{ik} - l_i) L^2 \epsilon^{-1} + \left(\frac{4}{3} + \frac{1}{3} l_{ik} - l_i \right) L^3 \right]$$

$$+ \delta_{k,\mathrm{t}} \left[-L\epsilon^{-3} - \frac{1}{3} L^3 \epsilon^{-1} - \frac{11}{12} L^4 - \left(l_{ik} - \frac{1}{2} l_i - \frac{1}{2} l_k \right) \epsilon^{-3} - (4 - 2l_{ik}) L\epsilon^{-2} \right.$$

$$\left. \left. - (l_{ik} - l_i) L^2 \epsilon^{-1} - \left(\frac{4}{3} + 3l_{ik} - 3l_i - \frac{2}{3} l_k \right) L^3 \right] \right\}$$

$$+ \delta_{i,0} \delta_{j,\mathrm{t}} \left\{ \delta_{k,0} \left[\frac{4}{3} \epsilon^{-4} - \frac{2}{3} L\epsilon^{-3} - \frac{1}{3} L^2 \epsilon^{-2} - \frac{1}{9} L^3 \epsilon^{-1} - \frac{1}{36} L^4 + \left(\frac{16}{3} - 2l_{ik} - \frac{4}{3} l_{ij} \right. \right. \right.$$

$$\left. \left. + \frac{2}{3} l_j \right) \epsilon^{-3} - \left(\frac{4}{3} - l_{ik} + \frac{2}{3} l_{ij} - \frac{1}{3} l_j \right) \left(2L\epsilon^{-2} + L^2 \epsilon^{-1} + \frac{1}{3} L^3 \right) \right]$$

$$
+ \delta_{k,\mathrm{t}} \Bigg[\frac{1}{2}\epsilon^{-4} - L\epsilon^{-3} + \frac{1}{3}L^3\epsilon^{-1} + \frac{1}{4}L^4 + \left(2 - \frac{5}{3}l_{ik} - \frac{1}{3}l_{ij} + \frac{1}{6}l_j + \frac{5}{6}l_k \right)\epsilon^{-3}
$$

$$
- \left(4 - \frac{4}{3}l_{ik} - \frac{2}{3}l_{ij} + \frac{1}{3}l_j - \frac{1}{3}l_k \right) L\epsilon^{-2} - \frac{1}{3}\left(l_{ik} - 4l_{ij} + 2l_j + l_k \right)L^2\epsilon^{-1}
$$

$$
+ \left(\frac{4}{3} - \frac{7}{9}l_{ik} + \frac{10}{9}l_{ij} - \frac{5}{9}l_j - \frac{4}{9}l_k \right) L^3 \Bigg] \Bigg\}
$$

$$
+ \delta_{i,\mathrm{t}}\delta_{j,\mathrm{t}} \Bigg\{ \delta_{k,0}\Bigg[-L\epsilon^{-3} + L^2\epsilon^{-2} + 2L^3\epsilon^{-1} + 2L^4 - \left(l_{ij} - \frac{1}{2}l_i - \frac{1}{2}l_j \right)\epsilon^{-3}
$$

$$
- \left(4 - 4l_{ik} + 2l_i \right)L\epsilon^{-2} + \left(4 + 2l_{ik} + 2l_{ij} - 5l_i - l_j \right)L^2\epsilon^{-1}
$$

$$
+ \left(8 + \frac{2}{3}l_{ik} + \frac{10}{3}l_{ij} - \frac{19}{3}l_i - \frac{5}{3}l_j \right)L^3 \Bigg]
$$

$$
+ \delta_{k,\mathrm{t}}\Bigg[2L^2\epsilon^{-2} + 2L^3\epsilon^{-1} + \frac{7}{6}L^4 + \left(2l_{ik} + 2l_{ij} - 2l_i - l_j - l_k \right)L\epsilon^{-2}
$$

$$
+ \left(8 - 2l_{ik} + 4l_{ij} - 3l_i - 2l_j - l_k \right)L^2\epsilon^{-1} + \left(8 - 4l_{ik} + \frac{14}{3}l_{ij} - \frac{7}{3}l_i - \frac{7}{3}l_j \right)L^3 \Bigg] \Bigg\}.
\tag{A.40}
$$

Here the UV singularities

$$
D_{12}^{\mathrm{UV}}(M_1, m_2; p_i, p_j, p_k) \overset{\mathrm{NLL}}{=} -4L^2\epsilon^{-1} - \frac{8}{3}L^3,
$$

$$
D_{12}^{\mathrm{UV}}(0, m_2; p_i, p_j, p_k) \overset{\mathrm{NLL}}{=} -4\left(\delta_{i,0} + \delta_{j,0} \right)\epsilon^{-3} + \left(\delta_{i,\mathrm{t}} + \delta_{j,\mathrm{t}} \right)\left(4L\epsilon^{-2} + 2L^2\epsilon^{-1} + \frac{2}{3}L^3 \right)
\tag{A.41}
$$

have been subtracted. While the above diagram, to NLL accuracy, does not depend on r_{ij} and r_{jk} for $p_j^2 = 0$, a dependency on r_{ij} is introduced for $p_j^2 = m_\mathrm{t}^2$.

Diagram 13.

$$
\tilde{\mathcal{M}}_2^{13,ijk} = \quad \overset{\mathrm{NLL}}{=} -\mathrm{i}\frac{g_2}{e}\mathcal{M}_0 \sum_{V_1,V_2,V_3=A,Z,W^\pm} \varepsilon^{V_1V_2V_3} I_i^{\bar{V}_1} I_j^{\bar{V}_2} I_k^{\bar{V}_3}
$$

$$
\times D_{13}(M_{V_1}, M_{V_2}, M_{V_3}; p_i, p_j, p_k),
\tag{A.42}
$$

where the loop integral D_{13} is defined in (B.6). This integral is free of UV singularities and yields

$$
D_{13}(M_1, M_2, M_3; p_i, p_j, p_k) \overset{\mathrm{NLL}}{=} 0,
$$

$$
D_{13}(0, M_2, M_3; p_i, p_j, p_k) \overset{\mathrm{NLL}}{=} \left(l_{ij} - l_{ik} \right)\left[\delta_{i,0}\left(L^2\epsilon^{-1} + \frac{5}{3}L^3 \right) - \frac{2}{3}\delta_{i,\mathrm{t}}L^3 \right]
$$

$$
+ \frac{1}{3}\delta_{i,\mathrm{t}}\left(l_2 - l_3 \right)L^3,
$$

$$D_{13}(M_1, 0, M_3; p_i, p_j, p_k) = D_{13}(0, M_3, M_1; p_j, p_k, p_i),$$
$$D_{13}(M_1, M_2, 0; p_i, p_j, p_k) = D_{13}(0, M_1, M_2; p_k, p_i, p_j). \qquad (A.43)$$

When one of the gauge bosons is a photon, it couples to two W bosons with equal masses, so the terms with the mass-dependent logarithms l_1, l_2, l_3 in (A.43) vanish in all physically relevant cases.

Diagram 14.

$$\tilde{\mathcal{M}}_2^{14,ijkl} = \quad \text{} \quad \overset{\text{NLL}}{=} \mathcal{M}_0 \sum_{V_1, V_2 = A, Z, W^\pm} I_i^{\bar{V}_1} I_j^{V_1} I_k^{\bar{V}_2} I_l^{V_2} D_{14}(M_{V_1}, M_{V_2}; p_i, p_j, p_k, p_l),$$

$$(A.44)$$

where the loop integral D_{14} is simply given by the product of one-loop integrals (A.3),

$$D_{14}(M_{V_1}, M_{V_2}; p_i, p_j, p_k, p_l) = D_0(M_{V_1}; p_i, p_j) \, D_0(M_{V_2}; p_k, p_l). \qquad (A.45)$$

Sum of two-loop diagrams involving gauge interactions. The complete contribution of all factorizable diagrams not involving Yukawa contributions is obtained by inserting the above results into (3.4). For the case of massless external fermions, we have explained in detail in appendix E of ref. [32] how the factorizable two-loop diagrams can be summed up to the total two-loop amplitude. To this purpose we have used relations between the scalar loop integrals which are listed in appendix B of ref. [32] and are valid in NLL approximation. For the general case of diagrams with massive and massless fermions, these relations receive only minor modifications which we indicate in appendix C of the present paper. Apart from that, the whole procedure remains exactly the same. So here we only present the result and refer to ref. [32] for more details.

The factorizable two-loop contributions can be written in the form

$$\tilde{\mathcal{M}}_2^{\mathrm{F}} \overset{\text{NLL}}{=} \mathcal{M}_0 \left\{ \frac{1}{2} \left[F_1^{\mathrm{F,sew}} \right]^2 + F_1^{\mathrm{F,sew}} \Delta F_1^{\mathrm{F,em}} + F_1^{\mathrm{F,sew}} \Delta F_1^{\mathrm{F,Z}} \right.$$

$$\left. + \frac{1}{2} \left[\Delta F_1^{\mathrm{F,em}} \right]^2 + \Delta F_1^{\mathrm{F,Z}} \Delta F_1^{\mathrm{F,em}} + G_2^{\mathrm{F,sew}} + \Delta G_2^{\mathrm{F,em}} \right\}, \qquad (A.46)$$

where the one-loop terms are given in (A.6). The additional two-loop terms read

$$e^2 G_2^{\mathrm{F,sew}} = \frac{1}{2} \sum_{i=1}^n \left[b_1^{(1)} g_1^2 \left(\frac{Y_i}{2} \right)^2 + b_2^{(1)} g_2^2 C_i \right] J(\epsilon, M_{\mathrm{W}}, Q^2; p_i, p_i),$$

$$\Delta G_2^{\mathrm{F,em}} = \frac{1}{2} \sum_{i=1}^n Q_i^2 \left\{ b_e^{(1)} \left[\Delta J(\epsilon, 0, Q^2; p_i, p_i) - \Delta J(\epsilon, 0, M_{\mathrm{W}}^2; p_i, p_i) \right] \right.$$

$$\left. + b_{\mathrm{QED}}^{(1)} \Delta J(\epsilon, 0, M_{\mathrm{W}}^2; p_i, p_i) \right\}, \qquad (A.47)$$

with the one-loop β-function coefficients (4.5) and (4.6), the SU(2) Casimir operator (2.18), and the two-loop functions

$$J(\epsilon, m, \mu^2; p_i, p_j) = \frac{1}{\epsilon}\left[I(2\epsilon, m; p_i, p_j) - \left(\frac{Q^2}{\mu^2}\right)^\epsilon I(\epsilon, m; p_i, p_j)\right],$$

$$\Delta J(\epsilon, m, \mu^2; p_i, p_j) = J(\epsilon, m, \mu^2; p_i, p_j) - J(\epsilon, M_{\mathrm{W}}, \mu^2; p_i, p_j), \qquad (A.48)$$

for $m = M_{\mathrm{W}}, M_{\mathrm{Z}}, 0$, which are combinations of one-loop functions I. The expressions (A.47) rely on the fact that the J-function, to NLL accuracy, involves only the LL parts of the I-function. In particular, no angular-dependent l_{ij}-terms are relevant for the J-function, so the identity (4.20) yields

$$J(\epsilon, m, \mu^2; p_i, p_j) \stackrel{\mathrm{NLL}}{=} \frac{1}{2}\Big[J(\epsilon, m, \mu^2; p_i, p_i) + J(\epsilon, m, \mu^2; p_j, p_j)\Big], \qquad (A.49)$$

and (4.21) can be generalized to the functions J and ΔJ.

In order to combine the terms in (A.47) with (5.5) we use

$$-\frac{1}{\epsilon}\left[\left(\frac{Q^2}{\mu_{\mathrm{R}}^2}\right)^\epsilon - 1\right]I(\epsilon, m; p_i, p_j) = J(\epsilon, m, \mu_{\mathrm{R}}^2; p_i, p_j) - J(\epsilon, m, Q^2; p_i, p_j) \qquad (A.50)$$

and a corresponding relation between ΔI and ΔJ.

A.3 Yukawa diagrams

Most diagrams with scalar bosons coupling to external fermions are suppressed, as explained in section 3.2.3. The only relevant Yukawa contributions from bare diagrams are presented in the following.

Yukawa diagram 1.

$$\tilde{\mathcal{M}}_2^{\mathrm{Y},1,ij} = \quad \raisebox{-1em}{} \quad \stackrel{\mathrm{NLL}}{=} -\frac{1}{e^2}\mathcal{M}_0 \sum_{V_1 = A, Z, W^\pm} \sum_{\Phi_2 = H, \chi, \phi^\pm} \hat{G}_i^{\Phi_2^+} G_i^{\Phi_2} I_i^{V_1} I_j^{\bar{V}_1}$$

$$\times D_{\mathrm{Y},1}(M_{V_1}, M_{\Phi_2}; p_i, p_j). \qquad (A.51)$$

The loop integral $D_{\mathrm{Y},1}$ is defined in (B.6) and yields

$$D_{\mathrm{Y},1}(m_1, M_2; p_i, p_j) \stackrel{\mathrm{NLL}}{=} D_{\mathrm{Y}}(m_1; p_i, p_j) \qquad (A.52)$$

with
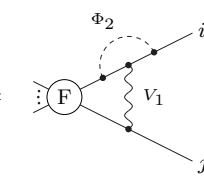
$$D_{\mathrm{Y}}(M_1; p_i, p_j) \stackrel{\mathrm{NLL}}{=} \frac{1}{6}L^3,$$

$$D_{\mathrm{Y}}(0; p_i, p_j) \stackrel{\mathrm{NLL}}{=} (\delta_{i,0} + \delta_{j,0})\left(\frac{1}{2}L\epsilon^{-2} + \frac{1}{2}L^2\epsilon^{-1} + \frac{1}{3}L^3\right) - \delta_{i,\mathrm{t}}\left(\frac{1}{4}L^2\epsilon^{-1} + \frac{1}{4}L^3\right)$$

$$- \delta_{j,\mathrm{t}}\left(\frac{3}{4}L^2\epsilon^{-1} + \frac{17}{12}L^3\right), \qquad (A.53)$$

where the UV singularities

$$D_{\mathrm{Y}}^{\mathrm{UV}}(M_1; p_i, p_j) \stackrel{\mathrm{NLL}}{=} \frac{1}{2} L^2 \epsilon^{-1} + \frac{1}{3} L^3,$$

$$D_{\mathrm{Y}}^{\mathrm{UV}}(0; p_i, p_j) \stackrel{\mathrm{NLL}}{=} \frac{1}{2} \left(\delta_{i,0} + \delta_{j,0} \right) \epsilon^{-3} - \left(\delta_{i,\mathrm{t}} + \delta_{j,\mathrm{t}} \right) \left(\frac{1}{2} L \epsilon^{-2} + \frac{1}{4} L^2 \epsilon^{-1} + \frac{1}{12} L^3 \right)$$

$$\text{(A.54)}$$
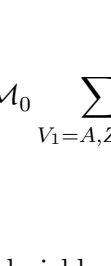
have been subtracted.

Yukawa diagram 2.

$$\tilde{\mathcal{M}}_2^{\mathrm{Y},2,ij} = \quad \stackrel{\mathrm{NLL}}{=} -\frac{1}{e^2} \mathcal{M}_0 \sum_{V_1 = A,Z,W^\pm} \sum_{\Phi_2 = H,\chi,\phi^\pm} \hat{G}_i^{\Phi_2^+} \hat{I}_i^{V_1} G_i^{\Phi_2} I_j^{\bar{V}_1}$$

$$\times D_{\mathrm{Y},2}(M_{V_1}, M_{\Phi_2}; p_i, p_j).$$

$$\text{(A.55)}$$

The loop integral $D_{\mathrm{Y},2}$ is defined in (B.6) and yields

$$D_{\mathrm{Y},2}(m_1, M_2; p_i, p_j) \stackrel{\mathrm{NLL}}{=} -D_{\mathrm{Y}}(m_1; p_i, p_j) \qquad \text{(A.56)}$$

with $D_{\mathrm{Y}}(m_1; p_i, p_j)$ from (A.53).

Yukawa diagram 3.

$$\tilde{\mathcal{M}}_2^{\mathrm{Y},3,ij} = \quad \stackrel{\mathrm{NLL}}{=} \frac{1}{e^2} \mathcal{M}_0 \sum_{\Phi_1, \Phi_2 = H,\chi,\phi^\pm} \hat{G}_i^{\Phi_2^+} G_i^{\Phi_1} \sum_{V_3 = A,Z,W^\pm} I_j^{\bar{V}_3} I_{\Phi_1 \Phi_2}^{V_3}$$

$$\times D_{\mathrm{Y},3}(M_{\Phi_1}, M_{\Phi_2}, M_{V_3}; p_i, p_j).$$

$$\text{(A.57)}$$

The loop integral $D_{\mathrm{Y},3}$ is defined in (B.6) and yields

$$D_{\mathrm{Y},3}(M_1, M_2, m_3; p_i, p_j) \stackrel{\mathrm{NLL}}{=} -D_{\mathrm{Y}}(m_3; p_i, p_j) \qquad \text{(A.58)}$$

with $D_{\mathrm{Y}}(m_3; p_i, p_j)$ from (A.53).

B. Definition of the loop integrals

In this appendix, we list the explicit expressions for the Feynman integrals that contribute to the one- and two-loop diagrams discussed in appendix A. In order to keep our expressions as compact as possible we define the momenta

$$\begin{aligned}
k_1 &= p_i + l_1, & k_2 &= p_i + l_2, & k_3 &= p_i + l_1 + l_2, \\
q_1 &= p_j - l_1, & q_2 &= p_j - l_2, & q_3 &= p_j - l_1 - l_2, & l_3 &= -l_1 - l_2, \\
r_1 &= p_k - l_1, & r_2 &= p_k - l_2, & r_3 &= p_k - l_1 + l_2, & l_4 &= l_1 - l_2.
\end{aligned} \qquad \text{(B.1)}$$

For propagators with mass m we use the notation

$$P(q, m) = q^2 - m^2 + i0 \tag{B.2}$$

and for triple gauge-boson couplings we write

$$\Gamma^{\mu_1\mu_2\mu_3}(l_1, l_2, l_3) = g^{\mu_1\mu_2}(l_1 - l_2)^{\mu_3} + g^{\mu_2\mu_3}(l_2 - l_3)^{\mu_1} + g^{\mu_3\mu_1}(l_3 - l_1)^{\mu_2}. \tag{B.3}$$

The normalization factors occurring in (2.9) are absorbed into the integration measure

$$\mathrm{d}\tilde{l}_i = (4\pi)^2 \left(\frac{4\pi\mu_{\mathrm{D}}^2}{e^{\gamma_{\mathrm{E}}}Q^2} \right)^{D/2-2} \mu_{\mathrm{D}}^{4-D} \frac{\mathrm{d}^D l_i}{(2\pi)^D} = \frac{1}{\pi^2} \left(e^{\gamma_{\mathrm{E}}}Q^2\pi \right)^{2-D/2} \mathrm{d}^D l_i, \tag{B.4}$$

and for the projection introduced in (3.12) we use the equality

$$\Pi_{ij} \left(\omega_{\kappa_i}\Gamma \right) = \frac{1}{2}\Pi_{ij} \left(\Gamma \right), \tag{B.5}$$

which holds if Γ does not involve γ_5 or $\omega_{\mathrm{R,L}}$, as it is the case in the following equations. We have explicitly verified that the NLL contributions from the projector $\tilde{\Pi}_{ij}$ in (3.13) cancel.

The integral functions D_h depend on the internal masses $m_1, m_2, \ldots$ and, through the momenta $p_i, p_j, \ldots$, on the kinematical invariants r_{ij} and on the masses $m_i^2 = p_i^2$ of the external particles. The definition of these integrals also involves the masses m_i', m_i'', m_i''' of the particles $\varphi_i', \varphi_i'', \varphi_i'''$ along the fermionic line i after one, two or three interactions with gauge bosons or scalar bosons, which possibly change the weak isospin of the external particle φ_i. We have found, however, that the dependence of the results on the masses along the fermionic lines is completely fixed by the external masses m_i, so we do not indicate the additional masses $m_i', \ldots$ in the arguments of the functions D_h.

With this notation we have

$$D_0(m_1; p_i, p_j) = \int \mathrm{d}\tilde{l}_1 \frac{4ik_1 q_1}{P(l_1, m_1)P(k_1, m_i')P(q_1, m_j')},$$

$$D_1(m_1, m_2; p_i, p_j) = \int \mathrm{d}\tilde{l}_1\mathrm{d}\tilde{l}_2$$
$$\times \frac{-16(k_1 q_1)(k_3 q_3)}{P(l_1, m_1)P(l_2, m_2)P(k_1, m_i')P(k_3, m_i'')P(q_1, m_j')P(q_3, m_j'')},$$

$$D_2(m_1, m_2; p_i, p_j) = \int \mathrm{d}\tilde{l}_1\mathrm{d}\tilde{l}_2$$
$$\times \frac{-16(k_1 q_3)(k_3 q_2)}{P(l_1, m_1)P(l_2, m_2)P(k_1, m_i')P(k_3, m_i'')P(q_2, m_j')P(q_3, m_j'')},$$

$$D_3(m_1, m_2, m_3; p_i, p_j) = \int \mathrm{d}\tilde{l}_1\mathrm{d}\tilde{l}_2$$
$$\times \frac{-2\Pi_{ij} \left[(\slashed{k}_3 + m_i'')\gamma^{\mu_2}(\slashed{k}_1 + m_i')\gamma^{\mu_1} \right] q_3^{\mu_3}\Gamma_{\mu_1\mu_2\mu_3}(l_1, l_2, l_3)}{P(l_1, m_1)P(l_2, m_2)P(l_3, m_3)P(k_1, m_i')P(k_3, m_i'')P(q_3, m_j')},$$

$$D_4(m_1, m_2; p_i, p_j) = \int \mathrm{d}\tilde{l}_1\mathrm{d}\tilde{l}_2$$

$$\times \frac{2\Pi_{ij}\left[(\not{k}_1 + m_i')\gamma^{\mu_2}(\not{k}_3 + m_i'')\gamma_{\mu_2}(\not{k}_1 + m_i')\not{q}_1\right]}{P(l_1,m_1)P(l_2,m_2)\left[P(k_1,m_i')\right]^2 P(k_3,m_i'')P(q_1,m_j')},$$

$$D_5(m_1,m_2;p_i,p_j) = \int d\tilde{l}_1 d\tilde{l}_2$$

$$\times \frac{2\Pi_{ij}\left[(\not{k}_1 + m_i''')\gamma^{\mu_2}(\not{k}_3 + m_i'')\not{q}_1(\not{k}_2 + m_i')\gamma_{\mu_2}\right]}{P(l_1,m_1)P(l_2,m_2)P(k_1,m_i''')P(k_3,m_i'')P(k_2,m_i')P(q_1,m_j')},$$

$$D_6(m_1,m_2,m_3,m_4;p_i,p_j) = \int d\tilde{l}_1 d\tilde{l}_2$$

$$\times \frac{-4k_1^{\mu_1}q_{1\mu_4}\left[\Gamma_{\mu_1\mu_2\mu_3}(l_1,l_2,l_3)\Gamma^{\mu_4\mu_2\mu_3}(l_1,l_2,l_3) + 2l_{2\mu_1}l_3^{\mu_4}\right]}{P(l_1,m_1)P(l_2,m_2)P(l_3,m_3)P(l_1,m_4)P(k_1,m_i')P(q_1,m_j')},$$

$$D_7(m_1,m_2,m_3;p_i,p_j) = \int d\tilde{l}_1 d\tilde{l}_2 \frac{-4k_1 q_1}{P(l_1,m_1)P(l_2,m_2)P(l_1,m_3)P(k_1,m_i')P(q_1,m_j')},$$

$$D_8(m_1,m_2,m_3,m_4;p_i,p_j) = \int d\tilde{l}_1 d\tilde{l}_2$$

$$\times \frac{-4k_1 q_1}{P(l_1,m_1)P(l_2,m_2)P(l_3,m_3)P(l_1,m_4)P(k_1,m_i')P(q_1,m_j')},$$

$$D_9(m_1,m_2,m_3,m_4;p_i,p_j) = \int d\tilde{l}_1 d\tilde{l}_2$$

$$\times \frac{4k_1^{\mu_1}q_1^{\mu_4}(l_2 - l_3)_{\mu_1}(l_2 - l_3)_{\mu_4}}{P(l_1,m_1)P(l_2,m_2)P(l_3,m_3)P(l_1,m_4)P(k_1,m_i')P(q_1,m_j')},$$

$$D_{10}(m_1,m_2,m_3;p_i,p_j) = D_7(m_1,m_2,m_3;p_i,p_j),$$

$$D_{11,0}(m_1,m_2,m_3,m_4;p_i,p_j) = \int d\tilde{l}_1 d\tilde{l}_2$$

$$\times \frac{4k_1^{\mu_1}q_1^{\mu_4}\,\mathrm{Tr}\left(\gamma_{\mu_1}\not{l}_2\gamma_{\mu_4}\not{l}_3\right)}{P(l_1,m_1)P(l_2,m_2)P(l_3,m_3)P(l_1,m_4)P(k_1,m_i')P(q_1,m_j')},$$

$$D_{11,m}(m_1,m_2,m_3,m_4;p_i,p_j) = -4D_8(m_1,m_2,m_3,m_4;p_i,p_j),$$

$$D_{12}(m_1,m_2;p_i,p_j,p_k) = \int d\tilde{l}_1 d\tilde{l}_2$$

$$\times \frac{-16(k_1q_1)(k_3r_2)}{P(l_1,m_1)P(l_2,m_2)P(k_1,m_i')P(k_3,m_i'')P(q_1,m_j')P(r_2,m_k')},$$

$$D_{13}(m_1,m_2,m_3;p_i,p_j,p_k) = \int d\tilde{l}_1 d\tilde{l}_2$$

$$\times \frac{8k_1^{\mu_1}q_2^{\mu_2}r_3^{\mu_3}\Gamma_{\mu_1\mu_2\mu_3}(-l_1,l_2,l_4)}{P(l_1,m_1)P(l_2,m_2)P(l_4,m_3)P(k_1,m_i')P(q_2,m_j')P(r_3,m_k')},$$

$$D_{14}(m_1,m_2;p_i,p_j,p_k,p_l) = D_0(m_1;p_i,p_j)D_0(m_2;p_k,p_l),$$

$$D_{Y,1}(m_1,m_2;p_i,p_j) = \int d\tilde{l}_1 d\tilde{l}_2$$

$$\times \frac{-2\Pi_{ij}\left[(\not{k}_1 + m_i')(\not{k}_3 + m_i'')(\not{k}_1 + m_i')\not{q}_1\right]}{P(l_1,m_1)P(l_2,m_2)\left[P(k_1,m_i')\right]^2 P(k_3,m_i'')P(q_1,m_j')},$$

$$D_{Y,2}(m_1, m_2; p_i, p_j) = \int d\tilde{l}_1 d\tilde{l}_2$$

$$\times \frac{-2\Pi_{ij}\left[(\slashed{k}_1 + m_i''')(\slashed{k}_3 + m_i'')\slashed{q}_1(\slashed{k}_2 + m_i')\right]}{P(l_1, m_1)P(l_2, m_2)P(k_1, m_i''')P(k_3, m_i'')P(k_2, m_i')P(q_1, m_j')},$$

$$D_{Y,3}(m_1, m_2, m_3; p_i, p_j) = \int d\tilde{l}_1 d\tilde{l}_2$$

$$\times \frac{2\Pi_{ij}\left[(\slashed{k}_3 + m_i'')(\slashed{k}_1 + m_i')\right]q_3 l_4}{P(l_1, m_1)P(l_2, m_2)P(l_3, m_3)P(k_1, m_i')P(k_3, m_i'')P(q_3, m_j')}.$$

$$(B.6)$$

The previous definitions are valid for diagrams with incoming fermions. In the case of an incoming antifermion φ_i, all masses $m_i, m_i', \ldots$ along the fermionic line i have to be multiplied by (-1), in the integral definitions (B.6) as well as in the projectors (3.12). But as mentioned in sections 2.2 and 3.2.2, the NLL results are insensitive to this transformation.

The various coupling matrices I_k^V and G_k^Φ, which are associated with the interactions along the fermionic lines $k = i, j, \ldots$, have been factorized from the loop integrals and can be found in appendix A. Here a comment is in order since, in principle, the fermion-mass terms in the numerator flip the chirality of the fermions and give rise to coupling matrices $\hat{I}_k^V$ and $\hat{G}_k^\Phi$ corresponding to opposite chirality states [see (2.29)]. However, as discussed in appendix A for the case of diagrams 4 and 5 [see text after (A.17)], we have found that the fermion-mass terms in the numerator are only relevant in the case of photon interactions, where the representations of the generators are independent of the chiralities, i.e. $\hat{I}_k^A = I_k^A$. Thus, all contributions can be expressed in terms of the operators I_k^V, which belong to the representations associated with the chiralities κ_k of the external fermions, and all coupling factors can be factorized as in appendix A.

C. Relations between loop integrals in NLL approximation

In order to combine the two-loop contributions of section A.2 we use relations between the loop integrals. These relations have been obtained from the explicit results listed in sections A.1 and A.2. They are valid after subtraction of the UV singularities and in NLL approximation.

For the case of massless fermionic particles, the relevant relations have been listed in appendix B of ref. [32]. We have found that, after only small modifications, they are all still valid for the case of massive fermionic particles. One trivial and obvious modification is the following change of arguments in the integral functions D_h:

$$D_h(\ldots; r_{ij}) \to D_h(\ldots; p_i, p_j), \quad \text{for } D_1, \ldots, D_{10}, D_{11,0}, D_{11,m}, \tag{C.1}$$

and similarly for the subtracted functions ΔD_h defined in (A.1). Many relations do not need further modifications, and we refer to appendix B of ref. [32] for them.

However, since the presence of fermion masses breaks the invariance of some diagrams with respect to an exchange of external or internal lines, certain relations obtained for massless fermions have to be modified by an appropriate reordering of arguments in the D_h-functions. We list these relations in the following. As in appendix A,

the symbols m_i are used to denote generic mass parameters, which can assume the values $m_i = M_W, M_Z, m_t, M_H$ or $m_i = 0$, and the symbols M_i are used to denote non-zero masses, i.e. $M_i = M_W, M_Z, m_t, M_H$.

In the second line of (B.2) in ref. [32] the arguments p_i, p_j have to be exchanged on the right-hand side. This relation becomes

$$D_2(m_1, m_2; p_i, p_j) = D_2(m_2, m_1; p_j, p_i). \tag{C.2}$$

In the relations (B.3) of ref. [32] the order of the mass parameters in D_2 has to be reversed, and the order of the momenta in the 3-leg integral D_{12} is now important:

$$
\begin{aligned}
D_3(M_1, m_2, m_3; p_i, p_j) &\overset{\text{NLL}}{=} \frac{1}{2} D_2(M_1, m_3; p_i, p_j) - D_4(m_3, M_1; p_i, p_j) \\
&\quad - 6 D_9(m_3, M_1, M_1, m_3; p_i, p_j), \\
\Delta D_3(M_W, M_W, m_1; p_i, p_j) &\overset{\text{NLL}}{=} \frac{1}{2} \Delta D_{12}(M_W, m_1; p_i, p_k, p_j) - \Delta D_4(m_1, M_W; p_i, p_j) \\
&\quad - 6 \Delta D_9(m_1, M_W, M_W, m_1; p_i, p_j), \\
\Delta D_3(m_1, M_W, M_W; p_i, p_j) &\overset{\text{NLL}}{=} \Delta D_3(M_W, m_1, M_W; p_i, p_j) + \Delta D_1(M_W, m_1; p_i, p_j) \\
&\quad + \Delta D_2(m_1, M_W; p_i, p_j) + \Delta D_4(M_W, m_1; p_i, p_j) \\
&\quad - \frac{1}{2} \Delta D_{12}(M_W, m_1; p_j, p_k, p_i). \tag{C.3}
\end{aligned}
$$

As in ref. [32], the first of these relations has been verified and is needed only if at most one of the masses m_2 and m_3 is zero.

The functions J and ΔJ defined in (A.48) of this paper now also depend on the external momenta p_i, p_j, and (B.6) and (B.7) of ref. [32] become

$$
\begin{aligned}
3 D_9(M_1, M_2, M_3, M_4; p_i, p_j) &\overset{\text{NLL}}{=} -J(\epsilon, M_W, Q^2; p_i, p_j), \\
3 \Delta D_9(0, M_2, M_3, 0; p_i, p_j) &\overset{\text{NLL}}{=} -\left[\Delta J(\epsilon, 0, Q^2; p_i, p_j) - \Delta J(\epsilon, 0, M_W^2; p_i, p_j) \right], \\
3\left[\Delta D_{11,0}(0,0,0,0; p_i, p_j) - \Delta D_{11,0}(0, M_2, M_3, 0; p_i, p_j) \right] &\overset{\text{NLL}}{=} -4 \Delta J(\epsilon, 0, M_W^2; p_i, p_j).
\end{aligned}
\tag{C.4}
$$

For the 3-leg integrals the order of the external momenta p_i, p_j, p_k becomes relevant and (B.8), (B.9) and (B.10) of ref. [32] generalize to

$$
\begin{aligned}
D_{12}(m_1, m_2; p_i, p_j, p_k) + D_{12}(m_2, m_1; p_i, p_k, p_j) &\overset{\text{NLL}}{=} D_0(m_1; p_i, p_j) D_0(m_2; p_i, p_k), \\
\sum_{\pi(i,j,k)} \text{sgn}(\pi(i,j,k))\, D_{12}(M_1, M_2; p_i, p_j, p_k) &\overset{\text{NLL}}{=} 0, \tag{C.5}
\end{aligned}
$$

where the sum runs over all permutations $\pi(i,j,k)$ of i,j,k, with sign $\text{sgn}(\pi(i,j,k))$, and

$$
\begin{aligned}
D_{13}(M_1, M_2, M_3; p_i, p_j, p_k) &\overset{\text{NLL}}{=} 0, \\
2 \Delta D_{13}(M_1, M_1, m_3; p_i, p_j, p_k) &= 2 \Delta D_{13}(m_3, M_1, M_1; p_k, p_i, p_j) \\
&= 2 \Delta D_{13}(M_1, m_3, M_1; p_j, p_k, p_i)
\end{aligned}
$$

$$\overset{\text{NLL}}{=} \Delta D_{12}(M_{\text{W}}, m_3; p_j, p_i, p_k) - \Delta D_{12}(M_{\text{W}}, m_3; p_i, p_j, p_k).$$
$$(C.6)$$

When fermion masses are involved, the last relation is only true (and only needed) if the two non-zero gauge-boson masses M_1 on the left-hand side are equal.

We have found that the relations from appendix B of ref. [32], together with the modifications presented above, are exactly the ones needed to combine the two-loop contributions of section A.2 into the complete amplitude (see end of appendix A).

D. Application to four-particle processes

Here we apply our results to four-particle processes involving light fermions, heavy fermions and gluons. We first examine four-fermion processes

$$\varphi_1(p_1)\, \varphi_2(p_2) \to \varphi_3(-p_3)\, \varphi_4(-p_4), \qquad (D.1)$$

where each of the φ_i may be a fermion, $\varphi_i = f_{\sigma_i}^{\kappa_i}$, or antifermion, $\varphi_i = \bar{f}_{\sigma_i}^{\kappa_i}$, with the notations from section 2, provided that the number of fermions and antifermions in the initial and final state is equal. We exclude top quarks from the initial state, $\varphi_{1,2} \neq t, \bar{t}$, but allow for bottom quarks there. The final state may contain any combination of massless or massive fermions and antifermions, including top and bottom quarks.

The scattering amplitudes for the processes (D.1) follow directly from our results for the generic $n \to 0$ process (2.1) by crossing symmetry, and the Mandelstam invariants are given by $s = r_{12} = r_{34}$, $t = r_{13} = r_{24}$, and $u = r_{14} = r_{23}$ with $r_{ij} = (p_i + p_j)^2$. In practice we can restrict ourselves to the calculation of s-channel amplitudes $f_{\sigma_1}^{\kappa_1} \bar{f}_{\sigma_2}^{\kappa_2} \to f_{\sigma_3}^{\kappa_3} \bar{f}_{\sigma_4}^{\kappa_4}$, i.e. amplitudes where the external fermion lines are connected between $f_{\sigma_1}^{\kappa_1}$ and $\bar{f}_{\sigma_2}^{\kappa_2}$ in the initial state and between $f_{\sigma_3}^{\kappa_3}$ and $\bar{f}_{\sigma_4}^{\kappa_4}$ in the final state. All other scattering amplitudes needed for the four-fermion processes can be obtained from the s-channel amplitudes by crossing symmetry.

In section D.1 we treat neutral-current four-fermion amplitudes where the particle pairs in the initial and final state are antiparticles of each other. Section D.2 is devoted to charged-current four-fermion amplitudes where the initial and final state each consist of a pair of isospin partners. Finally, in section D.3 we provide results for the annihilation of two gluons into a fermion pair, $g\,g \to f_\sigma^\kappa \bar{f}_\sigma^\kappa$. All other four-particle processes involving two gluons and two (anti)fermions, i.e. $g\,f_\sigma^\kappa \to g\,f_\sigma^\kappa$, $f_\sigma^\kappa \bar{f}_\sigma^\kappa \to g\,g$, etc., are related to $g\,g \to f_\sigma^\kappa \bar{f}_\sigma^\kappa$ by crossing symmetry.

In order to keep all results manifestly invariant with respect to crossing symmetry, we keep the hard scale Q^2, which enters the logarithms $L = \ln(Q^2/M_{\text{W}}^2)$, as a free parameter. In practical applications, Q^2 can be identified with the centre-of-mass energy s or, alternatively, with $|t|$ or $|u|$. This implies an ambiguity of NNLL order, which corresponds to the intrinsic error of the NLL approximation.

We present the results in the factorized form (5.18), using the notation

$$\mathcal{M}_X \overset{\text{NLL}}{=} \mathcal{M}_{0,X}(Q^2)\, f_X^{\text{sew}}\, f_X^{\text{Z}}\, f_X^{\text{em}}, \qquad (D.2)$$

where X denotes a specific process. In particular we separate the finite parts of the corrections, f_X^{sew} and f_X^{Z}, from the subtracted electromagnetic part f_X^{em}. The latter contains all soft/collinear $1/\epsilon$ poles that must be cancelled against real photon emission or, in the case of initial-state singularities, factorized. In f_X^{sew} and f_X^{Z} we will omit contributions of $\mathcal{O}(\epsilon)$ and $\mathcal{O}(\epsilon^2)$, since such terms are irrelevant after cancellation of the photonic soft/collinear singularities. The electromagnetic contributions f_X^{em} have the general form

$$f_X^{\mathrm{em}} \stackrel{\mathrm{NLL}}{=} 1 + \frac{\alpha_\epsilon}{4\pi}\,\Delta f_{1,X}^{\mathrm{em}} + \left(\frac{\alpha_\epsilon}{4\pi}\right)^2 \left[\frac{1}{2}\left(\Delta f_{1,X}^{\mathrm{em}}\right)^2 + \Delta g_{2,X}^{\mathrm{em}}\right] \tag{D.3}$$

with

$$
\begin{aligned}
\Delta f_{1,X}^{\mathrm{em}} \stackrel{\mathrm{NLL}}{=} &-\left(2\epsilon^{-2} - L^2 - \frac{2}{3}L^3\epsilon - \frac{1}{4}L^4\epsilon^2 + 3\epsilon^{-1} + 3L + \frac{3}{2}L^2\epsilon + \frac{1}{2}L^3\epsilon^2\right) C_{1,X,0}^{\mathrm{em}} \\
&+\left(\epsilon^{-1} + L + \frac{1}{2}L^2\epsilon + \frac{1}{6}L^3\epsilon^2\right)\left[2\left(L - 1 - l_{\mathrm{t}}\right) C_{1,X,\mathrm{t}}^{\mathrm{em}} - C_{1,X}^{\mathrm{ad,em}}\right] + \mathcal{O}(\epsilon^3), \\
\Delta g_{2,X}^{\mathrm{em}} \stackrel{\mathrm{NLL}}{=} &\left\{ l_{\mu_{\mathrm{R}}}\left[-2\epsilon^{-2} - \left(2L - l_{\mu_{\mathrm{R}}}\right)\epsilon^{-1} + l_{\mu_{\mathrm{R}}}L - \frac{1}{3}l_{\mu_{\mathrm{R}}}^2\right] b_e^{(1)} \right. \\
&\left.+ \left(\frac{3}{2}\epsilon^{-3} + 2L\epsilon^{-2} + L^2\epsilon^{-1}\right) b_{\mathrm{QED}}^{(1)}\right\} C_{1,X,0}^{\mathrm{em}} + \left[l_{\mu_{\mathrm{R}}}\left(2L\epsilon^{-1} + 4L^2 - l_{\mu_{\mathrm{R}}}L\right) b_e^{(1)} \right. \\
&\left. - \left(L\epsilon^{-2} + 2L^2\epsilon^{-1} + 2L^3\right) b_{\mathrm{QED}}^{(1)}\right] C_{1,X,\mathrm{t}}^{\mathrm{em}} + \mathcal{O}(\epsilon),
\end{aligned}
\tag{D.4}
$$

and the factors $C_{1,X,0}^{\mathrm{em}}, C_{1,X,\mathrm{t}}^{\mathrm{em}}, C_{1,X}^{\mathrm{ad,em}}$, which depend on the charges and masses of the external particles, are given in the next sections. The values for the β-function coefficients $b_e^{(1)}$ and $b_{\mathrm{QED}}^{(1)}$ can be found in (4.5) and (4.6).

D.1 Neutral-current four-fermion scattering

This section deals with s-channel neutral-current four-fermion amplitudes

$$f_\sigma^\kappa\,\bar{f}_\sigma^\kappa \to f_{\sigma'}^{\kappa'}\,\bar{f}_{\sigma'}^{\kappa'}\,, \tag{D.5}$$

where a fermion-antifermion pair annihilates and produces another fermion-antifermion pair. The Born diagram of such an amplitude is given by
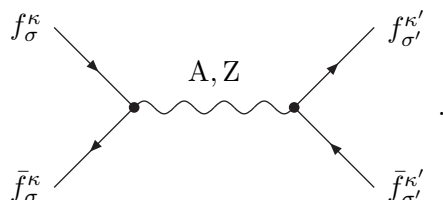
We allow for top quarks only in the final state. Both particles of the initial state must share the same chirality κ, and both particles of the final state must have the same chirality κ', otherwise the amplitude is suppressed in NLL accuracy. The electromagnetic charge quantum numbers of the external particles are given by $q_f = q_{f_\sigma^\kappa} = -q_{\bar{f}_\sigma^\kappa}$ and $q_{f'} = q_{f_{\sigma'}^{\kappa'}} = -q_{\bar{f}_{\sigma'}^{\kappa'}}$, the hypercharges by $y_f = y_{f_\sigma^\kappa} = -y_{\bar{f}_\sigma^\kappa}$ and $y_{f'} = y_{f_{\sigma'}^{\kappa'}} = -y_{\bar{f}_{\sigma'}^{\kappa'}}$,

the isospin components by $t_f^3 = t_{f_\sigma^\kappa}^3 = -t_{\bar{f}_\sigma^\kappa}^3$ and $t_{f'}^3 = t_{f_{\sigma'}^{\kappa'}}^3 = -t_{\bar{f}_{\sigma'}^{\kappa'}}^3$, and the isospin by $t_f = |t_f^3|$, $t_{f'} = |t_{f'}^3|$. We use z_f^Y and $z_{f'}^Y$ to denote the Yukawa factors (4.11) of the initial- and final-state particles, respectively.

The amplitude can be written in the factorized form (5.18),

$$\mathcal{M}_{\mathrm{NC}} \overset{\mathrm{NLL}}{=} \mathcal{M}_{0,\mathrm{NC}}(Q^2)\, f_{\mathrm{NC}}^{\mathrm{sew}}\, f_{\mathrm{NC}}^{\mathrm{Z}}\, f_{\mathrm{NC}}^{\mathrm{em}}. \tag{D.6}$$

The Born amplitude combined with the (non-diagonal) symmetric-electroweak contribution $f_{\mathrm{NC}}^{\mathrm{sew}}$ (5.23) reads

$$
\begin{aligned}
\mathcal{M}_{0,\mathrm{NC}}(Q^2)\, f_{\mathrm{NC}}^{\mathrm{sew}} \overset{\mathrm{NLL}}{=} \frac{1}{s}\, &\bar{v}(p_2,\kappa)\gamma^\mu u(p_1,\kappa)\, \bar{u}(-p_3,\kappa')\gamma_\mu v(-p_4,\kappa') \bigg\{ C_{0,\mathrm{NC}} \\
&+ \frac{\alpha_\epsilon}{4\pi}\left[-C_{0,\mathrm{NC}}\left((L^2 - 3L)\, C_{1,\mathrm{NC}}^{\mathrm{sew}} + L_{\mathrm{t}} \frac{\lambda_t^2}{2e^2}\left(z_f^Y + z_{f'}^Y \right) \right) + L\, C_{1,\mathrm{NC}}^{\mathrm{ad}} \right] \\
&+ \left(\frac{\alpha_\epsilon}{4\pi}\right)^2 \left[C_{0,\mathrm{NC}}\left(\left(\frac{1}{2}L^4 - 3L^3\right)\left(C_{1,\mathrm{NC}}^{\mathrm{sew}}\right)^2 + L^2 L_{\mathrm{t}} \frac{\lambda_t^2}{2e^2}\left(z_f^Y + z_{f'}^Y \right) C_{1,\mathrm{NC}}^{\mathrm{sew}} + g_{2,\mathrm{NC}}^{\mathrm{sew}} \right) \right. \\
&\left. - L^3\, C_{1,\mathrm{NC}}^{\mathrm{ad}}\, C_{1,\mathrm{NC}}^{\mathrm{sew}} \right] \bigg\} + \mathcal{O}(\epsilon),
\end{aligned}
\tag{D.7}
$$

where the Born term

$$C_{0,\mathrm{NC}} = g_1^2(Q^2)\frac{y_f y_{f'}}{4} + g_2^2(Q^2)\, t_f^3 t_{f'}^3 \tag{D.8}$$

is written in terms of couplings $g_i(Q^2)$ renormalized at the scale Q, whereas α_ϵ and the other couplings and mixing angles in the loop corrections are renormalized at the scale μ_{R}. The remaining terms in (D.7) read

$$
\begin{aligned}
C_{1,\mathrm{NC}}^{\mathrm{sew}} &= \frac{g_1^2}{e^2}\frac{y_f^2}{4} + \frac{g_2^2}{e^2}\, t_f(t_f+1) + (f \leftrightarrow f'), \\
C_{1,\mathrm{NC}}^{\mathrm{ad}} &= C_{0,\mathrm{NC}}\left[4\ln\left(\frac{u}{t}\right)\left(\frac{g_1^2}{e^2}\frac{y_f y_{f'}}{4} + \frac{g_2^2}{e^2}\, t_f^3 t_{f'}^3 \right) - 2\ln\left(\frac{-s}{Q^2}\right) C_{1,\mathrm{NC}}^{\mathrm{sew}} \right] \\
&\quad + 2g_2^2(Q^2)\frac{g_2^2}{e^2}\left[\ln\left(\frac{u}{t}\right) t_f t_{f'} - \left(\ln\left(\frac{t}{s}\right) + \ln\left(\frac{u}{s}\right) \right) t_f^3 t_{f'}^3 \right], \\
g_{2,\mathrm{NC}}^{\mathrm{sew}} &\overset{\mathrm{NLL}}{=} \left(\frac{1}{3}L^3 - l_{\mu_{\mathrm{R}}} L^2\right)\left[b_1^{(1)}\frac{g_1^2}{e^2}\frac{y_f^2}{4} + b_2^{(1)}\frac{g_2^2}{e^2}\, t_f(t_f+1) + (f \leftrightarrow f') \right] + \mathcal{O}(\epsilon). \tag{D.9}
\end{aligned}
$$

The values for the β-function coefficients $b_1^{(1)}$, $b_2^{(1)}$ are given in (4.5). The symmetric-electroweak result (D.7) is multiplied with the diagonal factors

$$f_{\mathrm{NC}}^{\mathrm{Z}} \overset{\mathrm{NLL}}{=} 1 + \frac{\alpha_\epsilon}{4\pi} 2L\, l_{\mathrm{Z}}\left[\left(\frac{g_2}{e} c_{\mathrm{W}} t_f^3 - \frac{g_1}{e} s_{\mathrm{W}} \frac{y_f}{2} \right)^2 + (f \leftrightarrow f') \right] + \mathcal{O}(\epsilon) \tag{D.10}$$

and $f_{\mathrm{NC}}^{\mathrm{em}}$. The latter is obtained from (D.3)–(D.4) with

$$C_{1,\mathrm{NC},0}^{\mathrm{em}} = q_f^2 + \delta_{f',0}\, q_{f'}^2, \qquad C_{1,\mathrm{NC,t}}^{\mathrm{em}} = \delta_{f',\mathrm{t}}\, q_{\mathrm{t}}^2,$$

$$C_{1,\mathrm{NC}}^{\mathrm{ad,em}} = 4\ln\left(\frac{u}{t}\right) q_f q_{f'} - 2\ln\left(\frac{-s}{Q^2}\right)\left(q_f^2 + q_{f'}^2\right), \tag{D.11}$$

where $q_{\mathrm{t}} = 2/3$, and the symbols

$$\delta_{f',\mathrm{t}} = \left\{\begin{array}{l} 1, \ f_{\sigma'} = t \\ 0, \ f_{\sigma'} \neq t \end{array}\right\}, \qquad \delta_{f',0} = 1 - \delta_{f',\mathrm{t}} \tag{D.12}$$

are used to distinguish between massive and massless fermions in the final state.

Note that only the electromagnetic contributions $f_{\mathrm{NC}}^{\mathrm{em}}$ depend on the fermion masses. The remaining contributions are simply complemented by the Yukawa contributions proportional to λ_t^2 in (D.7), otherwise they are equal to our results for massless fermions presented in section 8.4.1 of ref. [32].

D.2 Charged-current four-fermion scattering

In this section we treat s-channel charged-current four-fermion amplitudes $f_\sigma^\kappa \bar{f}_\rho^\lambda \to f_{\sigma'}^\kappa \bar{f}_{\rho'}^\lambda$, where the fermions f_σ and $f_{\sigma'}$ are the isospin partners of f_ρ and $f_{\rho'}$, respectively. We allow for a top-antibottom or bottom-antitop pair both in the initial and final state because the s-channel amplitude $t\,\bar{b} \to t\,\bar{b}$ arises via crossing symmetry as a contribution to the process $b\,\bar{b} \to t\,\bar{t}$.

For s-channel amplitudes with purely left-handed external fermions,

$$f_\sigma^{\mathrm{L}} \bar{f}_\rho^{\mathrm{L}} \to f_{\sigma'}^{\mathrm{L}} \bar{f}_{\rho'}^{\mathrm{L}}, \tag{D.13}$$

the Born diagram involves the exchange of a W boson:
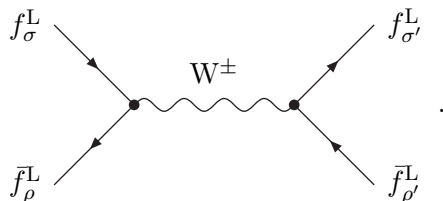
Most of the other combinations of chiralities for the external fermions yield contributions which are suppressed in NLL accuracy. The only exception is the s-channel amplitude

$$t^{\mathrm{R}} \bar{b}^{\mathrm{L}} \to t^{\mathrm{R}} \bar{b}^{\mathrm{L}} \tag{D.14}$$

or, via crossing symmetry, $b^{\mathrm{L}} \bar{t}^{\mathrm{R}} \to b^{\mathrm{L}} \bar{t}^{\mathrm{R}}$, where the exchange of a $\phi^\pm$ scalar boson in the Born diagram produces a non-suppressed contribution with right-handed top quarks:
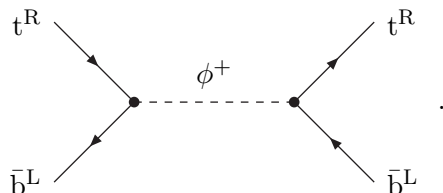
We start with the fully left-handed amplitude (D.13). The hypercharge quantum numbers of the external particles are given by $y_f = y_{f_\sigma^{\mathrm{L}}} = -y_{\bar{f}_\rho^{\mathrm{L}}}$ and $y_{f'} = y_{f_{\sigma'}^{\mathrm{L}}} = -y_{\bar{f}_{\rho'}^{\mathrm{L}}}$,

the isospin components by $t^3 = t^3_{f^L_\sigma} = t^3_{\bar{f}^L_\rho} = t^3_{f^L_{\sigma'}} = t^3_{\bar{f}^L_{\rho'}}$, and for left-handed fermions $|t^3| = 1/2$. The Yukawa factors (4.11) of the initial- and final-state particles are denoted by $z^Y_f = z^Y_{f^L_\sigma} = z^Y_{\bar{f}^L_\rho}$ and $z^Y_{f'} = z^Y_{f^L_{\sigma'}} = z^Y_{\bar{f}^L_{\rho'}}$, respectively.

As in the previous section, the amplitude (D.13) is written in the form

$$\mathcal{M}_{\mathrm{CC}} \overset{\mathrm{NLL}}{=} \mathcal{M}_{0,\mathrm{CC}}(Q^2)\, f^{\mathrm{sew}}_{\mathrm{CC}}\, f^{\mathrm{Z}}_{\mathrm{CC}}\, f^{\mathrm{em}}_{\mathrm{CC}}. \tag{D.15}$$

Combining the Born amplitude with the (non-diagonal) symmetric-electroweak contribution $f^{\mathrm{sew}}_{\mathrm{NC}}$ (5.23), we find

$$\mathcal{M}_{0,\mathrm{CC}}(Q^2)\, f^{\mathrm{sew}}_{\mathrm{CC}} \overset{\mathrm{NLL}}{=} \frac{1}{s}\, \bar{v}(p_2,\mathrm{L})\gamma^\mu u(p_1,\mathrm{L})\, \bar{u}(-p_3,\mathrm{L})\gamma_\mu v(-p_4,\mathrm{L}) \left\{ \frac{g_2^2(Q^2)}{2} \right.$$

$$+ \frac{\alpha_\epsilon}{4\pi}\left[-\frac{g_2^2(Q^2)}{2}\left((L^2 - 3L)\, C^{\mathrm{sew}}_{1,\mathrm{CC}} + L_{\mathrm t}\, \frac{\lambda_t^2}{2e^2}\left(z^Y_f + z^Y_{f'} \right) \right) + L\, C^{\mathrm{ad}}_{1,\mathrm{CC}} \right]$$

$$+ \left(\frac{\alpha_\epsilon}{4\pi}\right)^2 \left[\frac{g_2^2(Q^2)}{2}\left(\left(\frac{1}{2}L^4 - 3L^3\right)\left(C^{\mathrm{sew}}_{1,\mathrm{CC}}\right)^2 + L^2 L_{\mathrm t}\, \frac{\lambda_t^2}{2e^2}\left(z^Y_f + z^Y_{f'}\right)C^{\mathrm{sew}}_{1,\mathrm{CC}} + g^{\mathrm{sew}}_{2,\mathrm{CC}} \right) \right.$$

$$\left.\left. - L^3\, C^{\mathrm{ad}}_{1,\mathrm{CC}}\, C^{\mathrm{sew}}_{1,\mathrm{CC}} \right] \right\} + \mathcal{O}(\epsilon) \tag{D.16}$$

with

$$C^{\mathrm{sew}}_{1,\mathrm{CC}} = \frac{g_1^2}{e^2}\frac{y_f^2 + y_{f'}^2}{4} + \frac{3}{2}\frac{g_2^2}{e^2},$$

$$C^{\mathrm{ad}}_{1,\mathrm{CC}} = \frac{g_2^2(Q^2)}{2}\left[4\ln\left(\frac{u}{t}\right)\frac{g_1^2}{e^2}\frac{y_f y_{f'}}{4} - 2\left(\ln\left(\frac{t}{s}\right) + \ln\left(\frac{u}{s}\right)\right)\frac{g_2^2}{e^2} - 2\ln\left(\frac{-s}{Q^2}\right)C^{\mathrm{sew}}_{1,\mathrm{CC}} \right]$$

$$+ 2\ln\left(\frac{u}{t}\right)g_1^2(Q^2)\frac{y_f y_{f'}}{4}\frac{g_2^2}{e^2},$$

$$g^{\mathrm{sew}}_{2,\mathrm{CC}} \overset{\mathrm{NLL}}{=} \left(\frac{1}{3}L^3 - l_{\mu_{\mathrm R}}L^2\right)\left(b_1^{(1)}\frac{g_1^2}{e^2}\frac{y_f^2 + y_{f'}^2}{4} + \frac{3}{2}b_2^{(1)}\frac{g_2^2}{e^2} \right) + \mathcal{O}(\epsilon). \tag{D.17}$$

The $M_{\mathrm Z}$-dependent correction factor reads

$$f^{\mathrm{Z}}_{\mathrm{CC}} \overset{\mathrm{NLL}}{=} 1 + \frac{\alpha_\epsilon}{4\pi}\, L\, l_{\mathrm Z}\left(\frac{g_2^2}{e^2}c_{\mathrm w}^2 + 2\frac{g_1^2}{e^2}s_{\mathrm w}^2\frac{y_f^2 + y_{f'}^2}{4} \right) + \mathcal{O}(\epsilon), \tag{D.18}$$

and the electromagnetic factor $f^{\mathrm{em}}_{\mathrm{CC}}$ is obtained from (D.3)–(D.4) with

$$C^{\mathrm{em}}_{1,\mathrm{CC},0} = \frac{1}{2}\left[\delta_{f,0}\left(q_{f^L_\sigma}^2 + q_{\bar{f}^L_\rho}^2 \right) + \delta_{f',0}\left(q_{f^L_{\sigma'}}^2 + q_{\bar{f}^L_{\rho'}}^2 \right) + \left(\delta_{f,\mathrm t} + \delta_{f',\mathrm t}\right)q_{\mathrm b}^2 \right]$$

$$= \left[\delta_{f,0}\left(\frac{g_1^2}{e^2}c_{\mathrm w}^2\frac{y_f^2}{4} + \frac{1}{4}\frac{g_2^2}{e^2}s_{\mathrm w}^2 \right) + \frac{1}{2}\delta_{f,\mathrm t}\, q_{\mathrm b}^2 + (f \leftrightarrow f') \right],$$

$$C^{\mathrm{em}}_{1,\mathrm{CC},\mathrm t} = \frac{1}{2}\left(\delta_{f,\mathrm t} + \delta_{f',\mathrm t} \right)q_{\mathrm t}^2,$$

$$
\begin{aligned}
C_{1,\text{CC}}^{\text{ad,em}} &= 2 \left[\ln\left(\frac{-s}{Q^2}\right) \left(q_{f_\sigma^{\text{L}}} q_{\bar{f}_\rho^{\text{L}}} + q_{f_{\sigma'}^{\text{L}}} q_{f_{\rho'}^{\text{L}}} \right) - \ln\left(\frac{-t}{Q^2}\right) \left(q_{f_\sigma^{\text{L}}} q_{f_{\sigma'}^{\text{L}}} + q_{\bar{f}_\rho^{\text{L}}} q_{f_{\rho'}^{\text{L}}} \right) \right. \\
&\quad \left. - \ln\left(\frac{-u}{Q^2}\right) \left(q_{f_\sigma^{\text{L}}} q_{\bar{f}_{\rho'}^{\text{L}}} + q_{f_{\sigma'}^{\text{L}}} q_{\bar{f}_\rho^{\text{L}}} \right) \right] \\
&= 4 \ln\left(\frac{u}{t}\right) \frac{g_1^2}{e^2} c_{\text{W}}^2 \frac{y_f y_{f'}}{4} - \left(\ln\left(\frac{t}{s}\right) + \ln\left(\frac{u}{s}\right) \right) \frac{g_2^2}{e^2} s_{\text{W}}^2 \\
&\quad - 2 \ln\left(\frac{-s}{Q^2}\right) \left(\frac{g_1^2}{e^2} c_{\text{W}}^2 \frac{y_f^2 + y_{f'}^2}{4} + \frac{1}{2} \frac{g_2^2}{e^2} s_{\text{W}}^2 \right),
\end{aligned}
\tag{D.19}
$$

where $q_{\text{t}} = 2/3$, $q_{\text{b}} = -1/3$, and the symbols

$$
\delta_{f,\text{t}} = \left\{ \begin{array}{l} 1, \ f_\sigma = t \text{ or } f_\rho = t \\ 0, \text{ otherwise} \end{array} \right\}, \qquad \delta_{f,0} = 1 - \delta_{f,\text{t}}
\tag{D.20}
$$

and similarly for $f \to f'$, $f_\sigma \to f_{\sigma'}$, $f_\rho \to f_{\rho'}$ are used to distinguish between massive and massless fermions.

Again only the dependence of the electromagnetic contributions $f_{\text{CC}}^{\text{em}}$ on the fermion masses and the Yukawa terms in (D.16) are new compared with our results for massless fermions in section 8.4.2 of ref. [32].

Now we present the results for the s-channel amplitude $\text{t}^{\text{R}} \bar{\text{b}}^{\text{L}} \to \text{t}^{\text{R}} \bar{\text{b}}^{\text{L}}$ (D.14) which contributes via crossing symmetry to the process $\text{b}^{\text{L}} \bar{\text{b}}^{\text{L}} \to \text{t}^{\text{R}} \bar{\text{t}}^{\text{R}}$. We need the hypercharges $y_{\text{t}^{\text{R}}} = 4/3$, $y_{\text{b}^{\text{L}}} = 1/3$ and the Yukawa factors $z_{\text{t}^{\text{R}}}^{\text{Y}} = 2$, $z_{\text{b}^{\text{L}}}^{\text{Y}} = 1$. The amplitude reads

$$
\mathcal{M}_{\text{CCY}} \overset{\text{NLL}}{=} \mathcal{M}_{0,\text{CCY}}(Q^2) \, f_{\text{CCY}}^{\text{sew}} \, f_{\text{CCY}}^{\text{Z}} \, f_{\text{CCY}}^{\text{em}}
\tag{D.21}
$$

and is expressed through

$$
\begin{aligned}
\mathcal{M}_{0,\text{CCY}}(Q^2) \, f_{\text{CCY}}^{\text{sew}} &\overset{\text{NLL}}{=} -\frac{\lambda_t^2(Q^2)}{s} \, \bar{v}(p_2, \text{L}) u(p_1, \text{R}) \, \bar{u}(-p_3, \text{R}) v(-p_4, \text{L}) \left\{ 1 \right. \\
&+ \frac{\alpha_\epsilon}{4\pi} \left[-\left(L^2 - 3L \right) C_{1,\text{CCY}}^{\text{sew}} - L_{\text{t}} \frac{\lambda_t^2}{2e^2} \left(z_{\text{t}^{\text{R}}}^{\text{Y}} + z_{\text{b}^{\text{L}}}^{\text{Y}} \right) + L \, C_{1,\text{CCY}}^{\text{ad}} \right] \\
&+ \left(\frac{\alpha_\epsilon}{4\pi} \right)^2 \left[\left(\frac{1}{2} L^4 - 3L^3 \right) \left(C_{1,\text{CCY}}^{\text{sew}} \right)^2 + L^2 L_{\text{t}} \frac{\lambda_t^2}{2e^2} \left(z_{\text{t}^{\text{R}}}^{\text{Y}} + z_{\text{b}^{\text{L}}}^{\text{Y}} \right) C_{1,\text{CCY}}^{\text{sew}} + g_{2,\text{CCY}}^{\text{sew}} \right. \\
&\quad \left. \left. - L^3 \, C_{1,\text{CCY}}^{\text{ad}} C_{1,\text{CCY}}^{\text{sew}} \right] \right\} + \mathcal{O}(\epsilon)
\end{aligned}
\tag{D.22}
$$

with

$$
\begin{aligned}
C_{1,\text{CCY}}^{\text{sew}} &= \frac{g_1^2}{e^2} \frac{y_{\text{t}^{\text{R}}}^2 + y_{\text{b}^{\text{L}}}^2}{4} + \frac{3}{4} \frac{g_2^2}{e^2}, \\
C_{1,\text{CCY}}^{\text{ad}} &= 4 \ln\left(\frac{u}{s}\right) \frac{g_1^2}{e^2} \frac{y_{\text{t}^{\text{R}}} y_{\text{b}^{\text{L}}}}{4} - 2 \ln\left(\frac{-t}{Q^2}\right) C_{1,\text{CCY}}^{\text{sew}},
\end{aligned}
$$

$$g_{2,\mathrm{CCY}}^{\mathrm{sew}} \overset{\mathrm{NLL}}{=} \left(\frac{1}{3} L^3 - l_{\mu_{\mathrm{R}}} L^2 \right) \left(b_1^{(1)} \frac{g_1^2}{e^2} \frac{y_{\mathrm{tR}}^2 + y_{\mathrm{bL}}^2}{4} + \frac{3}{4} b_2^{(1)} \frac{g_2^2}{e^2} \right) + \mathcal{O}(\epsilon) \qquad \text{(D.23)}$$

and the M_{Z}-dependent factor

$$f_{\mathrm{CCY}}^{\mathrm{Z}} \overset{\mathrm{NLL}}{=} 1 + \frac{\alpha_\epsilon}{4\pi} 2L \, l_{\mathrm{Z}} \left[\frac{g_1^2}{e^2} s_{\mathrm{w}}^2 \frac{y_{\mathrm{tR}}^2}{4} + \left(\frac{1}{2} \frac{g_2}{e} c_{\mathrm{w}} + \frac{g_1}{e} s_{\mathrm{w}} \frac{y_{\mathrm{bL}}}{2} \right)^2 \right] + \mathcal{O}(\epsilon). \qquad \text{(D.24)}$$

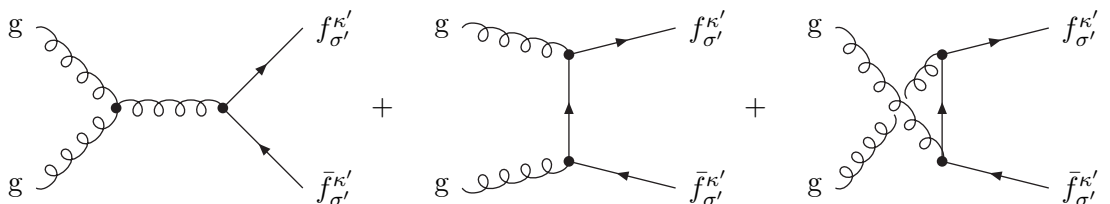The electromagnetic correction factor $f_{\mathrm{CCY}}^{\mathrm{em}}$ is obtained from (D.3)–(D.4) with

$$C_{1,\mathrm{CCY},0}^{\mathrm{em}} = q_{\mathrm{b}}^2, \qquad C_{1,\mathrm{CCY,t}}^{\mathrm{em}} = q_{\mathrm{t}}^2,$$
$$C_{1,\mathrm{CCY}}^{\mathrm{ad,em}} = 4 \ln\left(\frac{u}{s} \right) q_{\mathrm{t}} q_{\mathrm{b}} - 2 \ln\left(\frac{-t}{Q^2} \right) \left(q_{\mathrm{t}}^2 + q_{\mathrm{b}}^2 \right). \qquad \text{(D.25)}$$

D.3 Annihilation of two gluons into a fermion pair

This section completes the four-particle processes by amplitudes with two gluons in the initial state. The process

$$\mathrm{g\,g} \to f_{\sigma'}^{\kappa'} \, \bar{f}_{\sigma'}^{\kappa'} \qquad \text{(D.26)}$$

involves three diagrams at Born level,

and the corresponding Born amplitude in the high-energy limit reads

$$\mathcal{M}_{0,\mathrm{g}f} = -g_{\mathrm{s}}^2 \, \varepsilon_\mu(p_1) \varepsilon_\nu(p_2) \, \bar{u}(-p_3, \kappa') \times$$
$$\left\{ \frac{\mathrm{i}}{s} f^{abc} t^c \left[g^{\mu\nu}(p_1 - p_2)^\rho + g^{\nu\rho}(p_1 + 2p_2)^\mu - g^{\rho\mu}(2p_1 + p_2)^\nu \right] \gamma_\rho \right.$$
$$\left. + \frac{1}{t} t^a t^b \, \gamma^\mu(\slashed{p}_2 + \slashed{p}_4)\gamma^\nu + \frac{1}{u} t^b t^a \, \gamma^\nu(\slashed{p}_1 + \slashed{p}_4)\gamma^\mu \right\} v(-p_4, \kappa'), \qquad \text{(D.27)}$$

where g_{s} is the strong coupling, $\varepsilon_\mu(p_{1,2})$ are the polarization vectors of the initial-state gluons with colour indices a and b, t^a are the generators of the QCD SU(3) gauge group, and f^{abc} are the corresponding structure constants.

As discussed in section 6, our NLL results for n-fermion processes can be applied also to QCD processes involving fermions and gluons. The NLL amplitude for the process (D.26) assumes the usual factorized form,

$$\mathcal{M}_{\mathrm{g}f} \overset{\mathrm{NLL}}{=} \mathcal{M}_{0,\mathrm{g}f} \, f_{\mathrm{g}f}^{\mathrm{sew}} \, f_{\mathrm{g}f}^{\mathrm{Z}} \, f_{\mathrm{g}f}^{\mathrm{em}}, \qquad \text{(D.28)}$$

and the presence of the gluons affects only the factorized Born amplitude $\mathcal{M}_{0,\mathrm{g}f}$. The NLL correction factors $f_{\mathrm{g}f}^{\mathrm{sew}}$, $f_{\mathrm{g}f}^{\mathrm{Z}}$, and $f_{\mathrm{g}f}^{\mathrm{em}}$ are obtained from the general results of section 4

and section 5 by treating the reaction (D.26) as a $0 \to 2$ process, in the sense that the NLL correction factors receive contributions only from the final-state fermions.

The symmetric-electroweak operator $f_{\mathrm{g}f}^{\mathrm{sew}}$ is diagonal for this process,

$$
\begin{aligned}
f_{\mathrm{g}f}^{\mathrm{sew}} \overset{\mathrm{NLL}}{=}\ & 1 - \frac{\alpha_\epsilon}{4\pi} \left\{ \left[L^2 - 3L + 2L \ln\left(\frac{-s}{Q^2}\right) \right] C_{1,\mathrm{g}f}^{\mathrm{sew}} + L_{\mathrm{t}} \frac{\lambda_t^2}{2e^2} z_{f'}^{\mathrm{Y}} \right\} \\
& + \left(\frac{\alpha_\epsilon}{4\pi}\right)^2 \left\{ \left[\frac{1}{2} L^4 - 3L^3 + 2L^3 \ln\left(\frac{-s}{Q^2}\right) \right] \left(C_{1,\mathrm{g}f}^{\mathrm{sew}}\right)^2 + L^2 L_{\mathrm{t}} \frac{\lambda_t^2}{2e^2} z_{f'}^{\mathrm{Y}} C_{1,\mathrm{g}f}^{\mathrm{sew}} + g_{2,\mathrm{g}f}^{\mathrm{sew}} \right\} \\
& + \mathcal{O}(\epsilon),
\end{aligned} \tag{D.29}
$$

and simply multiplies the Born amplitude (D.27). The terms $C_{1,\mathrm{g}f}^{\mathrm{sew}}$ and $g_{2,\mathrm{g}f}^{\mathrm{sew}}$ used here as well as the two other correction factors $f_{\mathrm{g}f}^{\mathrm{Z}}$ and $f_{\mathrm{g}f}^{\mathrm{em}}$ can be obtained from the corresponding results (D.9)–(D.11) of the neutral-current four-fermion amplitude in section D.1 by setting all electroweak quantum numbers of the initial-state fermions (y_f, t_f^3, t_f, q_f) to zero, keeping only the final-state quantum numbers $y_{f'}, t_{f'}^3, t_{f'}, q_{f'}$.

D.4 Comparison with effective field-theory results

The four-fermion amplitudes presented in this appendix can be compared with the results of refs. [24, 25] based on soft-collinear effective theory (SCET). To this end we have to use the results in section VII of ref. [25], omitting QCD contributions. We have found agreement at NLL accuracy for the symmetric-electroweak and M_{Z}-dependent parts of our results.

In the SCET framework, the full electroweak theory is matched at the high scale $\mu = Q$ to an effective theory $\mathrm{SCET}_{\mathrm{EW}}$ where the degrees of freedom above the scale Q are integrated out. In NLL accuracy, only the tree-level expressions of the corresponding matching coefficients are relevant. These matching coefficients are evolved from the scale $\mu = Q$ down to the scale $\mu = M_{\mathrm{W}}$ using anomalous-dimension matrices calculated in $\mathrm{SCET}_{\mathrm{EW}}$. This step yields LL and NLL contributions which agree with the symmetric-electroweak parts $f_{\mathrm{NC}}^{\mathrm{sew}}$ (D.7) and $f_{\mathrm{CC}}^{\mathrm{sew}}$ (D.16) of the neutral- and charged-current amplitudes presented here. At the low scale $\mu = M_{\mathrm{W}}$, $\mathrm{SCET}_{\mathrm{EW}}$ is matched to another effective theory SCET_{γ} where the massive gauge bosons are integrated out. The loop corrections resulting from this second matching agree with the factors $f_{\mathrm{NC}}^{\mathrm{Z}}$ (D.10) and $f_{\mathrm{CC}}^{\mathrm{Z}}$ (D.18) arising in our calculation from the difference in the W- and Z-boson masses.

Finally, the matching coefficients in SCET_{γ} are evolved down to some finite scale $\mu_0 < M_{\mathrm{W}}$ ($\mu_0 = 30\,\mathrm{GeV}$ for the numerics in ref. [25]), which acts as a cut-off for the singular contributions due to soft and collinear photons. Due to the different regularization employed in our calculation these contributions cannot directly be compared with our electromagnetic factors $f_{\mathrm{NC}}^{\mathrm{em}}$ and $f_{\mathrm{CC}}^{\mathrm{em}}$.

In addition to the results of ref. [25], our analysis in section D.2 also includes the charged-current t-channel amplitude for the process $\mathrm{b}\,\bar{\mathrm{b}} \to \mathrm{t}\,\bar{\mathrm{t}}$ and, in particular, the tree-level exchange of a scalar boson in the case of right-handed top quarks.

Our results concerning four-particle processes with two gluons and two quarks in section D.3 are in agreement with the comments on these reactions in ref. [25].

References

[1] M. Kuroda, G. Moultaka and D. Schildknecht, *Direct one loop renormalization of* $\mathrm{SU}(2)_L \times \mathrm{U}(1)_Y$ *four fermion processes and running coupling constants*, *Nucl. Phys.* **B 350** (1991) 25;
G. Degrassi and A. Sirlin, *Gauge invariant selfenergies and vertex parts of the standard model in the pinch technique framework*, *Phys. Rev.* **D 46** (1992) 3104.

[2] A. Denner, S. Dittmaier and R. Schuster, *Radiative corrections to* $\gamma\gamma \to W^+W^-$ *in the electroweak standard model*, *Nucl. Phys.* **B 452** (1995) 80 [hep-ph/9503442];
A. Denner, S. Dittmaier and T. Hahn, *Radiative corrections to* $ZZ \to ZZ$ *in the electroweak standard model*, *Phys. Rev.* **D 56** (1997) 117 [hep-ph/9612390];
A. Denner and T. Hahn, *Radiative corrections to* $W^+W^- \to W^+W^-$ *in the electroweak standard model*, *Nucl. Phys.* **B 525** (1998) 27 [hep-ph/9711302].

[3] M. Beccaria, G. Montagna, F. Piccinini, F.M. Renard and C. Verzegnassi, *Rising bosonic electroweak virtual effects at high energy* e^+e^- *colliders*, *Phys. Rev.* **D 58** (1998) 093014 [hep-ph/9805250];
P. Ciafaloni and D. Comelli, *Sudakov enhancement of electroweak corrections*, *Phys. Lett.* **B 446** (1999) 278 [hep-ph/9809321].

[4] W. Beenakker, A. Denner, S. Dittmaier, R. Mertig and T. Sack, *High-energy approximation for on-shell W pair production*, *Nucl. Phys.* **B 410** (1993) 245;
W. Beenakker, A. Denner, S. Dittmaier and R. Mertig, *On shell W pair production in the TeV range*, *Phys. Lett.* **B 317** (1993) 622.

[5] G.J. Gounaris, J. Layssac and F.M. Renard, *The processes* $e^-e^+ \to \gamma\gamma$, $Z\gamma$, ZZ *in SM and MSSM*, *Phys. Rev.* **D 67** (2003) 013012 [hep-ph/0211327].

[6] E. Accomando, A. Denner and S. Pozzorini, *Electroweak-correction effects in gauge boson pair production at the LHC*, *Phys. Rev.* **D 65** (2002) 073003 [hep-ph/0110114];
W. Hollik and C. Meier, *Electroweak corrections to* γZ *production at hadron colliders*, *Phys. Lett.* **B 590** (2004) 69 [hep-ph/0402281];
E. Accomando, A. Denner and A. Kaiser, *Logarithmic electroweak corrections to gauge-boson pair production at the LHC*, *Nucl. Phys.* **B 706** (2005) 325 [hep-ph/0409247];
E. Accomando, A. Denner and C. Meier, *Electroweak corrections to* $W\gamma$ *and* $Z\gamma$ *production at the LHC*, *Eur. Phys. J.* **C 47** (2006) 125 [hep-ph/0509234];
E. Accomando and A. Kaiser, *Electroweak corrections and anomalous triple gauge-boson couplings in* WW *and* WZ *production at the LHC*, *Phys. Rev.* **D 73** (2006) 093006 [hep-ph/0511088].

[7] E. Accomando, A. Denner and S. Pozzorini, *Logarithmic electroweak corrections to* $e^+e^- \to \nu_e\bar{\nu}_e W^+W^-$, *JHEP* **03** (2007) 078 [hep-ph/0611289].

[8] M. Beccaria, P. Ciafaloni, D. Comelli, F.M. Renard and C. Verzegnassi, *Logarithmic expansion of electroweak corrections to four-fermion processes in the TeV region*, *Phys. Rev.* **D 61** (2000) 073005 [hep-ph/9906319].

[9] U. Baur, O. Brein, W. Hollik, C. Schappacher and D. Wackeroth, *Electroweak radiative corrections to neutral-current Drell-Yan processes at hadron colliders*, *Phys. Rev.* **D 65** (2002) 033007 [hep-ph/0108274];
S. Dittmaier and M. Krämer, *Electroweak radiative corrections to W-boson production at hadron colliders*, *Phys. Rev.* **D 65** (2002) 073007 [hep-ph/0109062];

U. Baur and D. Wackeroth, *Electroweak radiative corrections to* $p\overset{(-)}{p} \to W^{\pm} \to \ell^{\pm}\nu$ *beyond the pole approximation*, *Phys. Rev.* **D 70** (2004) 073015 [hep-ph/0405191];

V.A. Zykunov, *Weak radiative corrections to the Drell-Yan process for large invariant mass of a dilepton pair*, *Phys. Rev.* **D 75** (2007) 073019 [hep-ph/0509315];

C.M. Carloni Calame, G. Montagna, O. Nicrosini and A. Vicini, *Precision electroweak calculation of the production of a high transverse-momentum lepton pair at hadron colliders*, *JHEP* **10** (2007) 109 [arXiv:0710.1722];

S. Brensing, S. Dittmaier, M. Krämer and A. Mück, *Radiative corrections to W-boson hadroproduction: higher-order electroweak and supersymmetric effects*, *Phys. Rev.* **D 77** (2008) 073006 [arXiv:0710.3309].

[10] M. Beccaria, P. Ciafaloni, D. Comelli, F.M. Renard and C. Verzegnassi, *The role of the top mass in b production at future lepton colliders*, *Phys. Rev.* **D 61** (2000) 011301 [hep-ph/9907389];

M. Beccaria, F.M. Renard and C. Verzegnassi, *Top quark production at future lepton colliders in the asymptotic regime*, *Phys. Rev.* **D 63** (2001) 053013 [hep-ph/0010205];

E. Maina, S. Moretti, M.R. Nolten and D.A. Ross, *One-loop weak corrections to the* $b\bar{b}$ *cross section at TeV energy hadron colliders*, *Phys. Lett.* **B 570** (2003) 205 [hep-ph/0307021];

S. Moretti, M.R. Nolten and D.A. Ross, *Weak corrections to gluon-induced top-antitop hadro-production*, *Phys. Lett.* **B 639** (2006) 513 [*Erratum ibid.* **B 660** (2008) 607] [hep-ph/0603083];

M. Beccaria, G. Macorini, F.M. Renard and C. Verzegnassi, *Single top production in the t-channel at LHC: a realistic test of electroweak models*, *Phys. Rev.* **D 74** (2006) 013008 [hep-ph/0605108];

J.H. Kühn, A. Scharf and P. Uwer, *Electroweak effects in top-quark pair production at hadron colliders*, *Eur. Phys. J.* **C 51** (2007) 37 [hep-ph/0610335];

W. Bernreuther, M. Fücker and Z.-G. Si, *Weak interaction corrections to hadronic top quark pair production*, *Phys. Rev.* **D 74** (2006) 113005 [hep-ph/0610334].

[11] E. Maina, S. Moretti and D.A. Ross, *One-loop weak corrections to gamma/Z hadro-production at finite transverse momentum*, *Phys. Lett.* **B 593** (2004) 143 [*Erratum ibid.* **B 614** (2005) 216] [hep-ph/0403050];

J.H. Kühn, A. Kulesza, S. Pozzorini and M. Schulze, *Logarithmic electroweak corrections to hadronic Z + 1 jet production at large transverse momentum*, *Phys. Lett.* **B 609** (2005) 277 [hep-ph/0408308]; *One-loop weak corrections to hadronic production of Z bosons at large transverse momenta*, *Nucl. Phys.* **B 727** (2005) 368 [hep-ph/0507178]; *Electroweak corrections to hadronic photon production at large transverse momenta*, *JHEP* **03** (2006) 059 [hep-ph/0508253]; *Electroweak corrections to large transverse momentum production of W bosons at the LHC*, *Phys. Lett.* **B 651** (2007) 160 [hep-ph/0703283]; *Electroweak corrections to hadronic production of W bosons at large transverse momenta*, *Nucl. Phys.* **B 797** (2008) 27 [arXiv:0708.0476];

W. Hollik, T. Kasprzik and B.A. Kniehl, *Electroweak corrections to W-boson hadroproduction at finite transverse momentum*, *Nucl. Phys.* **B 790** (2008) 138 [arXiv:0707.2553].

[12] M. Ciccolini, A. Denner and S. Dittmaier, *Strong and electroweak corrections to the production of Higgs+2 jets via weak interactions at the LHC*, *Phys. Rev. Lett.* **99** (2007) 161803 [arXiv:0707.0381]; *Electroweak and QCD corrections to Higgs production via vector-boson fusion at the LHC*, *Phys. Rev.* **D 77** (2008) 013002 [arXiv:0710.4749].

[13] C.M. Carloni-Calame, S. Moretti, F. Piccinini and D.A. Ross, *Full one-loop electro-weak corrections to three-jet observables at the Z pole and beyond*, arXiv:0804.3771.

[14] M. Ciafaloni, P. Ciafaloni and D. Comelli, *Bloch-Nordsieck violating electroweak corrections to inclusive TeV scale hard processes*, *Phys. Rev. Lett.* **84** (2000) 4810 [`hep-ph/0001142`]; *Electroweak Bloch-Nordsieck violation at the TeV scale: 'strong' weak interactions?*, *Nucl. Phys.* **B 589** (2000) 359 [`hep-ph/0004071`]; *Electroweak double logarithms in inclusive observables for a generic initial state*, *Phys. Lett.* **B 501** (2001) 216 [`hep-ph/0007096`]; *Bloch-Nordsieck violation in spontaneously broken Abelian theories*, *Phys. Rev. Lett.* **87** (2001) 211802 [`hep-ph/0103315`]; *Enhanced electroweak corrections to inclusive boson fusion processes at the TeV scale*, *Nucl. Phys.* **B 613** (2001) 382 [`hep-ph/0103316`]; *Towards collinear evolution equations in electroweak theory*, *Phys. Rev. Lett.* **88** (2002) 102001 [`hep-ph/0111109`];
P. Ciafaloni and D. Comelli, *Electroweak evolution equations*, *JHEP* **11** (2005) 022 [`hep-ph/0505047`].

[15] U. Baur, *Weak boson emission in hadron collider processes*, *Phys. Rev.* **D 75** (2007) 013005 [`hep-ph/0611241`].

[16] A. Denner and S. Pozzorini, *One-loop leading logarithms in electroweak radiative corrections. I: results*, *Eur. Phys. J.* **C 18** (2001) 461 [`hep-ph/0010201`]; *One-loop leading logarithms in electroweak radiative corrections. II: factorization of collinear singularities*, *Eur. Phys. J.* **C 21** (2001) 63 [`hep-ph/0104127`].

[17] S. Pozzorini, *Electroweak radiative corrections at high energies*, `hep-ph/0201077`.

[18] V.S. Fadin, L.N. Lipatov, A.D. Martin and M. Melles, *Resummation of double logarithms in electroweak high energy processes*, *Phys. Rev.* **D 61** (2000) 094002 [`hep-ph/9910338`].

[19] M. Melles, *Resummation of Yukawa enhanced and subleading Sudakov logarithms in longitudinal gauge boson and Higgs production*, *Phys. Rev.* **D 64** (2001) 014011 [`hep-ph/0012157`]; *Electroweak radiative corrections in high energy processes*, *Phys. Rept.* **375** (2003) 219 [`hep-ph/0104232`].

[20] M. Melles, *Subleading Sudakov logarithms in electroweak high energy processes to all orders*, *Phys. Rev.* **D 63** (2001) 034003 [`hep-ph/0004056`]; *Electroweak renormalization group corrections in high energy processes*, *Phys. Rev.* **D 64** (2001) 054003 [`hep-ph/0102097`]; *Resummation of angular dependent corrections in spontaneously broken gauge theories*, *Eur. Phys. J.* **C 24** (2002) 193 [`hep-ph/0108221`].

[21] J.H. Kühn, A.A. Penin and V.A. Smirnov, *Summing up subleading Sudakov logarithms*, *Eur. Phys. J.* **C 17** (2000) 97 [`hep-ph/9912503`];
J.H. Kühn, S. Moch, A.A. Penin and V.A. Smirnov, *Next-to-next-to-leading logarithms in four-fermion electroweak processes at high energy*, *Nucl. Phys.* **B 616** (2001) 286 [*Erratum ibid.* **B 648** (2003) 455] [`hep-ph/0106298`].

[22] J.H. Kühn, F. Metzler and A.A. Penin, *Next-to-next-to-leading electroweak logarithms in W-pair production at ILC*, *Nucl. Phys.* **B 795** (2008) 277 [`arXiv:0709.4055`].

[23] C.W. Bauer, S. Fleming and M.E. Luke, *Summing Sudakov logarithms in $B \to X_s\gamma$ in effective field theory*, *Phys. Rev.* **D 63** (2000) 014006 [`hep-ph/0005275`];
C.W. Bauer, S. Fleming, D. Pirjol and I.W. Stewart, *An effective field theory for collinear and soft gluons: heavy to light decays*, *Phys. Rev.* **D 63** (2001) 114020 [`hep-ph/0011336`];
C.W. Bauer and I.W. Stewart, *Invariant operators in collinear effective theory*, *Phys. Lett.* **B 516** (2001) 134 [`hep-ph/0107001`];
C.W. Bauer, D. Pirjol and I.W. Stewart, *Soft-collinear factorization in effective field theory*, *Phys. Rev.* **D 65** (2002) 054022 [`hep-ph/0109045`].

[24] J.-Y. Chiu, F. Golf, R. Kelley and A.V. Manohar, *Electroweak Sudakov corrections using effective field theory*, *Phys. Rev. Lett.* **100** (2008) 021802 [`arXiv:0709.2377`]; *Electroweak corrections in high energy processes using effective field theory*, *Phys. Rev.* **D 77** (2008) 053004 [`arXiv:0712.0396`].

[25] J.-Y. Chiu, R. Kelley and A.V. Manohar, *Electroweak corrections using effective field theory: applications to the LHC*, *Phys. Rev.* **D 78** (2008) 073006 [`arXiv:0806.1240`].

[26] M. Melles, *Mass gap effects and higher order electroweak Sudakov logarithms*, *Phys. Lett.* **B 495** (2000) 81 [`hep-ph/0006077`];
M. Hori, H. Kawamura and J. Kodaira, *Electroweak Sudakov at two loop level*, *Phys. Lett.* **B 491** (2000) 275 [`hep-ph/0007329`];
W. Beenakker and A. Werthenbach, *New insights into the perturbative structure of electroweak Sudakov logarithms: breakdown of conventional exponentiation*, *Phys. Lett.* **B 489** (2000) 148 [`hep-ph/0005316`]; *Electroweak two-loop Sudakov logarithms for on-shell fermions and bosons*, *Nucl. Phys.* **B 630** (2002) 3 [`hep-ph/0112030`].

[27] A. Denner, M. Melles and S. Pozzorini, *Two-loop electroweak angular-dependent logarithms at high energies*, *Nucl. Phys.* **B 662** (2003) 299 [`hep-ph/0301241`].

[28] S. Pozzorini, *Next-to-leading mass singularities in two-loop electroweak singlet form factors*, *Nucl. Phys.* **B 692** (2004) 135 [`hep-ph/0401087`].

[29] B. Feucht, J.H. Kühn and S. Moch, *Fermionic and scalar corrections for the Abelian form factor at two loops*, *Phys. Lett.* **B 561** (2003) 111 [`hep-ph/0303016`];
B. Feucht, J.H. Kühn, A.A. Penin and V.A. Smirnov, *Two-loop Sudakov form factor in a theory with mass gap*, *Phys. Rev. Lett.* **93** (2004) 101802 [`hep-ph/0404082`];
B. Jantzen, J.H. Kühn, A.A. Penin and V.A. Smirnov, *Two-loop electroweak logarithms*, *Phys. Rev.* **D 72** (2005) 051301 [*Erratum ibid.* **D 74** (2006) 019901] [`hep-ph/0504111`].

[30] B. Jantzen, J.H. Kühn, A.A. Penin and V.A. Smirnov, *Two-loop electroweak logarithms in four-fermion processes at high energy*, *Nucl. Phys.* **B 731** (2005) 188 [*Erratum ibid.* **B 752** (2006) 327] [`hep-ph/0509157`].

[31] B. Jantzen and V.A. Smirnov, *The two-loop vector form factor in the Sudakov limit*, *Eur. Phys. J.* **C 47** (2006) 671 [`hep-ph/0603133`].

[32] A. Denner, B. Jantzen and S. Pozzorini, *Two-loop electroweak next-to-leading logarithmic corrections to massless fermionic processes*, *Nucl. Phys.* **B 761** (2007) 1 [`hep-ph/0608326`].

[33] A. Denner and S. Pozzorini, *An algorithm for the high-energy expansion of multi-loop diagrams to next-to-leading logarithmic accuracy*, *Nucl. Phys.* **B 717** (2005) 48 [`hep-ph/0408068`].

[34] A. Denner, B. Jantzen and S. Pozzorini, *Two-loop electroweak Sudakov logarithms for massive fermion scattering*, `arXiv:0801.2647`.

[35] W. Bernreuther et al., *Two-loop QCD corrections to the heavy quark form factors: the vector contributions*, *Nucl. Phys.* **B 706** (2005) 245 [`hep-ph/0406046`].